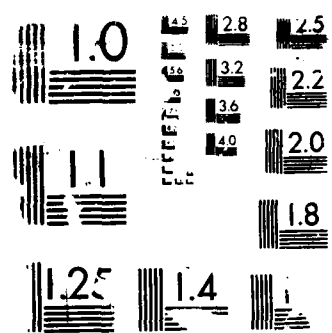


UNCLASSIFIED

THE HEAT EQUATION: (U) AIR FORCE INST
WRIGHT-PATTERSON AFB OH SCHOOL OF ENGI
DEC 87 AFIT/GEP/ENP/87D-5

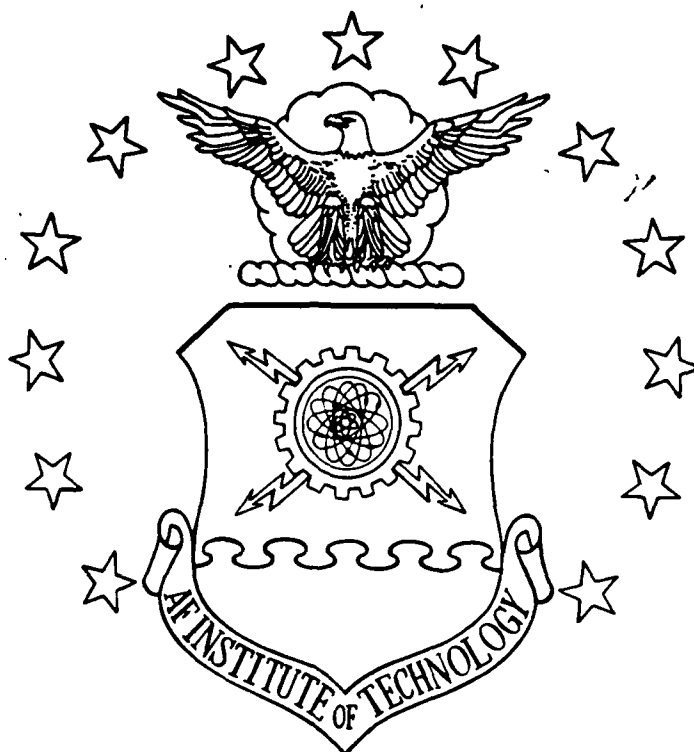
MI

F/G 12/1



400 COPY RESOLUTION TEST CHART

AD-A189 591



PREDICTING OSCILLATORY FINITE
DIFFERENCE SOLUTIONS TO THE HEAT
EQUATION: A COMPARATIVE STUDY OF
THE COEFFICIENT AND MATRIX METHODS

THESIS

Thomas M. Dipp
Captain, USAF

AFIT/GEP/ENP/87D-5

DTIC
ELECTE
MAR 03 1988
S H D

DEPARTMENT OF THE AIR FORCE
AIR UNIVERSITY

AIR FORCE INSTITUTE OF TECHNOLOGY

Wright-Patterson Air Force Base, Ohio

DISTRIBUTION STATEMENT A

Approved for public release;
Distribution Unlimited

88 3 01 04 6

AFIT/GEP/ENP/87D-5

PREDICTING OSCILLATORY FINITE
DIFFERENCE SOLUTIONS TO THE HEAT
EQUATION: A COMPARATIVE STUDY OF
THE COEFFICIENT AND MATRIX METHODS

THESIS

Thomas M. Dipp
Captain, USAF

AFIT/GEP/ENP/87D-5

DTIC
ELECTE
MAR 03 1988
SH

Approved for public release, distribution unlimited

AFIT/GEP/ENP/87D-5

PREDICTING OSCILLATORY FINITE DIFFERENCE SOLUTIONS
TO THE HEAT EQUATION: A COMPARATIVE STUDY
OF THE COEFFICIENT AND MATRIX METHODS

THESIS

Presented to the Faculty of the School of Engineering
of the Air Force Institute of Technology

Air University

In Partial Fulfillment of the
Requirements for the Degree of
Master of Science in Physics

Thomas M. Dipp, B.S.

Captain, USAF

December 1987

Approved for public release; distribution unlimited

Preface

This study began as an attempt to compare a new method for predicting stability with the coefficient method. The new method, using Pade' approximants and systems of linear equations, had predicted the oscillatory behavior discovered by a previous thesis (8; 14:246). To do a comparative study, a new approach using the space and time step domain was developed. Also, for a comparative study it was felt that a survey of many finite difference methods for both the one and two dimensional cases was required, so this thesis looks at five popular finite difference methods.

I would like to thank Dr. Bernard Kaplan of the Air Force Institute of Technology for letting me pursue this independent study as just that, an independent study, while always demanding quality results. His guidance kept me from getting too far off track at times. Also, I would like to express my thanks to Dr. N. Pagano of AFWAL/MLBC for sponsoring this study. Finally, I would like to express my thanks to Major Lupo, whose door was always open, especially when it came to questions about mainframe computers, and without whose support the graphics in this thesis would still just be numbers floating around somewhere in the VAX computer.

-- Thomas M. Dipp



For	<input checked="checked" type="checkbox"/>
SI	<input type="checkbox"/>
ed	<input type="checkbox"/>
con	<input type="checkbox"/>
Availability Codes	
Dist	Special
A-1	

Table of Contents

	Page
Preface	ii
List of Figures	v
Notation and Abbreviations	vii
Abstract	ix
I. Introduction	1
Background	1
The Two Dimensional Transient Heat (Diffusion) Equation	2
Problem Statement	3
Scope	3
Approach	4
Sequence of Presentation	5
Computer	5
II. Finite Difference Approximations	7
Fully Explicit (EX) Approximation	8
DuFort-Frankel (DF) Approximation	8
Crank-Nicolson (CN) Approximation	9
Peaceman-Rachford (ADI) Approximation	9
Fully Implicit (IM) Approximation	10
Methods of Solution	11
III. Stability, Oscillations, and Accuracy	13
Coefficient Method	14
Full Matrix Method	20
Pade' Approach to the Amplification Matrix	21
Non-Disastrous Consequences from Oscillatory Terms	27
Relating Coefficient and Matrix Methods	29
IV. Computational Approach	32
Domain Graphs	32
Stability and Behavioral Components	33
Reading h-k Domain Graphs	36
Comparison of h-k Domain Graphs with Conventional Graphs	40
V. Results	47

Problem #1	47
Problem #2	48
h-k Domain Graph Solutions	49
Fully Implicit Results	50
Fully Explicit Results	50
DuFort-Frankel Results	56
Crank-Nicolson Results	68
Peaceman-Rachford ADI Results	74
VI. Conclusions and Recommendations	78
Conclusions	78
Recommendations	84
Appendix A: h-k Domain Graphs for the Slope of the Maximum Error Versus Time	87
Appendix B: General Structure Diagram of Programs . . .	94
Appendix C: Example Stability Derivations	97
Appendix D: Relating Coefficient and Matrix Methods . .	102
Bibliography	105
Vita	107

List of Figures

Figure	Page
1. Coefficient and Matrix Method Stability Predictions .	17
2. Matrix Non-Disastrous Oscillations, and r Versus N Coordinate System, Both Superimposed on the h - k Domain	18
3. Coefficient Method Stability Curves, and Discrete Solution Points	19
4. Comparison Graphs for 1-D Cases	41
5. Comparison Graphs for 1-D Cases	42
6. Comparison Graphs for 2-D Cases	44
7. Comparison Graphs for 2-D Cases	45
8. IM Maximum Errors	51
9. EX Maximum Numeric Time Oscillations	52
10. EX Maximum Spatial Error Oscillations	53
11. EX Maximum Errors	54
12. DF Maximum Numeric Time Oscillations, Analytic Start	57
13. DF Maximum Spatial Error Oscillations, Analytic Start	58
14. DF Maximum Errors, Analytic Start	59
15. DF Maximum Numeric Time Oscillations, IM Start	60
16. DF Maximum Spatial Error Oscillations, IM Start . . .	61
17. DF Maximum Errors, IM Start	62
18. DF Maximum Numeric Time Oscillations, CN Start, and DF Maximum Spatial Error Oscillations, CN Start . . .	63
19. DF Maximum Errors, CN Start, and CN Maximum Errors, $t=0.50$ s	64
20. CN Maximum Numeric Time Oscillations, $t=0.50$ s, and CN Maximum Spatial Error Oscillations, $t=0.50$ s . . .	69

Figure	Page
21. CN Maximum Numeric Time Oscillations	70
22. CN Maximum Spatial Error Oscillations	71
23. CN Maximum Errors	72
24. ADI Maximum Numeric Time Oscillations, and ADI Maximum Spatial Error Oscillations	75
25. ADI Maximum Errors	76

Notation and Abbreviations

$\Delta x = \Delta y = h$ = spatial increment between nodal points.

$N_x = N_y = N$ = total spatial node points in x or y direction.

$L = Nh$ = total length of rod or square plate in x or y direction.

$\Delta t = k$ = time increment (seconds)

t = time (seconds)

M = total time nodes.

$T = Mk$ = total time to solution

a = thermal diffusivity, here always = 1.0

$r = a\Delta t/\Delta x^2 = a\Delta t/\Delta y^2 = ak/h^2$

$U(i,j,n)$ = temperature at the i th, j th node at time step n ,
= $U(i\Delta x, j\Delta y, n\Delta t) = U(x,y,t)$

$[B]$ = notation for matrix B

$\langle b \rangle$ = notation for column matrix b

EX = Fully Explicit Method

DF = DuFort-Frankel Method

CN = Crank-Nicolson Method

ADI = Peaceman-Rachford Alternating Direction Implicit Method

IM = Fully Implicit Method

1-D = one dimensional

2-D = two dimensional

FDM = Finite Difference Method

$[A]$ = Pade' exponential matrix A

$[G]$ = amplification or growth matrix G

$s=1(1)n = s$ varies from 1 to n by increments of (1), i.e.
 $s = 1, 2, 3, \dots, n-1, n$

$Z_s, Z_{\square, n} = 1\text{-D and } 2\text{-D matrix } A \text{ eigenvalues}$

$G_s, G_{\square, n} = 1\text{-D and } 2\text{-D amplification matrix eigenvalues}$

$\pi = 3.141592654\dots$

Abstract

This thesis compared the coefficient method with the full matrix method for predicting stability and oscillatory behavior of Finite Difference Methods, FDMs, used in solving the one and two dimensional transient heat (diffusion) equation with Dirichlet boundary conditions. Five FDMs were used: the fully implicit, fully explicit, DuFort-Frankel, Crank-Nicolson, and Peaceman-Rachford ADI.

Analytically, the Pade' method was found to be equivalent to the matrix method in predicting stability and oscillations. The matrix method was shown to be more severe than the coefficient method in predicting both stable and non-oscillatory step size constraints. Also, the matrix method, while mathematically more rigorous, proved to be more difficult to derive and analyze, possibly limiting its usefulness. Ultimately, it was found that the coefficient method's predictions could be derived from the matrix method for two-level FDMs.

Numerically, all methods were solved repeatedly and the results investigated for oscillatory behavior and maximum errors in the h - k , or space and time step, domain. These results allowed functional comparison with stability and oscillatory predictions made by the coefficient and full matrix methods. Neither the coefficient nor matrix method's stability and oscillatory predictions were significantly

violated for two-level FDMs. Finally, the matrix method could generally predict when non-disastrous oscillations would occur, based on moderate step size constraints.

PREDICTING OSCILLATORY FINITE DIFFERENCE SOLUTIONS
TO THE HEAT EQUATION: A COMPARATIVE STUDY
OF THE COEFFICIENT AND MATRIX METHODS

I. Introduction

Background

Finite difference methods (FDMs) have become increasingly important to the advancement of science and technology as ever faster and more powerful digital computers are developed to handle the complex and often analytically intractable problems arising in science and industry. One such problem, the transient heat (diffusion) partial differential equation, is often solved using finite difference methods. However, as with all numerical methods, the behavior of a finite difference method used to numerically solve a problem must be understood before the method can be applied with the reasonable hope of getting anything more than useless significant digits from a computer. In the relatively recent past, methods proven to be unconditionally stable have been embraced only to find that unacceptable errors and oscillations were occurring, such as in the Crank-Nicolson, DuFort-Frankel, and Peaceman-Rachford alternating direction implicit FDMs.

Stability is a condition where errors introduced into the FDM are bounded as time progresses. Von Neuman and Goldstein

note four major sources of errors in describing physical systems: 1) Mathematical models of nature are approximations, 2) Most descriptions require measured data, 3) truncation error due to most descriptions involving an infinite continuum, and limiting processes cannot be completed, and 4) roundoff error caused by the fact that calculations cannot be carried out with an infinite number of digits (15:6). The last source of error listed above is the most important source in the study of FDM stability and results from the fact that finite difference methods involve limited precision in computer arithmetic. Consequently, errors are introduced at each time step of the calculations, and would grow without bound if the FDM were not stable. Even if a method is stable, errors and oscillations that would eventually damp out with time, may produce unacceptable inaccuracies in a given solution. As a result, a knowledge of techniques for predicting stability and oscillations, and how well these techniques work, is needed before solving a problem on the computer.

The Two Dimensional Transient Heat (Diffusion) Equation

The heat equation is a parabolic partial differential equation, and in two dimensions has the form

$$U(x,y,t)_t = a [U(x,y,t)_{xx} + U(x,y,t)_{yy}]$$

where $U(x,y,t)$ is the temperature, 'a' is the thermal diffusivity, t is the time, and x and y are the spatial dimensions of length. Partial differentiation of $U(x,y,t)$ with respect to t , x , and y is denoted, in standard notation, by subscripted variables.

Problem Statement

The goal of this thesis is to compare the coefficient and full matrix (Pade' approximant) methods of predicting stability and oscillatory behavior of FDMs used in solving the transient heat (diffusion) equation.

Scope

Five finite difference approximations to the transient heat (diffusion) equation are used in this study:

1. Fully Implicit (IM)
2. Fully Explicit (EX)
3. DuFort-Frankel (DF)
4. Crank-Nicolson (CN)
5. Peaceman-Rachford Alternating Direction Implicit (ADI)

Both the one (1-D) and two (2-D) dimensional FDMs are analyzed, except in the case of the ADI method which has no 1-D representation. Also, the one and two dimensional FDMs are each used to solve a different test problem. Both

problems are boundary value problems using Dirichlet boundary conditions, both assume a thermal diffusivity of one, and both the rod and the square have unit lengths. For the two dimensional case, only the standard $\Delta x = \Delta y$ plane is used. The number of spatial nodes varies from three to 25 and the number of time steps varies from four to 100. All nodes and all time steps are included in the oscillation and error analysis.

Approach

First, two previous theses, where oscillations were found to exist in the ADI (8:56) and DF (4:62) FDMs, were reviewed. Next, published oscillatory solutions were reproduced for 1-D cases in Smith (13:124), Twizell (14:206), and Lawson and Morris (10:1217). From this experience, it was realized that no h-k domain studies comparing stability and oscillation predictions had been done. A literary search was conducted and no comparative domain studies were found. Two problems with known analytical solutions, which were previously used in showing oscillatory behavior, were selected for indepth stability analysis in the h-k domain (13:124;4:19;8:19). For such a comparison study, a survey of many FDMs in the h-k domain was indicated. Computer modules to determine stability components were developed and computer programs for the one and two dimensional FDMs were written. Numerical solutions to the problems using the FDMs were graphed in the h-k domain and compared with predicted functional restrictions on h and k obtained from the coefficient method and Pade' approximant

(full matrix) method. Finally, the analytic development of the coefficient, Pade' approximant, and full matrix methods were explored to determine the relationships among the methods.

Sequence of Presentation

Chapter 2 introduces general finite difference approximations and the finite difference equations for the five FDMs used in this thesis. Stability, oscillations, and accuracy are discussed in Chapter 3, along with the coefficient method and full matrix (Pade' approximant) method for predicting stability and oscillations. Because of the new approach to graphing FDM stability components and errors in the h - k domain, which uses 2 dimensional contour plots of three dimensions, Chapter 4 covers the rationale behind the domain approach, what it includes, how to read the domain graphs, and comparisons with conventional stability graphs. Chapter 5 presents the numerical results for maximum time and spatial oscillations, as well as for maximum absolute errors, as well as comparisons with stability predictions. Finally, conclusions and observations are given in Chapter 6.

Computer

A VAX 11/780 32 bit computer was used. Programs were written in FORTRAN 77. All calculations were done using double precision to reduce the effects of round off error.

Extensive use of structured programming technique was applied to insure that code was readable and modular, allowing quick program design with reliability. Graphs were drawn using standard library routines provided by Major Lupo (11), and hardcopy output was obtained with an Imagen Laser Printer.

II. Finite Difference Approximations

All finite difference methods involve approximations to differential equations. Since the analytic solution for the heat equation for all space and time may be impossible or not practical to derive, numerical solutions based on a knowledge of the present state of a system and the rates of change to that system must be developed instead. These numerical solutions are accomplished by using approximations to the partial derivatives in the governing partial differential equation, and involve replacing the actual derivatives by approximate derivatives built from truncated Taylor series expansions. The details of this process can be found in numerous texts (1:532-538, 578-597; 13:6-24; 14:31-37).

A fundamental result is that space and time are no longer an infinite continuum, but become discretized by the truncation of the derivative expressions. In effect, the result is a finite grid of difference approximations based on adjacent time and space point values, or nodes. Inevitably, it is this discretization that introduces truncation error into the numerical solution.

Five finite difference approximations commonly used to solve the heat equation are the fully explicit, fully implicit, Crank-Nicolson, DuFort-Frankel, and Peaceman-Rachford alternating direction implicit methods. In

listing the finite difference approximations, the following notation is implemented:

$$\begin{aligned} \Delta x = \Delta y = h, \Delta t = k, x = ih, y = jh, t = nk \quad \text{where} \\ i, j, \text{ and } n \text{ are integers and} \\ U(x,y,t) = U(ih,jh,nk) = U(i,j,n) \quad \text{with} \\ a = 1, r = ak/h^2. \end{aligned}$$

Fully Explicit (EX) Approximation

One of the easiest methods to implement, the EX calculates the temperatures at each new time step only in terms of the old temperatures at the previous time step. The formulas for one and two dimensions are (9:155,235):

$$U(i,n+1) = (1-2r)U(i,n) + r[U(i+1,n) + U(i-1,n)] \quad (1)$$

$$\begin{aligned} U(i,j,n+1) = (1-4r)U(i,j,n) + r[U(i+1,j,n) \\ + U(i-1,j,n) + U(i,j+1,n) + U(i,j-1,n)] \end{aligned} \quad (2)$$

DuFort-Frankel (DF) Approximation

The DuFort-Frankel approximation is a three level explicit method that overcomes the instability of the fully explicit method (9:238). It was the goal of the DF method to have the calculational ease of an explicit method without the instability associated with the fully explicit method. Forms for the one and two dimensional approximations are (9:157,239):

$$(1+2r)U(i,n+1) = 2r[U(i+1,n) + U(i-1,n)] \quad (3)$$

$$+ (1-2r)U(i,n-1)$$

$$(1+4r)U(i,j,n+1) = 2r[U(i+1,j,n) + U(i-1,j,n)] \quad (4)$$

$$+ U(i,j+1,n) + U(i,j-1,n)] + (1-4r)U(i,j,n-1)$$

Crank-Nicolson (CN) Implicit Approximation

The Crank-Nicolson method equally weights and combines the fully explicit and fully implicit methods. The goal of the CN method was to reduce the truncation error of the IM method and hopefully improve accuracy. The one and two dimensional forms are (9:160,242):

$$(2+2r)U(i,n+1) - r[U(i+1,n+1) + U(i-1,n+1)] \quad (5)$$

$$= (2-2r)U(i,n) + r[U(i+1,n) + U(i-1,n)]$$

$$(2+4r)U(i,j,n+1) - r[U(i+1,j,n+1) + U(i-1,j,n+1)] \quad (6)$$

$$+ U(i,j+1,n+1) + U(i,j-1,n+1)]$$

$$= (2-4r)U(i,j,n) + r[U(i+1,j,n) + U(i-1,j,n)$$

$$+ U(i,j+1,n) + U(i,j-1,n)]$$

Peaceman-Rachford (ADI) Approximation

The ADI method also combines the EX and IM methods, similar to CN method. However, the ADI method alternates in its use of the EX and IM methods. ADI solves a given time step explicitly in one direction and implicitly in the other,

and then reverses the EX and IM directions in solving for the next time step. Both time steps must have the same duration and both should be completed for a stable solution. The goal of the ADI method was to have the speed of tridiagonal matrices instead of the time problems of the IM method. It has the following form in two dimensions (9:246-247):

$$\begin{aligned} (1+2r)U(i,j,n+1) - r[U(i+1,j,n+1) + U(i-1,j,n+1)] & \quad (7a) \\ = (1-2r) U(i,j,n) + r[U(i,j+1,n) + U(i,j-1,n)] \end{aligned}$$

to advance from time step n to $n+1$, followed by

$$\begin{aligned} (1+2r)U(i,j,n+2) - r[U(i,j+1,n+2) + U(i,j-1,n+2)] & \quad (7b) \\ = (1-2r)U(i,j,n+1) + r[U(i+1,j,n+1) + U(i-1,j,n+1)] \end{aligned}$$

to advance from time step $n+1$ to $n+2$.

Fully Implicit (IM) Approximation

By replacing the second order spatial derivatives with the second order backward-difference approximation, this method computes the temperatures at the new time step based on temperatures at neighboring node points which are also at the new time step. The one and two dimensional form are (9:159,242):

$$(1+2r)U(i,n+1) - r[u(i+1,n+1) + U(i-1,n+1)] = U(i,n) \quad (8)$$

$$(1+4r)U(i,j,n+1) - r[U(i+1,j,n+1) + U(i-1,j,n+1)] \quad (9)$$

$$+ U(i,j+1,n+1) + U(i,j-1,n+1)] = U(i,j,n)$$

Methods of Solution

The EX and DF methods are explicit and are readily solved with one equation for each unknown. However, the DF method requires two initial time steps be known before it becomes explicit. Therefore, the DF method is often started by using another method to calculate the first time step from the initial and boundary conditions. Initial time steps were calculated using the analytic solution and the IM method, because they do not introduce oscillations into the first time step. However, the one dimensional case was also started using the CN method for comparison with an FDM that could oscillate.

The CN, ADI, and IM are all implicit formulations, and require that a system of simultaneous equations be solved in order to calculate the unknowns. The systems of equations have the general form:

$$[A]\langle x \rangle = \langle b \rangle$$

where $[A]$ is an $N \times N$ matrix for the one dimensional case and an $N^2 \times N^2$ matrix for the two dimensional case, $\langle x \rangle$ is a column vector composed of the new temperatures at $t+k$, $\langle b \rangle$ is a column vector containing the old temperatures and boundary conditions, and $N = L/h$, where $L = x_2 - x_1$. x_1 and x_2

represent the length of a 1-D rod or the side of a 2-D square plate.

One dimensional solutions of the column vector $\langle x \rangle$ for the CN and IM methods were obtained efficiently and accurately by using a tridiagonal solver. Since the ADI method alternately solves using the EX and IM methods, the ADI method also obtained solutions for $\langle x \rangle$ by using a tridiagonal solver. Finally, the two dimensional CN and IM methods were solved to at least 13 significant digits of accuracy by using Gauss-Seidel Iteration combined with Successive Over-Relaxation (1:428,434).

At least 10 digits of accuracy and precision was constantly maintained in the numerical solutions of the FDMs since 1) double precision was used exclusively in all the finite difference programs, 2) matrix sizes for direct matrix methods did not exceed 25x25 with no more than 100 time steps, and 3) two dimensional implicit matrices were solved using Gauss-Seidel iteration until 13 digits of numerical convergence were achieved.

III. Stability, Oscillations, and Accuracy

Stability is a property of FDMs which guarantees that the numerical solution to the finite difference equation will not grow without bound as time progresses. As such, stability is a property that is independent of the actual partial differential equation. Since numerical error introduced during the calculations, mainly from roundoff error, can be treated as perturbations to the vector of initial values, numerical error is subject to the same arithmetic operations as the vector of initial values (13:48,53). Therefore, stability also guarantees that numerical error is bounded (3:98).

Stability has also been given more specific definitions, such as conditional or unconditional stability, and Ao-stability or Lo-stability. Conditional stability refers to a finite difference equation that is only stable for certain values of step sizes for time and space, and unstable for all other step sizes (9:167). Unconditionally stable FDMs have no step size restrictions, and are stable over the whole h - k domain. Ao-stability guarantees unconditional stability while Lo-stability not only guarantees unconditional stability, but also guarantees no oscillations as well (14:213-215). These definitions, when applied to the five types of FDMs use in this thesis, are as follows:

EX	Conditional (1:581), Neither Ao nor Lo (13:122)
DF	Unconditional (13:153), Ao (definition, 13:120)
CN	Unconditional (13:56), Ao (13:121)
ADI	Unconditional (definition, 13:120), Ao (14:240)
IM	Unconditional (1:582), Lo (13:121)

However, stability does not guarantee accuracy. This is because stability is a necessary, but not sufficient, condition for accuracy (9:167). Also, a FDM may be stable, yet still experience oscillations which can have disastrous effects on the accuracy of a solution (12:281-84). Further, the stability of an FDM can depend on other factors, such as the type of boundary conditions employed (9:167). Still, because stability is necessary to accuracy, it is an important first step in analyzing any FDM. Accuracy and computational efficiency must become secondary considerations (9:167).

Two methods of analyzing stability and oscillations were investigated and used: the coefficient method and the Pade' (full matrix) method. Their description follows, beginning with the coefficient method.

Coefficient Method

The coefficient method is an easy to use and understand method of predicting stability and oscillations in FDMs. In this method, the FDM behavior for all of the nodal points is approximated by applying the finite difference equations to a

one nodal point grid with homogeneous boundary conditions. Consequently, since only one nodal point is examined, the coefficient method is often considered a crude one nodal point approximation when applied to predicting the stability of all the nodal points.

Myers, in his book, Analytical Methods in Conduction Heat Transfer, provides a clear and concise look at the one dimensional case of the coefficient method (12:282). This method has been directly extended to the two dimension heat equations in previous papers on the subject of stability and oscillations (8:10-14, 4:10-12). Resulting ratios for the one and two dimensional cases, Equations (1) through (9), are listed below:

Fully Explicit 1-D:	$p = 1-2r$
Fully Explicit 2-D:	$p = 1-4r$
DuFort-Frankel 1-D:	$p = (1-2r)/(1+2r)$
DuFort-Frankel 2-D:	$p = (1-4r)/(1+4r)$
Crank-Nicolson 1-D:	$p = (1-r)/(1+r)$
Crank-Nicolson 2-D:	$p = (1-2r)/(1+2r)$
Peaceman-Rachford 2-D:	$p = (1-2r)/(1+2r)$
Fully Implicit 1-D:	$p = 1/(1+2r)$
Fully Implicit 2-D:	$p = 1/(1+4r)$

where p is the ratio of the new to old temperatures at the single node point, and is defined as:

$$1-D: p = U(i,n+1)/U(i,n)$$

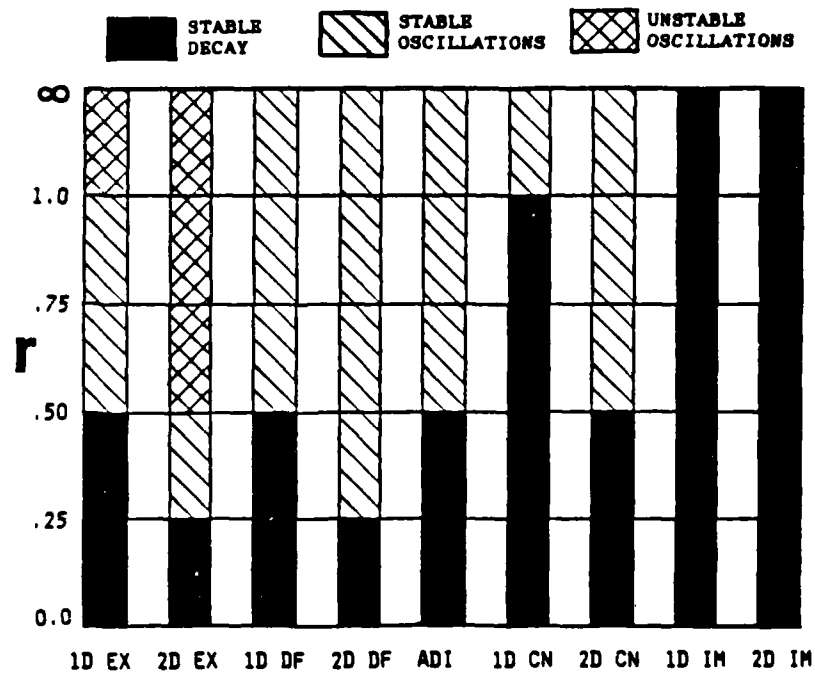
$$2-D: p = U(i,j,n+1)/U(i,j,n)$$

Stability and oscillatory behavior of a finite difference method can then be inferred from the various values the p-ratio takes on as the value of r changes, where $r=k/h^2$ is a positive number ranging from zero to infinity. This behavior is described by Myers and in summary is as follows (12:282):

$p > 1$	Unstable, No oscillations = unstable growth
$0 < p < 1$	Stable, No oscillations = stable decay
$-1 < p < 0$	Stable, Oscillations = stable oscillations
$p < -1$	Unstable, Oscillations = unstable oscillations

Values of the p-ratio, and hence the predicted behavior of Equations (1) through (9), can be calculated algebraically or graphically for various values of r . Figure 3 (top) is a graph that has been modified to show the behavior of all the previously listed p-ratios as a function of r (8:14). From the graph, it is easily seen that the EX method is the only predicted conditionally stable method, that the IM method is the only predicted Lo-stable method, and that the rest are unconditionally stable but can display conditional oscillatory behavior depending on the value of r . Figure 1 (top) summarizes the predicted behavior by using a bar chart to

COEFFICIENT METHOD STABILITY



FULL MATRIX METHOD STABILITY

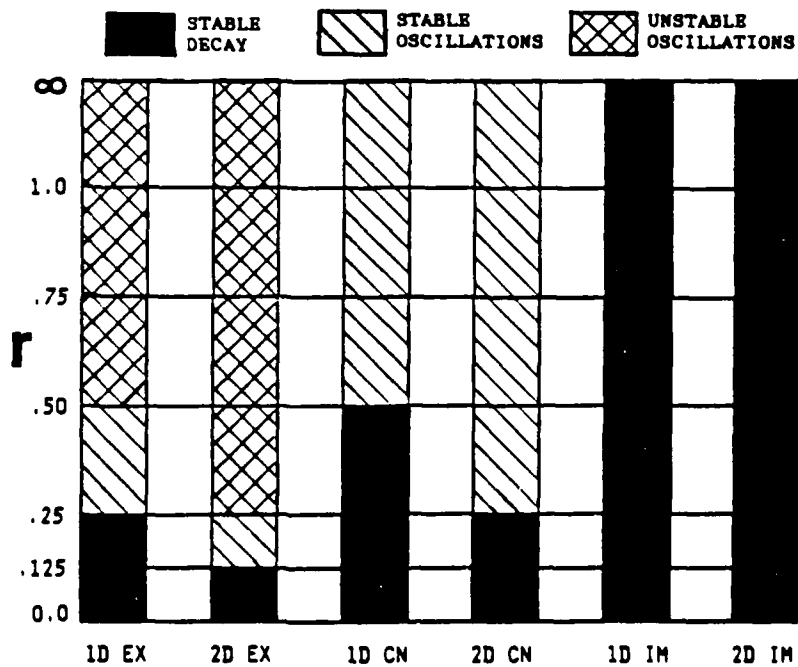
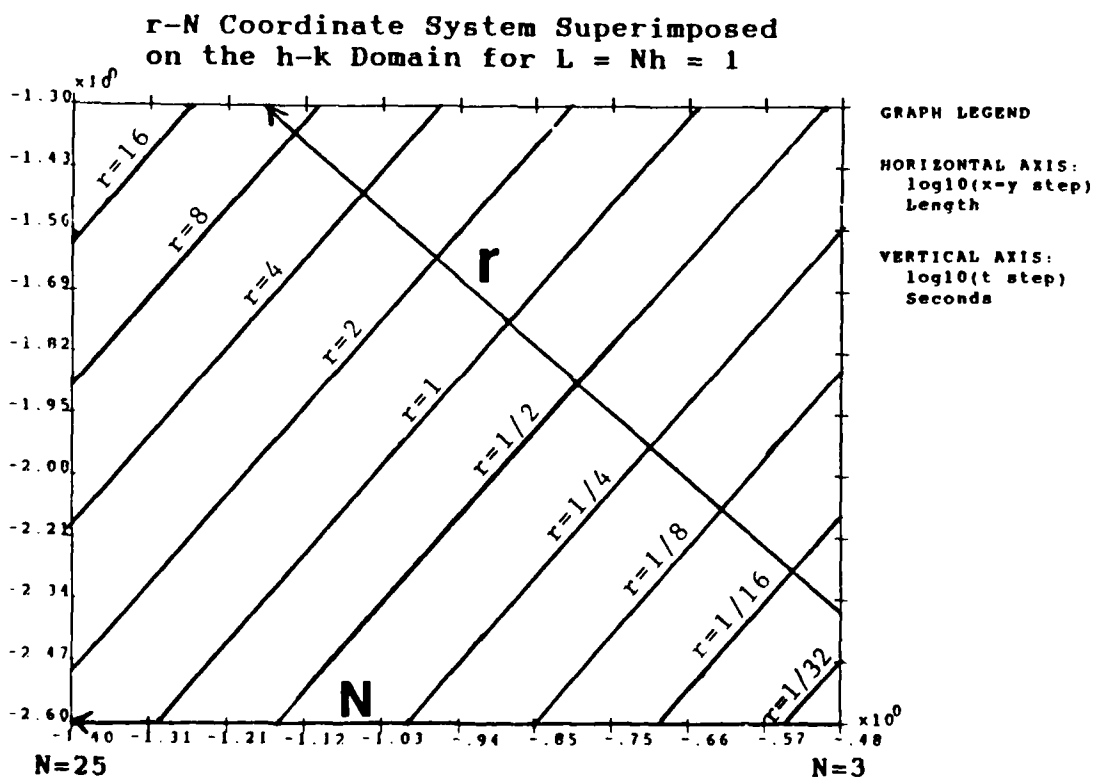
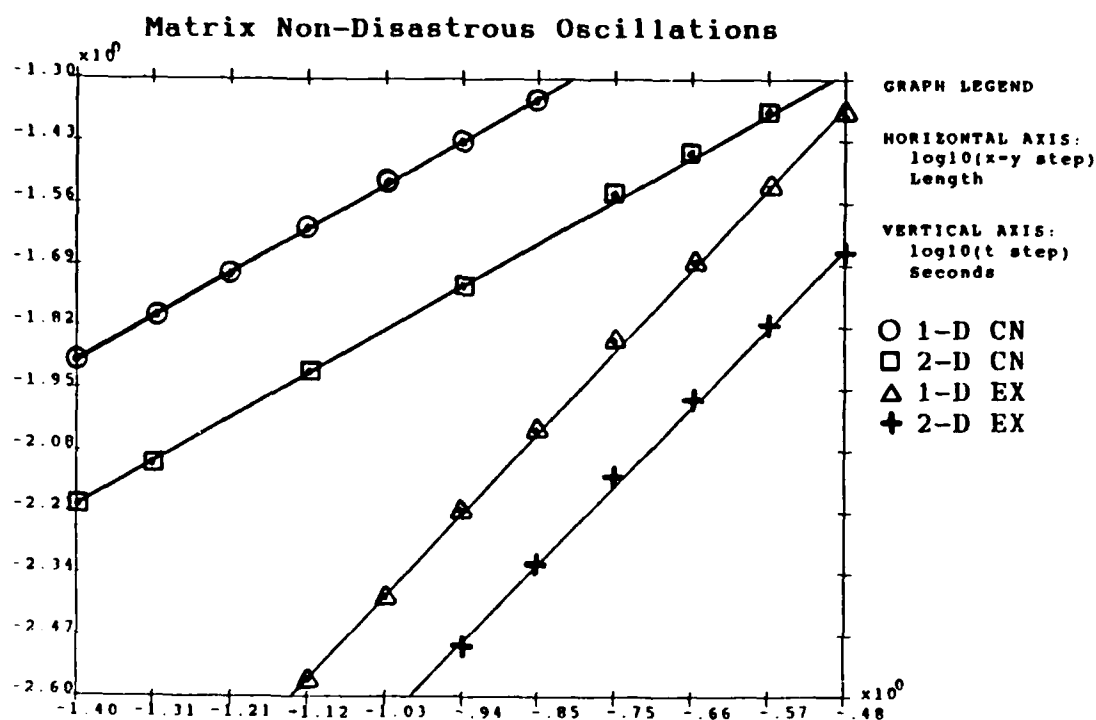
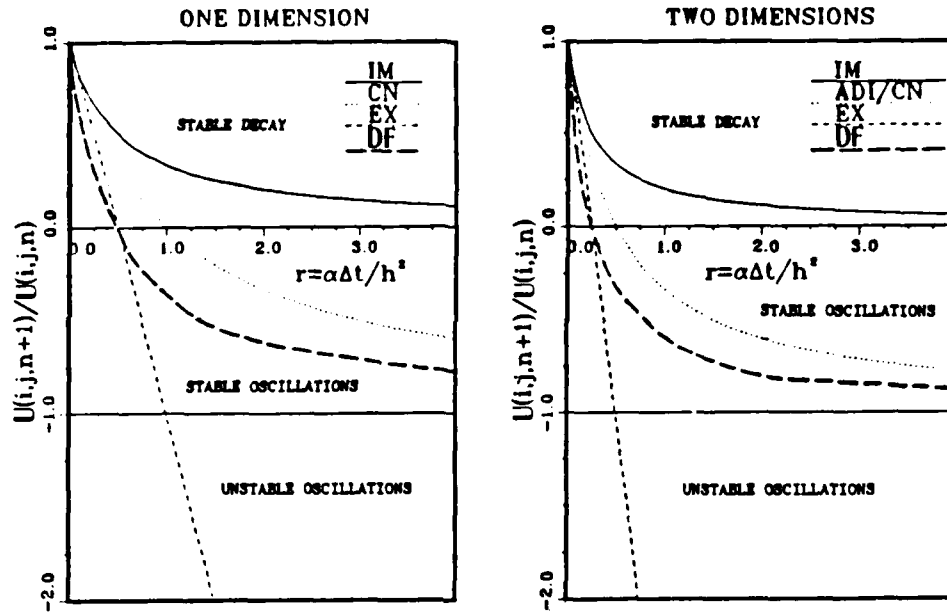


Figure 1. Coefficient and Matrix Method Stability Predictions



**Figure 2. Matrix Non-Disastrous Oscillations,
and r Versus N Coordinate System, Both
Superimposed on the h-k Domain**

COEFFICIENT METHOD STABILITY CURVES



NUMBER OF 2-D TIME AND SPACE STEPS, M AND N, SUPERIMPOSED ON H-K DOMAIN

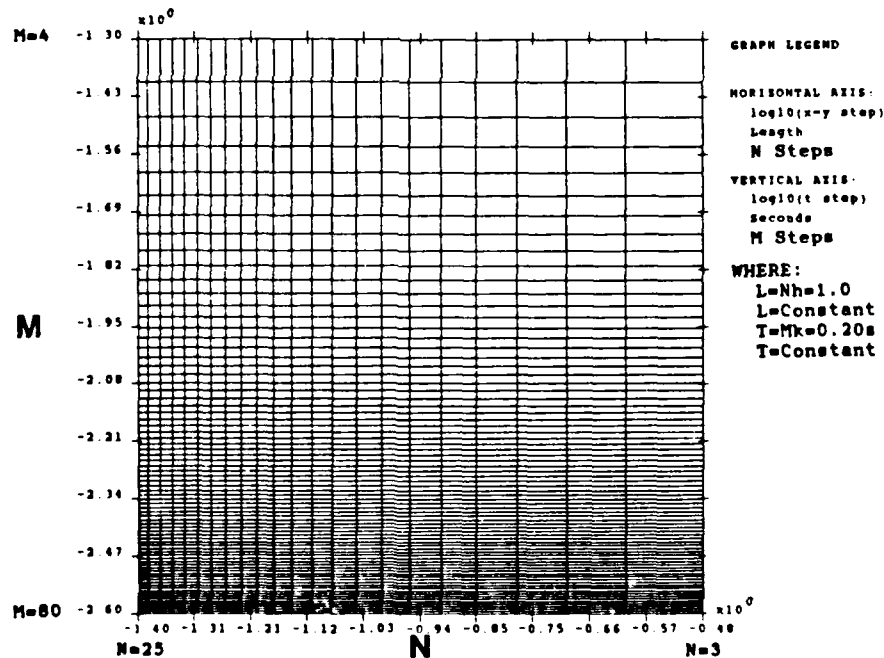


Figure 3. Coefficient Method Stability Curves, and Discrete Solution Points

display all the various behaviors versus common values of r where the behavior of the FDMs change. The values of r where changes are predicted for various of the FDMs are $r=1/4$, $r=1/2$, and $r=1$. Finally, notice that the 1-D DF, 2-D ADI, and 2-D CN all share the exact same p -ratios, and hence, same predicted behaviors.

Full Matrix Method

The full matrix method used to predict stability and oscillatory behavior is similar to the coefficient method, but uses the entire matrix to determine the behavioral characteristics of the finite difference equation. As such, it is much more complicated and requires a knowledge of matrices, matrix eigenvalues and eigenvectors, and matrix stability. There are two basic ways to approach matrix stability which are equivalent but involve generating the amplification matrix differently. The most straightforward approach is to generate, in matrix form, the simultaneous system of equations necessary to describe the FDM. For a simple two-level FDM, where two time levels are involved in the numerical calculations, the resulting matrix that is generated is the amplification matrix. The amplification matrix, $[G]$, must be in the form where

$$\langle U(i,j,n+1) \rangle = [G] \langle U(i,j,n) \rangle$$

which can be easily and directly achieved for explicit

methods, but requires for implicit forms, such as CN, the following set of manipulations:

$$\begin{aligned} [B]\langle U_{n+1} \rangle &= [C]\langle U_n \rangle \text{ be changed to} \\ \langle U(i,j,n+1) \rangle &= [B]^{-1}[C]\langle U(i,j,n) \rangle \text{ or} \\ \langle U(i,j,n+1) \rangle &= [G]\langle U(i,j,n) \rangle \end{aligned}$$

where $[G]$ is now a composite amplification matrix, $[B]$ and $[C]$ are generic implicit and explicit matrices respectively, and the constant vector of boundary conditions and zeros has been omitted. It is apparent then that the amplification matrix determines the numerical solution after repeated matrix multiplication for each time step taken, such that:

$$\langle U(i,j,n) \rangle = [G]^n \langle U(i,j,0) \rangle$$

A second way to obtain the amplification matrix describing the FDM is to use the Pade' Approach.

Pade' Approach to the Amplification Matrix

The Pade' approach to deriving the amplification matrix is presented in detail by Smith (13:111-119). This approach begins by replacing the partial differential equation with a first order system of ordinary differential equations, which are then solved to get an exponential matrix solution. The exponential matrix solution can then be written in the form of

a recurrence relation. Finally, the exponential matrix solution is approximated with an arbitrary Pade' approximant to the exponential matrix. The 1-D process proceeds, in brief, as follows (13:111):

$$\frac{dU(t)}{dt} = \frac{U(x-h,t) - 2U(x,t) + U(x+h,t)}{h^2}$$

neglecting truncation error in the approximation to the derivative. Next, this can be written in matrix form as (13:112):

$$d\langle U(t) \rangle / dt = [A] \langle U(t) \rangle + \langle b \rangle \quad (10)$$

where $\langle U(t) \rangle = [U_1, U_2, \dots, U_{N-1}]^T$, $\langle b \rangle$ is a column vector that is made up of the known boundary-values and zeros, and matrix $[A]$ is a tridiagonal matrix of order $(N-1)$ whose tridiagonal elements are $1/h^2$, $-2/h^2$, and $1/h^2$. The solution to Equation (10) is given by Smith as (13:113):

$$\langle U(t) \rangle = -[A]^{-1} \langle b \rangle + ([A]^{-1} \langle b \rangle + \langle g \rangle) \exp(t[A])$$

with the initial condition, $\langle U(0) \rangle = \langle g \rangle$, and with $\langle b \rangle$ independent of t . Then, if all the boundary conditions are set to zero to study stability, the following recurrence relation for the one dimension case can be obtained (13:113):

$$\langle U(t+k) \rangle = \exp(k[A]) \langle U(t) \rangle \quad (11)$$

or, if the solution vector is replaced by the initial perturbation vector $\langle E(0) \rangle$, then (13:113):

$$\langle E(t+k) \rangle = \exp(k[A]) \langle E(t) \rangle \quad (12)$$

The Pade' approximants to an exponential function with a real argument are then used to derive a rational function, $R_{S,T}(x)$, which is called the (S,T) Pade' approximant, and has the form (13:116):

$$\begin{aligned} R_{S,T}(x) &= (1+p_1x+\dots+p_Tx^T)/(1+q_1x+\dots+q_Sx^S) \\ &= \{P_T(x)\}/\{Q_S(x)\} \end{aligned}$$

Listed below are three Pade' approximants to the exponential matrix that result in three well-known FDMs when x is replaced by $k[A]$ (13:117).

<u>(S,T)</u>	<u>$R_{S,T}(x)$</u>	<u>FDM</u>
(0,1)	$1+x$	Fully Explicit
(1,0)	$1/(1-x)$	Fully Implicit
(1,1)	$(1+x/2)/(1-x/2)$	Crank-Nicolson

The recurrence relation for the EX method then becomes equal to $\langle E(t+k) \rangle = ([I]+k[A])\langle E(t) \rangle$, where $[I]$ is the identity matrix. So for n time steps from the initial error

vector, $\langle E(t_n) \rangle = ([I] + k[A])^n \langle E(0) \rangle$. The recurrence relation for the one dimensional case is also the recurrence relation for the two dimension case if $[A] = [B] + [C]$, where $[B]$ and $[C]$ are the component matrices of a two dimensional FDM matrix broken up into block matrix form (14:221). Finally, the amplification matrix, $[G]$, is then obtained directly from the (S,T) Pade' approximant (13:122).

Once the amplification matrix $[G]$ has been obtained, it becomes necessary to derive all the eigenvalues of the amplification matrix. Smith gives the general equation for the eigenvalues, Z_s , of a common tridiagonal matrix as

$$Z_s = b + 2\sqrt{ac} \cos \frac{s\pi}{N}, \quad s = 1(1)N-1 \quad (13)$$

where a , b , and c are the three elements of a tridiagonal matrix, from left to right (13:59). For the standard Pade' tridiagonal matrix elements, the eigenvalues of matrix $[A]$ then become:

$$Z_s = -\frac{4}{h^2} \sin^2 \frac{s\pi}{2N}, \quad s = 1(1)N-1 \quad (14)$$

For two dimensions, the eigenvalues of matrix $[A]$ can be derived by using Equation (13) and the definition of $[A] = [B] + [C]$ as (14:221):

$$Z_{m,n} = -\frac{4}{h^2} \left(\sin^2 \frac{m\pi}{2N} + \sin^2 \frac{n\pi}{2N} \right), \quad m=1(1)N-1, \quad n=1(1)N-1 \quad (15)$$

The eigenvalues for [A] are then plugged into the equation of the amplification matrix, [G], replacing the matrix [A], as shown by Smith (13:120-124) and Twizell (14:212-215), to obtain the eigenvalues of the amplification matrix, [G]. Substitution of the N-1 unique eigenvalues is possible because the associated N-1 linearly independent eigenvectors can be used as a basis, or coordinate system, in N-1 dimensional space. The vector of initial errors, $\langle E(0) \rangle$, can then be represented as a linear combination of constants, C_s , multiplied by the N-1 respective eigenvectors of matrix [A]. Once this is assumed to have been done, the eigenvalues operating on the eigenvector components of the initial error vector replaces the matrix multiplication of [A] $\langle E(0) \rangle$. This replacement of the amplification matrix by its eigenvalues is possible because of the definition of a matrix eigenvalue and eigenvector as satisfying (13:120):

$$[A] \langle V_s \rangle = Z_s \langle V_s \rangle \quad (16)$$

where Z_s is an eigenvalue, and V_s is its associated eigenvector. Therefore, the error grows as (13:120):

$$\langle E(t_n) \rangle = \sum_{s=1}^{N-1} C_s [R_{s,\tau}(kZ_s)]^n \langle V_s \rangle, \quad s=1(1)N-1 \quad (17)$$

where the error will decay only if $|R_{s,\tau}(kZ_s)| < 1$ (13:120).

Note that $R_{s,\tau}(kZ_s)$ represents the amplification matrix eigenvalues, and may be referred to as G_s , the growth factor associated with $\langle V_s \rangle$. The amplification matrix eigenvalues, G_s and $G_{m,n}$, for the finite difference methods used in this study are listed below:

$$\text{EX 1-D: } G_s = 1 + kZ_s$$

$$\text{EX 2-D: } G_{m,n} = 1 + kZ_{m,n}$$

$$\text{DF 1-D: } G_s = \frac{2rC_s + \sqrt{1 - 4r^2(1 - C_s^2)}}{1 + 2r}$$

$$\text{DF 2-D: } G_{m,n} = \frac{2r(C_m + C_n) + \sqrt{1 - 4r^2(4 - (C_m + C_n)^2)}}{1 + 4r}$$

$$\text{CN 1-D: } G_s = \frac{1 + 0.5 kZ_s}{1 - 0.5 kZ_s}$$

$$\text{CN 2-D: } G_{m,n} = \frac{1 + 0.5 kZ_{m,n}}{1 - 0.5 kZ_{m,n}}$$

$$\text{ADI 2-D: } G_{m,n} = \frac{(1 + 0.5 kZ_n)(1 + 0.5 kZ_m)}{(1 - 0.5 kZ_m)(1 - 0.5 kZ_n)}$$

$$\text{IM 1-D: } G_s = \frac{1}{1 - kZ_s}$$

$$\text{IM 2-D: } G_{m,n} = \frac{1}{1 - kZ_{m,n}}$$

where $Z_s = Z_m = Z_n = \text{Equation (14)}$, $Z_{m,n} = \text{Equation (15)}$,
 $C_s = C_m = C_n = \cos(s\pi/N)$, and the indices s , m , and n all
 vary independently as $1(1)N-1$. The 1-D growth factors listed
 above can be found in Smith (13:120-123,150-53).
 Amplification matrix eigenvalues for the 2-D cases were
 derived for this thesis in a manner similar to the 1-D cases
 (see Appendix C for example).

By applying the same criteria to the maximum and minimum
 amplification matrix eigenvalues as was applied in the
 coefficient method toward the p-ratios, the same set of four
 FDM stability and oscillatory behaviors can be predicted.
 Using approximations for large N , several predictions based on
 the full matrix method have been summarized in Figure 1. It
 should be emphasized that the matrix stability predictions in
 Figure 1 are the full matrix method predictions based on
 extreme eigenvalues and large N approximations, and are
 therefore worst case predictions that should never be
 violated. Consequently, it is not surprising that the full
 matrix method is found to be much more severe in its
 constraints on the values of r , requiring smaller values of r ,
 than the coefficient method.

Non-Disastrous Consequences from Oscillatory Terms

In addition to predicting the stability and oscillatory
 behavior of FDMs, the matrix method can even be applied to
 determine when the oscillations are disastrous or not
 disastrous to the solution. This is extremely useful since

the matrix method imposes severe constraints, more severe than usually needed, because the range of eigenvalues of the amplification matrix vary and are not all as large as the extreme values used in the predictions. Lawson and Morris (10:1214) pointed out that oscillatory terms will not have disastrous effects if the highest-frequency component, $C_{N-1}\langle V_{N-1} \rangle$, decays to zero faster than the lowest-frequency component, $C_1\langle V_1 \rangle$, where from the equation of the initial errors:

$$\langle E(0) \rangle = \sum_{s=1}^{N-1} C_s \langle V_s \rangle \quad , \quad s=1(1)N-1$$

in which $E(0)$ was represented as a linear combination of constants, C_s , multiplied by the eigenvectors of the $[A]$ matrix (10:1214). Functional relationships for the above inequalities have been derived for the EX, CN, and IM methods, and are listed below for the EX and CN methods:

$$1\text{-D EX:} \quad 2/k - 4/h^2 > \pi^2/L^2 \quad (18)$$

$$2\text{-D EX:} \quad 2/k - 8/h^2 > 2\pi^2/L^2 \quad (19)$$

$$1\text{-D CN:} \quad k/h < L/\pi \quad (20)$$

$$2\text{-D CN:} \quad k/h < L/(2\pi) \quad (21)$$

where $k = \Delta t$, $h = \Delta x = \Delta y$, and L is the length of the rod or

the length of one side of the square FDM mesh, such that $N=L/h$. Also, the above equations are approximations based on large N .

By transforming from an h, k, L coordinate system to an r, N coordinate system (see Figure 2), the relationships are easier to see in terms of the familiar r coefficient. The transformed equations are listed below:

$$1\text{-D EX: } r < 1/\{2+\pi^2/(2N^2)\}$$

$$2\text{-D EX: } r < 1/(4+\pi^2/N^2)$$

$$1\text{-D CN: } r < N/\pi$$

$$2\text{-D CN: } r < N/(2\pi)$$

The above functional relations, where r is set equal to the expression on the right side of the equations, are plotted on the h - k domain in Figure 2. These restrictions on the functional relationship in the h - k domain are less severe than the stable decay restrictions based on the extreme eigenvalues of the matrix method.

Relating Coefficient and Matrix Methods

In deriving the full matrix method stability predictions summarized in Figure 1, extreme eigenvalues for large N approximations were used. It would be simpler to apply a single value representing all the eigenvalues of the matrix method, that didn't depend on large N approximations, in deriving the matrix method predictions. Further, in picking a

single value, it should provide good predictions if the single quantity expresses the statistical expectation, or arithmetic mean, value of the amplification matrix eigenvalues. These expectation values are discrete, and are defined for Equation (14), a common component of the amplification matrix eigenvalue equations, as follows:

$$\langle Z_s \rangle = \frac{1}{N-1} \sum_{s=1}^{N-1} Z_s = -\frac{2}{h^2}, \quad N \geq 2 \quad s = 1, 2, \dots, N-1$$

where N is the number of spatial node points, and h is the spatial step size. Using this result, the expectation value of the 1-D EX amplification matrix eigenvalues is:

$$\text{EX 1-D: } \langle G_s \rangle = 1 - 2r$$

where for this equation, $\langle G_s \rangle$ denotes the expectation value of G_s .

Comparing the 1-D EX result above with the 1-D EX coefficient method p-ratio, an interesting relationship is seen . . . both equations are the same. In effect, the coefficient method has been derived from the more mathematically rigorous matrix method. This is an important result since it indicates that the coefficient method is not simply a crude, single node point approximation applied to all the node points. Instead, the coefficient method is firmly

related to the matrix method and statistically considers all the nodes.

Next, the above results and conclusions need to be checked with the other FDMs used in this study. For the FDMs in this study, the expectation values for all the 1-D and 2-D amplification matrix eigenvalues were derived and are tabulated in Appendix D. The results of the derivations indicate that the expectation value of the amplification matrix eigenvalues is equal to the coefficient method p-ratio for two-level FDMs. For three-level FDMs, the expectation values diverge from the p-ratios, as would be expected, since the behavior of the three FDMs in this study which have the same p-ratio is obviously different. Therefore, the coefficient method is seen to be a worse approximation for three-level FDMs, but may still be statistically related to all the nodes in a different manner. In conclusion, for two level FDMs, the coefficient method should provide good predictions due to its relation to the matrix method.

IV. Computational Approach

The computational approach used to examine stability predictions will be discussed in this chapter. Topics included will be the domain approach, stability components, how to read the domain graphs, and comparisons of domain graphs with representative conventional graphs.

Domain Graphs

Domain graphs provide a simple and comprehensive way to compare all functional relationships based on h , k , L , and time for predicting FDM stability, oscillations, and accuracy. Because it is the most basic of all possible representations, the h - k domain graph is one of the best ways to display a vast array of possible coefficients. Almost all other coefficients and conventional graphs can be found as simple points or lines on a domain graph. Another advantage of domain graphs is that they are extendible. Therefore, the predicted functional relationship does not have to be known and built into the graph when it is made. Consequently, the domain graph is useful for comparing other stability predictions in the future. However, the domain graph does have one chief drawback. Limited domains are a problem since the number of computations needed to solve many heat equations increases approximately as the total number of node points that must be

calculated in the domain. For large numbers of maximum time and space steps on the domain, the total number of node points to be calculated approaches:

$$1\text{-D, general:} \quad (n_x^2/2)(n_t^2/2) \quad \text{and} \quad (22)$$

$$2\text{-D, } \Delta x = \Delta y \text{ plane:} \quad (n_{xy}^3/3)(n_t^2/2) \quad \text{and} \quad (23)$$

$$2\text{-D, general:} \quad (n_x^2/2)(n_y^2/2)(n_t^2/2) \quad (24)$$

where n_x and n_y are the maximum number of steps in the x and y directions respectively, n_{xy} is the maximum number of steps in the x and y directions for the $\Delta x = \Delta y$ plane (a square grid is assumed, so x and y steps are equal), and n_t is the maximum number of steps in time to reach the solution. In addition, all steps up to and including the above maximum numbers are assumed to be used, starting with one step in each dimension. To simplify comparison of the domain graphs, the same domains were used on all graphs. As a result, equations (22) and (23) show that the domain graphs in this study were limited by the two dimensional case. Ultimately, the domain graph is a technique that, with the advent of faster and more powerful digital computers, promises to see more use in the analysis of methods for predicting FDM behavior.

Stability and Behavioral Components

After having selected the h-k domain as the best way to compare various stability properties, oscillations, and final errors, one of the major difficulties that had to be overcome

in using the approach was that of precisely defining what was to be displayed in the h - k domain, and then designing algorithms that allowed the computer to automatically find and quantify the information to be displayed. Various FDM behavioral diagnostics were examined, and the following were selected as a minimal, yet complete, set: maximum number of time oscillations, maximum number of spatial error oscillations, growth or decay of errors, and maximum error in the final solution.

In chapter 3, stability analysis using the p -ratio and the eigenvalues of the matrix method predicted four FDM behaviors. These four behaviors can concisely be displayed as combinations of individual stability components separated onto two graphs: one graph for the growth or decay of roundoff error as determined by whether the numerical solution is bounded, and a second graph for showing whether the numerical solution oscillates or not.

In a previous paper (8:29), the basic method used to prove stability was to show decreasing rms and maximum error as functions of time for a given solution of the heat equation. This diagnostic was adopted, but since stability is only a necessary condition for accuracy, this diagnostic can only be used to prove stability, and can not be used to prove a solution is unstable. So if the numeric versus analytic solution errors grow in time, then the solution may or may not be stable with respect to the numerical roundoff errors.

However, since all the methods are unconditionally stable, except for the EX method, these graphs play a minor role in this thesis, and have only been included in Appendix A to show that they are an unreliable stability diagnostic. To implement this diagnostic so that a digital computer could automatically determine the trend of error growth with time, a line was curve fitted, using least squares techniques, to the maximum error versus time at each time step. Finally, if the slope of the fitted line is negative, indicating decreasing error, the FDM is stable at that point on the h - k domain.

Since stability is a concept based on the growth or decay of numerically induced errors and oscillations in time, all nodes for each heat equation solution in the h - k domain were tracked with respect to time. The maximum number of slope changes for any of the single, fixed spatial nodes was counted as the number of oscillations for stability purposes. In addition, spatial oscillations, although not directly predicted by p -ratios or matrix eigenvalues, are graphed. Two reasons for including spatial oscillations exist. One, various texts (13:124; 14:206-207,213) show spatial oscillations when discussing stability, and the danger could occur of associating stability predictions with spatial oscillations in the final solution, as was incorrectly done in a previous paper (8:29). Secondly, oscillations predicted by stability methods in time are, for practical purposes, only really important if they result in spatial oscillations in the final solution. Since the actual solution in a general

partial differential equation could be oscillating, the analytic solution was subtracted from the numerical FDM solution to get the actual number of slope change oscillations with respect to the analytic solution. So, the spatial oscillation graphs display the maximum number of error slope change oscillations in either spatial direction for the two dimensional FDMs.

Lastly, whether a solution oscillates or not is a secondary consideration to the final maximum error in the solution. Also, since the matrix method can even be used to generate functional relationships in the $h-k$ domain that predict when the oscillations are disastrous or not disastrous to the final solution, these predictions must be examined. Therefore, $h-k$ domain graphs of the maximum error of all the node points in the final solution have been included in the analysis. For all error calculations, the error used is the absolute error, defined as: $\text{error} = |U(i,j,n) - T(x,y,t)|$, where U is the numerical solution to the FDM and T is the analytic solution to the partial differential equation.

Reading $h-k$ Domain Graphs

The domain graphs used in this thesis are not conventional, so this section provides the extra information needed to make using the domain graphs easier and more effective. First, two partial differential equation problems were used, one for the one dimensional case, and one for the

two dimensional case. The domains were all chosen to cover the same range in spatial and temporal step sizes, so that the resulting graphs could be compared directly. Logarithmic scales were used on the axes because most of the predicted functional relationships become simple lines on a logarithmic scale. Also, since exact solutions are computed, the h-k domain is made up of a discrete set of step sizes that exactly step through the space and time dimensions in n_x , n_y , and n_t steps. Therefore, the values of the z-axis are actually only computed at discrete points, even though they are shown as a continuum of values. As a result, the contour graphs introduce winding ribbons and waves that are mainly artifacts of the discrete points used. Reference bottom Figure 3, where lines intersect, to see the locations of the 2-D discrete points.

The graphs for both the one and two dimensional transient heat equations FDMs are all three dimensional graphs plotted as two dimensional contour graphs, and are read very much like two dimensional contour maps used in navigation. These graphs can be broken down into just four types, depending on what the z-axis, which is represented by the contour lines, itself represents. These graphs were chosen, because while harder to visualize topography on than three dimensional graphs, they are much easier to use to visualize the predicted functional relationships on than three dimensional graphics. The contour lines can then represent the following: 1) maximum numeric node time oscillations, 2) maximum spatial error oscillations,

3) maximum absolute error in the final solution, and 4) the slope of the maximum absolute error versus time (found in Appendix A). Otherwise, all horizontal and vertical axes are the same for all the graphs, all the h-k domains are the same for each graph, and all the graphs are the same size for ease of use and behavioral comparison. In addition, both the one and two dimensional solutions for each FDM will generally be placed together on a page, also for easy comparison of behavior changes. All the horizontal axes represent the logarithms of the x-steps. In the two dimensional case, the x-step = y-step plane is used for 3 reasons: 1) most FDMs are normally derived for this plane, 2) the same form of h-k domain graph can be used, and 3) it reduces the total number of nodal points to be calculated per domain. All vertical axes represent the logarithms of the time steps, and are exactly the same for both the one and two dimensional graphs.

To actually read a z-axis iso-value, the following should be observed. Contour line numbers increase with increasing values, after any z-axis mapping transforms have been used, of the z-axis. Contour line numbers are always located to the right of their respective contour line. The actual value of the z-axis iso-level line can be obtained by using the following equation:

$$(L\#-SL\#)(Offset)+(Start\ z\ value) \quad (25)$$

where L# is the number of the line you wish to find the z-axis value of, SL# is the number of the line for the starting z value, and Offset is the +/- offset value used for each contour. Once equation (25) has been calculated, the appropriate inverse z-axis transform must be performed. Four z-axis transforms have been used: linear, log10, modlog10, and mod2log10, where:

$$\text{modlog10}(z) = \text{sgn}(z) * \log_{10}(\text{abs}(z) + 1)$$

$$\text{mod2log10}(z) = \text{modlog10}(\log_{10}(z))$$

with mod2log10 only being used for the EX method to display the maximum errors in the final solution, which are all positive z values of extreme dynamic range.

However, it is not the intent of this paper to require careful reading and extraction of values off the contour plots, and they can be used in a much simpler fashion. To simplify reading important information off the contour graphs, two types of contour lines are used, solid and dotted. For oscillation graphs, regions of the h-k domain with solid lines are oscillating and regions of the domain with dotted lines are not oscillating. For maximum error graphs, dotted contour lines show regions where the maximum solution error is less than 10% of the range of the actual analytic solution's values. Therefore, regions of a maximum error graph's h-k domain with dotted lines have maximum errors that are not too disastrous to the final solution. Finally, for the slope of

the maximum error graphs in Appendix A, negative slopes indicate stable regions and are shown as dotted lines, while the stability of solid lines can not be proved using this diagnostic.

Comparison of h-k Domain Graphs with Conventional Graphs

Comparison of the h-k Domain Graphs with conventional graphs is accomplished for two reasons. One, it provides verification of the computer implementations of the FDMs and diagnostics using previous published results. Secondly, it shows how to understand, conventionally, what the h-k domain graphs represent. Figures 4 and 5 show the one dimensional analogs for points on the h-k domain versus conventional graphs, where the number of time steps is 10, and space steps is 14 (using Problem 1 of Chapter 5). For this point in the h-k domain, the diagnostics predict the following values:

FDM	time osc	space osc	max error	slope max error	time	r
1-D IM:	<u>0</u>	<u>1</u>	<u>.0329</u>	<u>-0.206</u>	.25s	4.90
1-D CN:	<u>8</u>	<u>9</u>	<u>.0104</u>	<u>-1.09</u>	.25s	4.90

where the underlined values can be found on Figures 4 and 5.

The 1-D CN method is compared side by side with the 1-D IM method. The IM method is used as a reference since the IM method is known to be non-oscillatory due to its Lo-stability. As seen in Figures 4 and 5, the program correctly identifies

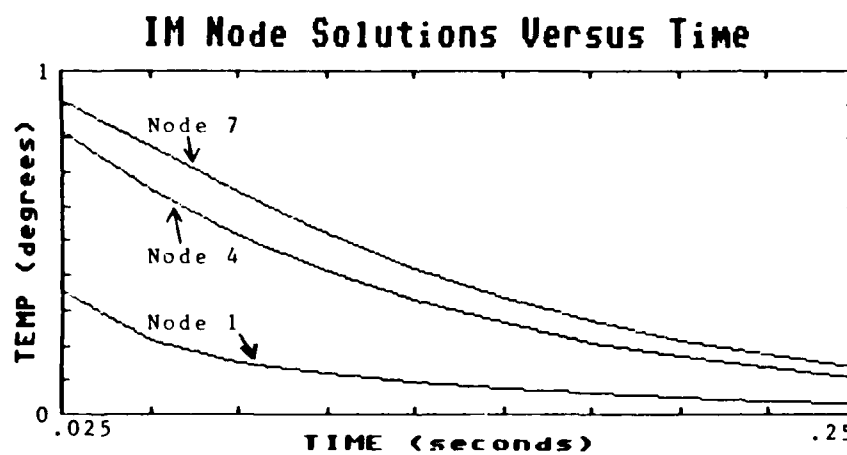
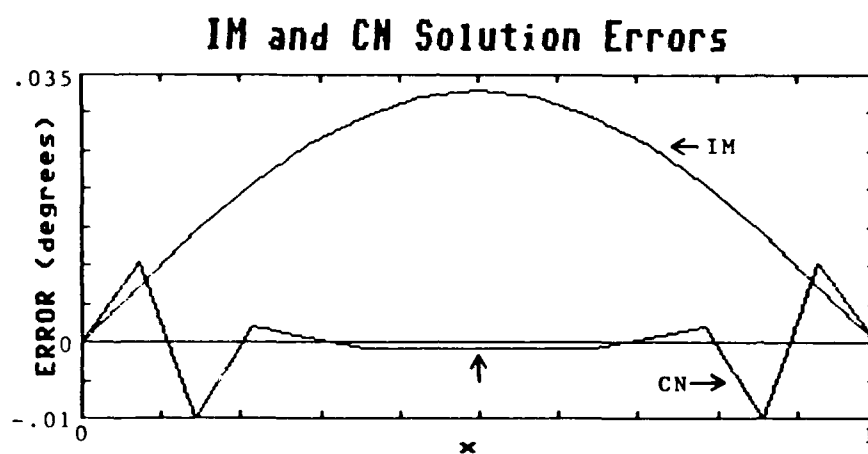
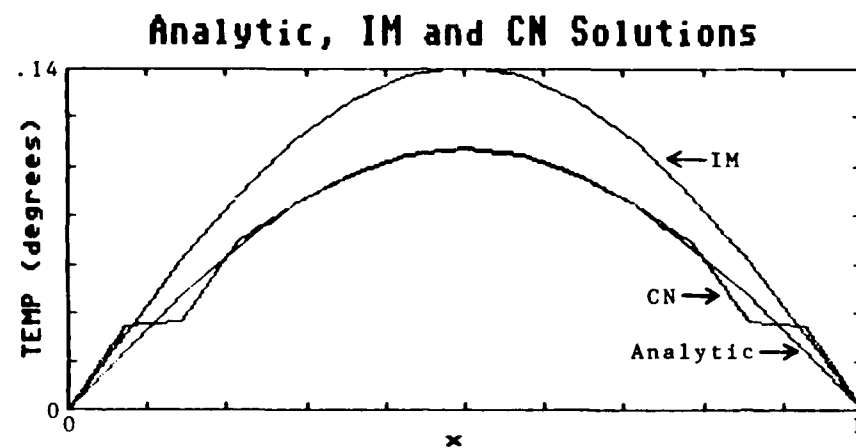
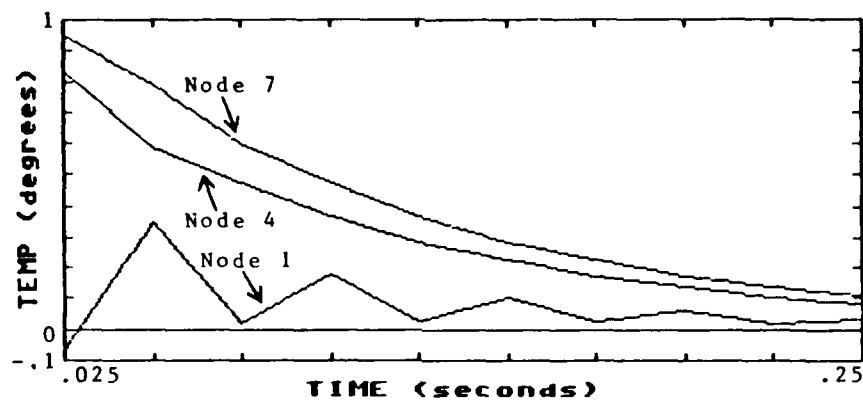
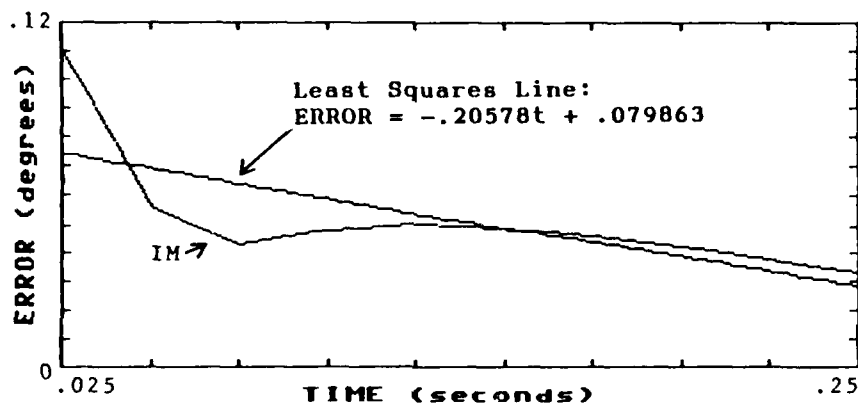


Figure 4. Comparison Graphs for 1-D Cases

CN Node Solutions Versus Time



IM Maximum Error Versus Time



CN Maximum Error Versus Time

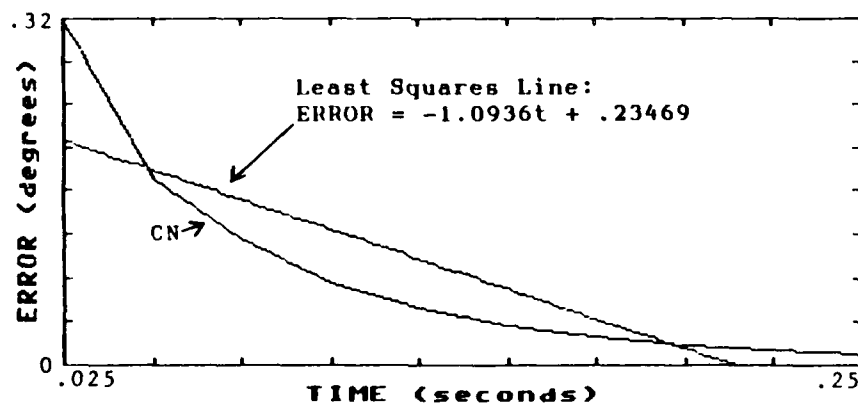


Figure 5. Comparison Graphs for 1-D Cases

the maximum error, the negative slope, and the number of slope changes related to oscillations. Note that the number of spatial oscillations for the CN case is nine, and not the seven easily counted on the graph, since the rise in the center of the graph is too small to be seen.

Figures 6 and 7 use graphs from two previous papers on stability and the programs in this thesis have been used to calculate behavior that should be seen in the graphs (4:23,24; 8:42,46). The results are as follows:

FDM	time osc	space osc	max error	slope max error	time	r
2-D IM:	0	<u>1</u>	<u>8.06</u>	-298	.4s	10.0
2-D ADI:	2	<u>3</u>	<u>10.5</u>	-1058	.4s	10.0
2-D CN:	2	<u>5</u>	<u>148</u>	<u>-425</u>	.4s	10.0
2-D CN:	6	7	4.45	<u>-674</u>	.2s	2.5
2-D DF:	<u>6</u>	1	18.7	-.0707	.2s	1.0

where again, the implicit method provides a reference value, and the underlined values can be found in the figures. Note that the last two sets of numbers are at .2s so that the values can also be read off the appropriate domain graphs in this thesis. These values agree well with the previous thesis graphs. However, the previous thesis graph in Figure 7 only shows the oscillatory behavior in time of one spatial node. Since the point calculated in the h-k domain is the maximum value of all the spatial nodes, the one node graph only shows

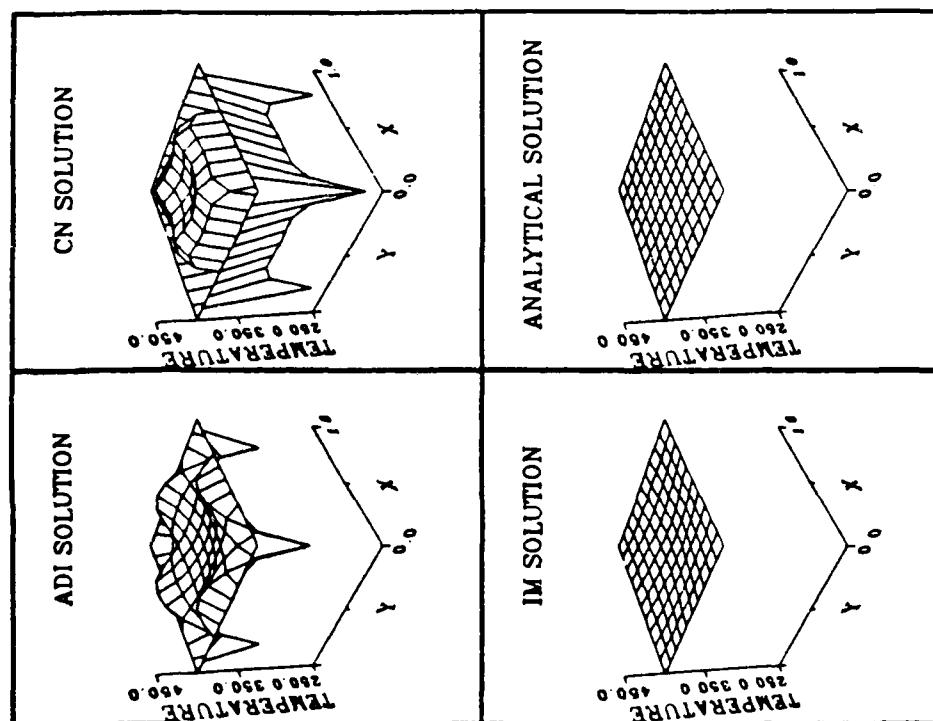


Figure 6. Comparison Graphs for 2-D Cases

Figure 18. Numerical Solutions Problem #2
Time=0.4 $\Delta t=0.1$ $h=0.1$ $r=\Delta t/h=10.0$

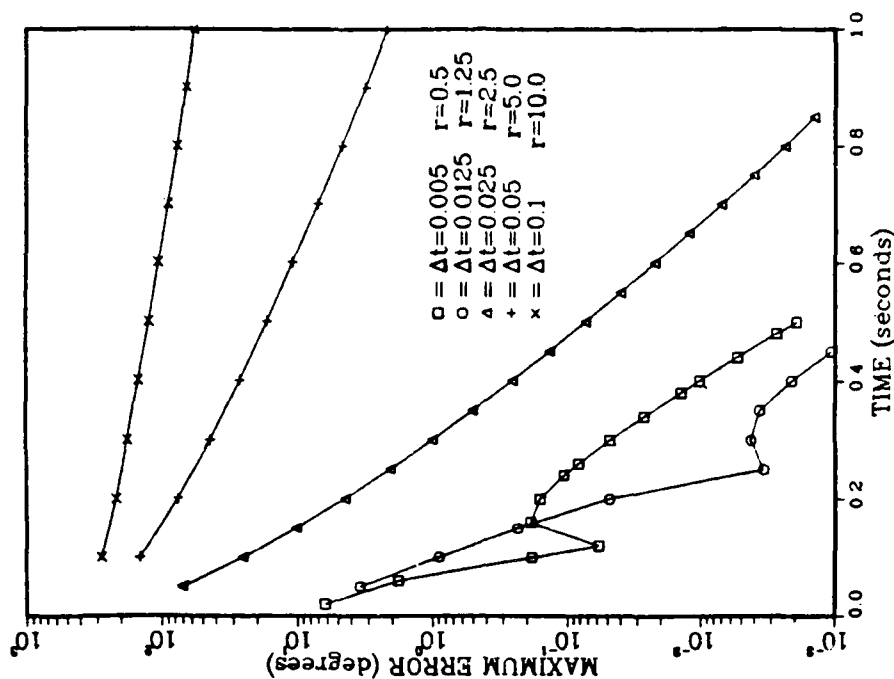


Figure 22. CN Solutions Problem #2 $h=0.1$
Maximum Error vs Time For Various
Values Of r In The Oscillatory Region

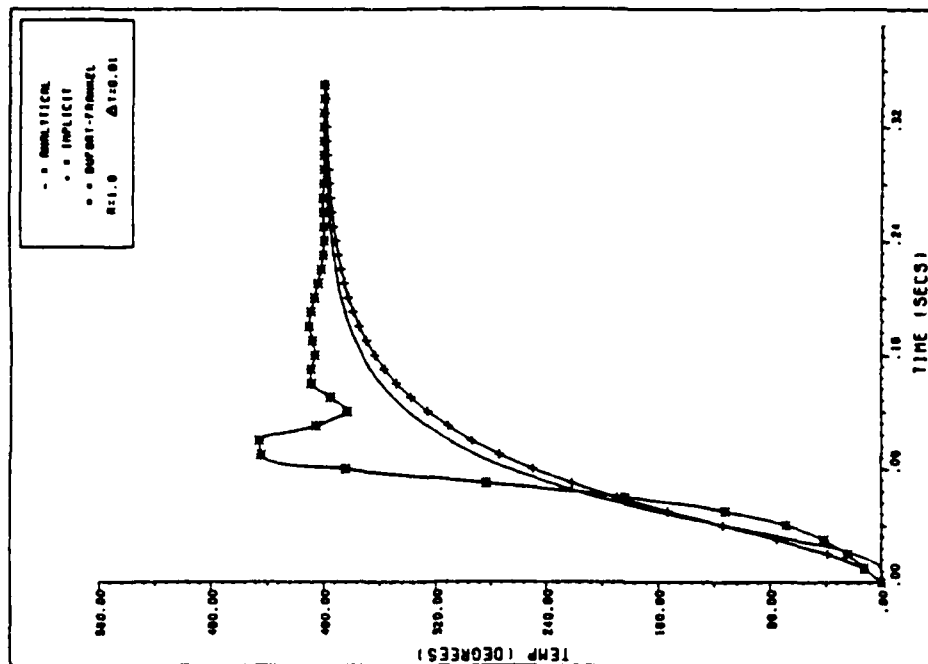


FIG 3. NUMERICAL SOLUTIONS PROBLEM #1 (NODE 41)

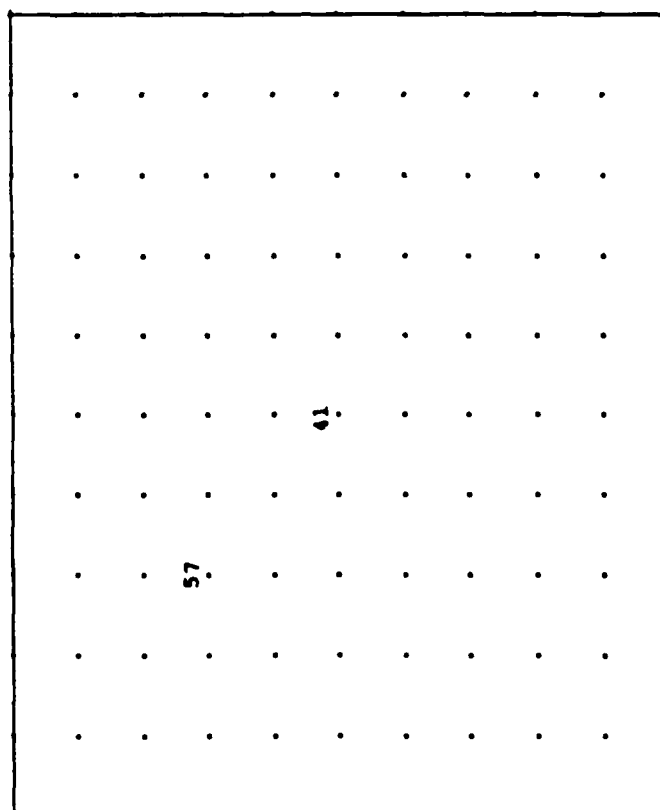


FIG 2. FINITE DIFFERENCE GRID IMPOSED ON A UNIT SQUARE ($H = 0.1$)

Figure 7. Comparison Graphs for 2-D Cases

5 slope change oscillations, and not the maximum value of six. Note that in Figure 6, the CN graph of the maximum error versus time for a fixed solution time and various values of r would trace out a straight line on the h - k domain, and shows the power and versatility of being able to represent several types of line graphs for several types of prediction coefficients on one h - k domain graph. Finally, note that zero time oscillations result from the implicit method, so zero oscillations denotes no time oscillations, yet 1 spatial error oscillation means the solution is not oscillating in space. This apparent contradiction occurs because the solution of the analytic solution has one slope change, and a monotonically decreasing IM solution also has one slope change. Therefore, one slope change is not considered a spatial error oscillation for the analytic problems used in this thesis.

V. Results

This chapter presents the h-k domain graphs generated by using the EX, DF, CN, ADI, and IM methods. These graphs were generated using two sample problems with known analytical solutions. First, the two problems will be examined. Then, the h-k domain graphs will be investigated and the predictions from the coefficient and matrix methods compared with the graphs.

Problem #1

The first problem is used in conjunction with all the one dimensional FDMs, and was used by Smith (13:124) in discussing stability, and is equivalent to problems used by Lawson and Morris (10:1212) and Twizell (14:205-206) in studying stability. The problem is:

$$\begin{aligned}U(x,t)_t &= U(x,t)_{xx} & 0 < x < 1 & \quad t > 0 & \quad \text{satisfying} \\U(0,t) &= U(1,t) = 0 & & \quad t > 0 \\U(0,x) &= 1 & 0 \leq x \leq 1 & \quad t = 0 & \quad \text{and}\end{aligned}$$

so that x varies from $x_1=0$ to $x_2=1$ in length, and time t varies from $t_1=0$ to $t_2=0.25$ in seconds. Partial differentiation of $U(x,t)$ with respect to t and x is denoted, in standard concise notation, by subscripted variables. For

the 1-D CN FDM, t_2 is also set equal to 0.50 seconds to compare the domain graphs at two different final times so that the domains remain constant, but the number of time steps used increases. The general analytic solution is found in Carslaw and Jaeger, and for problem #1 becomes (2:96):

$$U(x,t) = \sum_{n=1}^{\infty} \frac{4}{n\pi} \exp(-n^2\pi^2 t) \sin(n\pi x)$$

$$n = 1, 3, 5, \dots$$

Problem #2

The second problem was used in two previous theses to discover oscillatory behavior and examine the accuracy of the EX, DF, CN, ADI, and IM FDMs (4:19,8:19). The problem is:

$$U(x,y,t)_t = U(x,y,t)_{xx} + U(x,y,t)_{yy} \quad \text{with}$$

$$U(x,0,t) = U(x,1,t) = U(1,y,t) = U(0,y,t) = 400$$

$$U(x,y,0) = 0 \quad \text{where}$$

$$0 < x < 1 \quad \text{and} \quad 0 < y < 1$$

The analytic solution is (8:19-20):

$$U(x,y,t) = 400 (1-f(x,y,t)) \quad \text{where}$$

$$f(x,y,t) = g(x,t) h(y,t) \quad \text{where}$$

$$g(x,t) = \sum_{n=1}^{\infty} \frac{4}{n\pi} \exp(-n^2\pi^2 t) \sin(n\pi x)$$

$$h(y,t) = \sum_{n=1}^{\infty} \frac{4}{n\pi} \exp(-n^2\pi^2 t) \sin(n\pi y)$$

$$n = 1, 3, 5 \dots$$

h-k Domain Graph Solutions

Approximately 25 and 1.6 million total node points were calculated in the 2-D and 1-D problem respectively, in order to calculate each set of FDM domain graphs. The 2-D problem, as was expected from Equations (22) and (23), limited the size of the domains that could be calculated, since the VAX computer could calculate an average of 1.1 million node points per hour. Double precision accuracy was maintained with minimum series term calculations in the analytic solutions. The minimum number of series terms needed at each time step was calculated in the programs based on curve fitted power functions approximating the minimum terms needed versus solution time. Oscillations are given as the number of slope changes and maximum absolute errors are given in degrees. The slope of the maximum error versus time has dimensions of degrees/second (Appendix A). The spatial step size associated with the horizontal axes have units of length, while the vertical axes representing the time step duration have units

of seconds. The specific units for degrees and length, whether °K or °F, meters or feet, will depend on the choice of thermal diffusivity (α), which has a value of 1 for the problems used in this thesis.

Fully Implicit Results

The IM method was included in this study as a reference for comparing the behavior of other FDMs, since it was known to be Lo-stable (14:214). As a result, no IM h-k domain graphs for oscillations have been included, since the entire domains are devoid of contour lines. No contour lines can be drawn because all the points in the h-k domain return 0 as the maximum number of numeric node time oscillations, and 1 as the maximum number of spatial error oscillations.

The IM maximum error graphs show the least influence of an r type functional dependence in the domain. From Figure 8, the accuracy of the IM method appears to depend largely on using smaller time steps, with less dependence on the space step size, once a certain number of space steps has been used.

Fully Explicit Results

The results of the EX method provide easily understood graphs in the h-k domain, and are presented in Figures 9 through 11. The r correlation in the graphs is extremely high, with the solid contour lines representing time oscillations winding back and forth about the $r=0.5$ line for

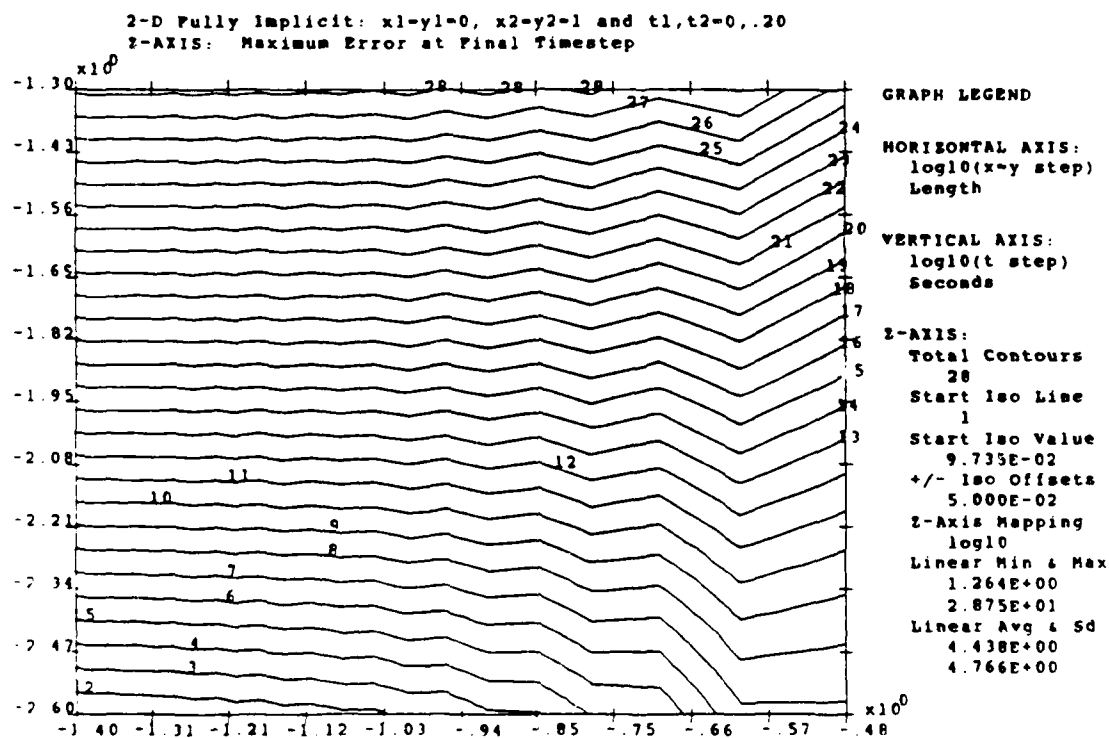
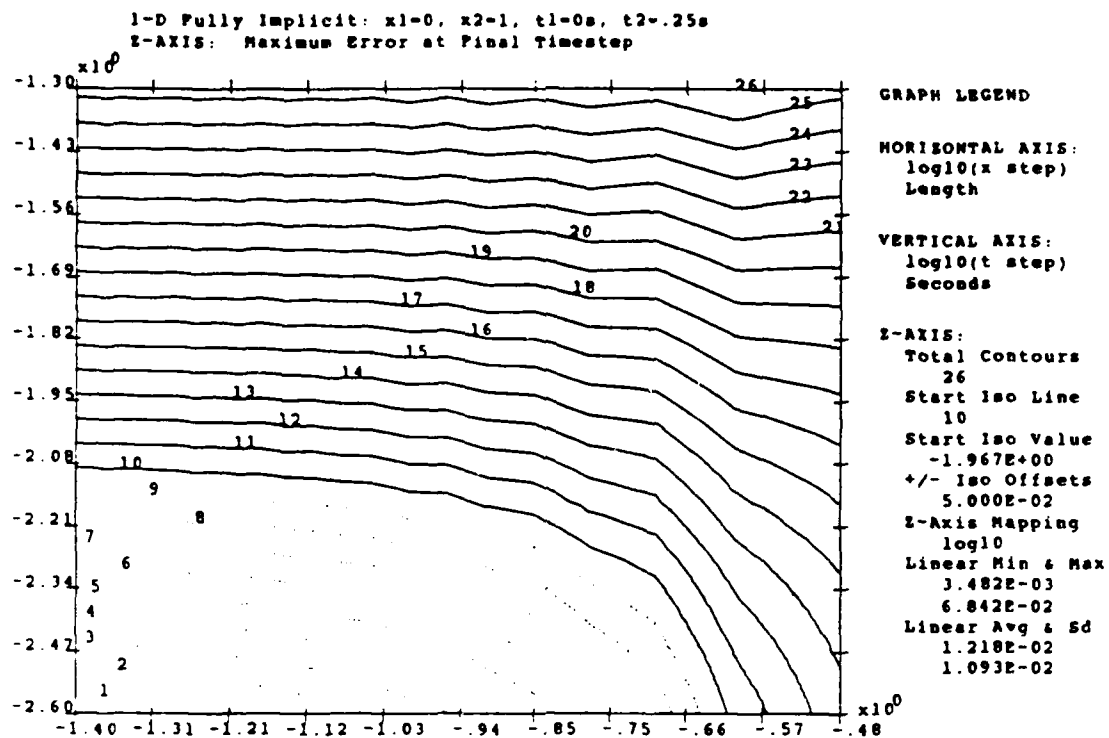


Figure 8. IM Maximum Errors

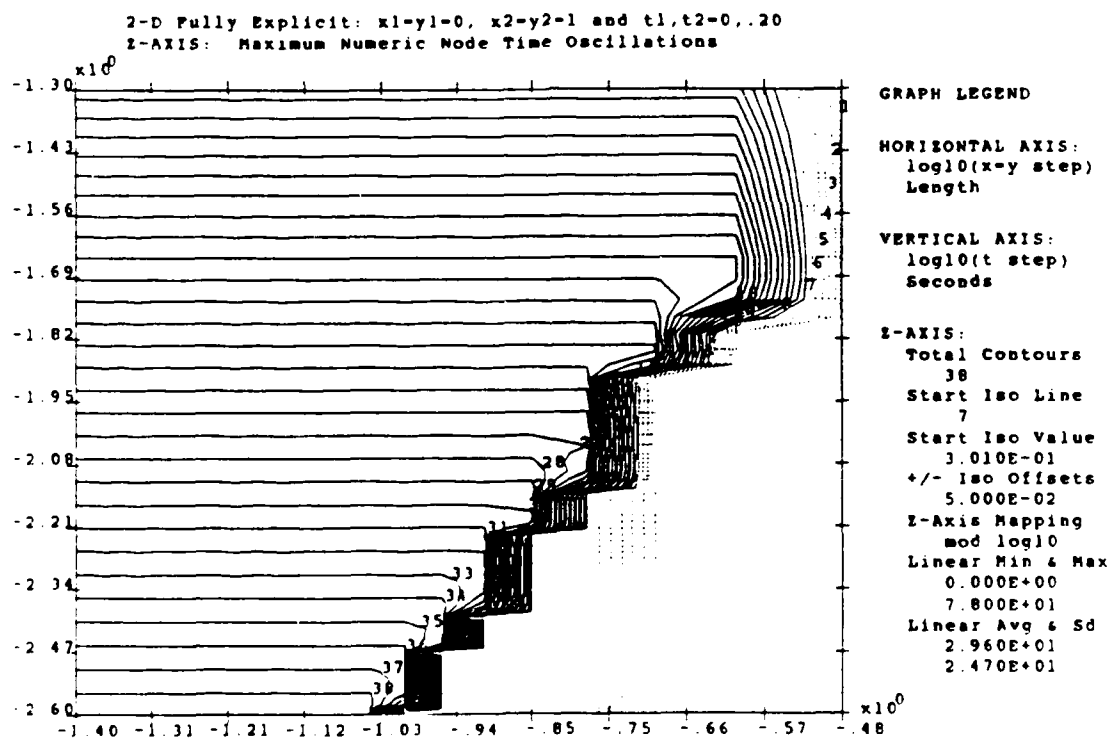
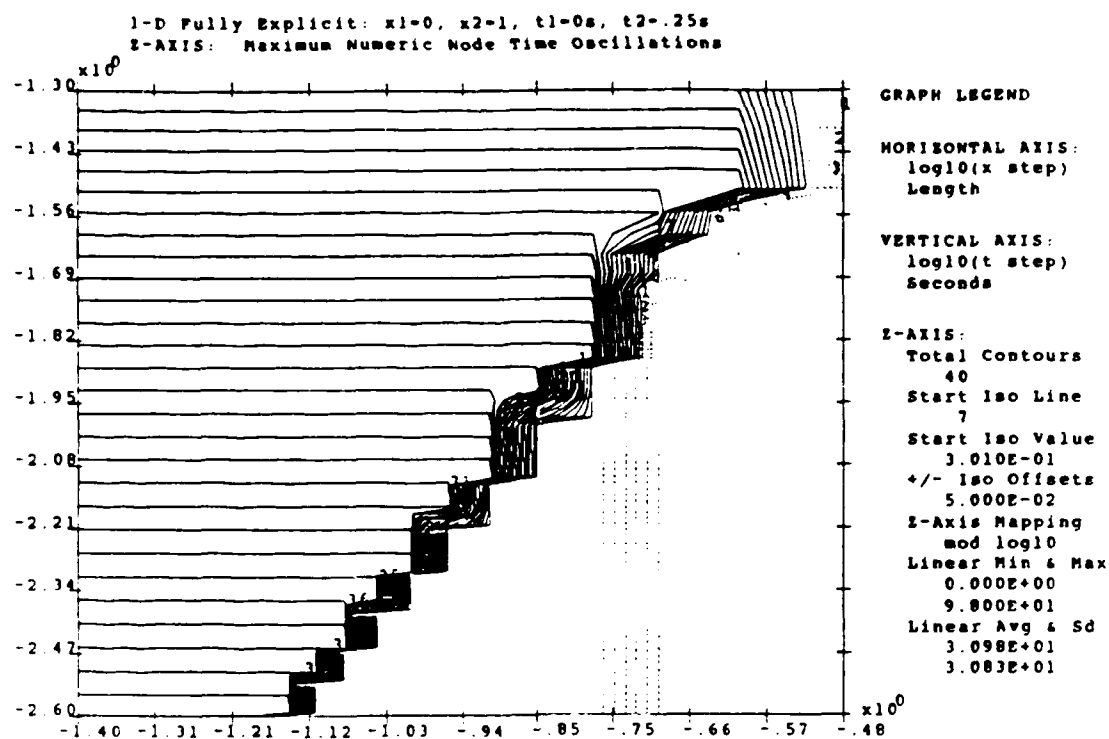


Figure 9. EX Maximum Numeric Time Oscillations

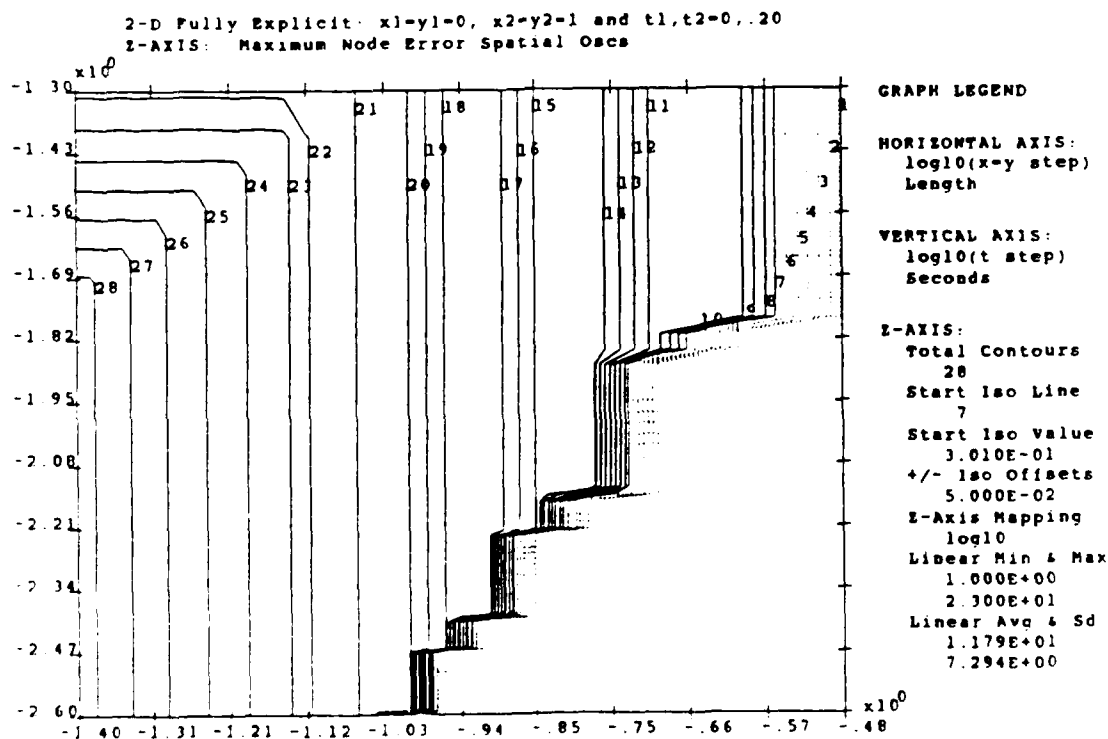
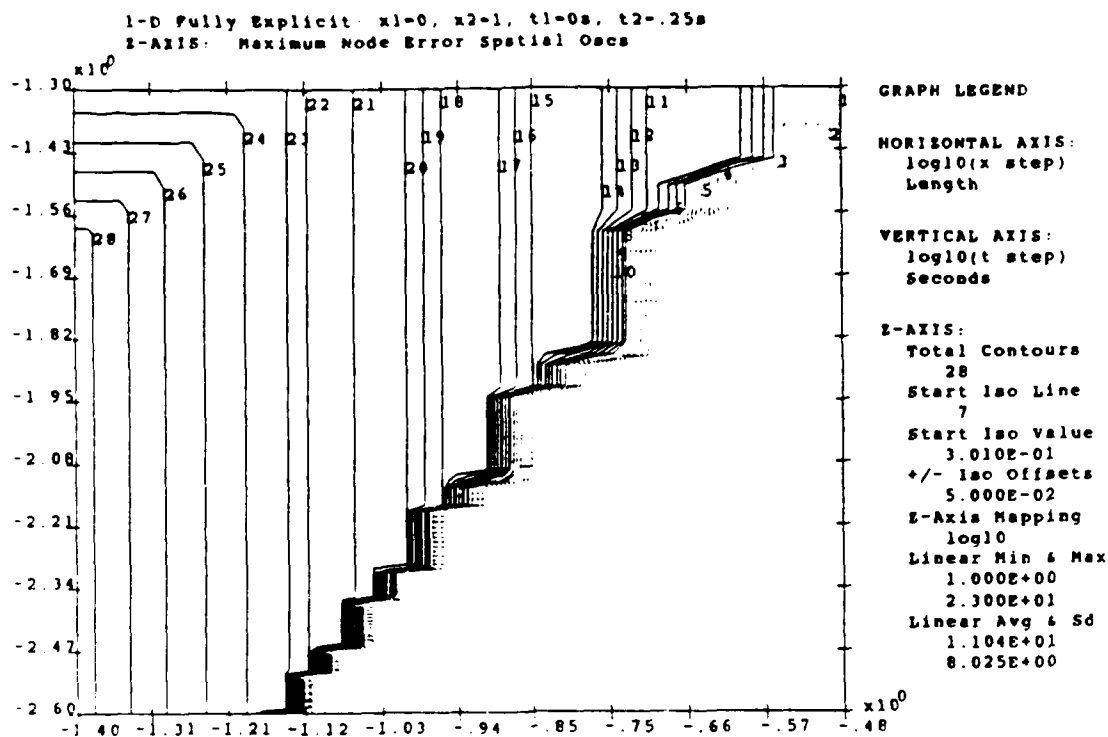


Figure 10. EX Maximum Spatial Error Oscillations

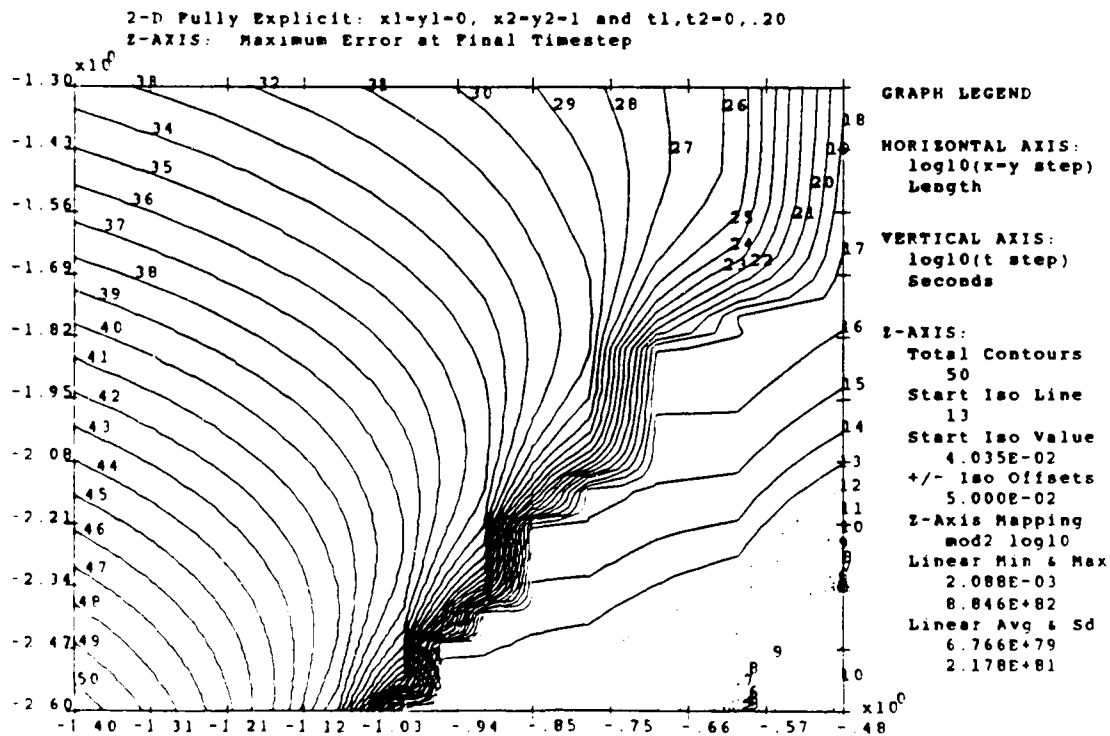
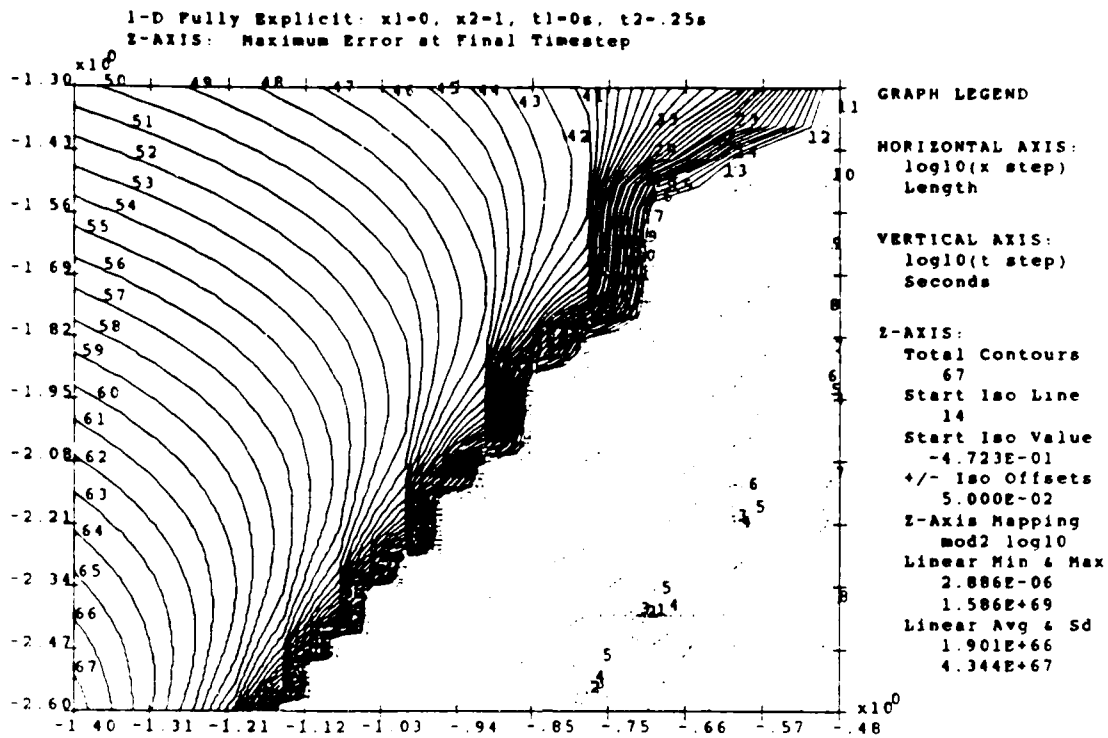


Figure 11. EX Maximum Errors

the 1-D case, and $r=0.25$ for the 2-D case. Note that the discrete winding back and forth of the contour lines appears to be largely an artifact of using discrete solution points (see Figure 3). The best fit r values mentioned above match exactly with the predicted coefficient method values where $r>0.5$ and $r>0.25$ are predicted as regions where time oscillations begin to occur. As a matter of fact, it is seen from Figure 9 that as r increases from the predicted starting values for the oscillations, a sort of turbulent zone is encountered where the number of oscillations increases until it reaches the maximum number of slope changes that the number of time step nodes will allow, and then remains at that maximum, as shown by the horizontal lines reaching to the time axis. Therefore, a line perpendicular to the r lines would show that with increasing r the oscillations also increase until the maximum time oscillations allowed are reached. The matrix method predictions for the start of 1-D and 2-D oscillations are $r>0.25$ and $r>0.125$ respectively. So the matrix method is better at predicting when no oscillations will occur, while the coefficient method appears better at predicting when oscillations start to occur, for these example problems. The actual EX method r variation is small compared to the coefficient predictions, and by itself is not significant enough to discredit the coefficient method as generally valid.

Figure 10 shows the corresponding results for spatial error oscillations. In this case, uncharacteristic of the

rest of the FDMs examined, the spatial oscillations also match the same r values as the time oscillations in Figure 9, so predicted stability oscillations in time correlate well with the actual spatial oscillations in the final solution. Also, the same type of turbulence is seen, but this time the oscillations increase until the maximum number of spatial oscillations is reached, as shown by the vertical lines.

Maximum errors for each solution point are graphed in Figure 11. Once again, these match, uncharacteristically, very closely with the r values observed for the oscillations. Based on the matrix method error predictions for large N , the matrix method is successful at predicting what r lines below which the errors from the oscillations are not disastrous, even when N is only about 3 on the domain graph. This is very good for a first order approximation of the trigonometric functions in the eigenvalues of the amplification matrix.

DuFort-Frankel Results

The DF results involve jump starting the three-level method with three different methods to get the first time level. Both the analytic solution and IM jump starts are graphed for both the 1-D and 2-D cases, and the CN method is used to jump start the 1-D method as well. Figures 12-14 and 15-17 are the results of the analytic solution and IM jump starts, respectively, while Figures 18-19 show the results of using the CN jump start to the DF method.

Z-AXIS: Maximum Numeric Node Time Oscillations



HORIZONTAL AXIS:
log10(x step)
length

VERTICAL AXIS:
log10(t step)
Seconds

```

Z-AXIS:
  Total Contours
    40
  Start Iso Line
    7
  Start Iso Value
    3.010E-01
  +/- Iso Offsets
    5.000E-02
  Z-Axis Mapping
    mod log10
  Linear Min & Max
    0.000E+00
    9.700E+01
  Linear Avg & Sd
    1.558E+01
    2.413E+01

```

Z-AXIS: Maximum Numeric Node Time Oscillations



HORIZONTAL AXIS:
log10(x-y step)
Length

VERTICAL AXIS:
log10(t step)
Seconds

```

Z-AXIS:
  Total Contours
    28
  Start Iso Line
    7
  Start Iso Value
    3.010E-01
  +/- Iso Offsets
    5 000E-02
  Z-Axis Mapping
    mod log10
  Linear Min & Max
    0.000E+00
    2.200E+01
  Linear Avg & Sd
    4.671E+00
    4.905E+00

```

Figure 12. DF Maximum Numeric Time Oscillations,
Analytic Start

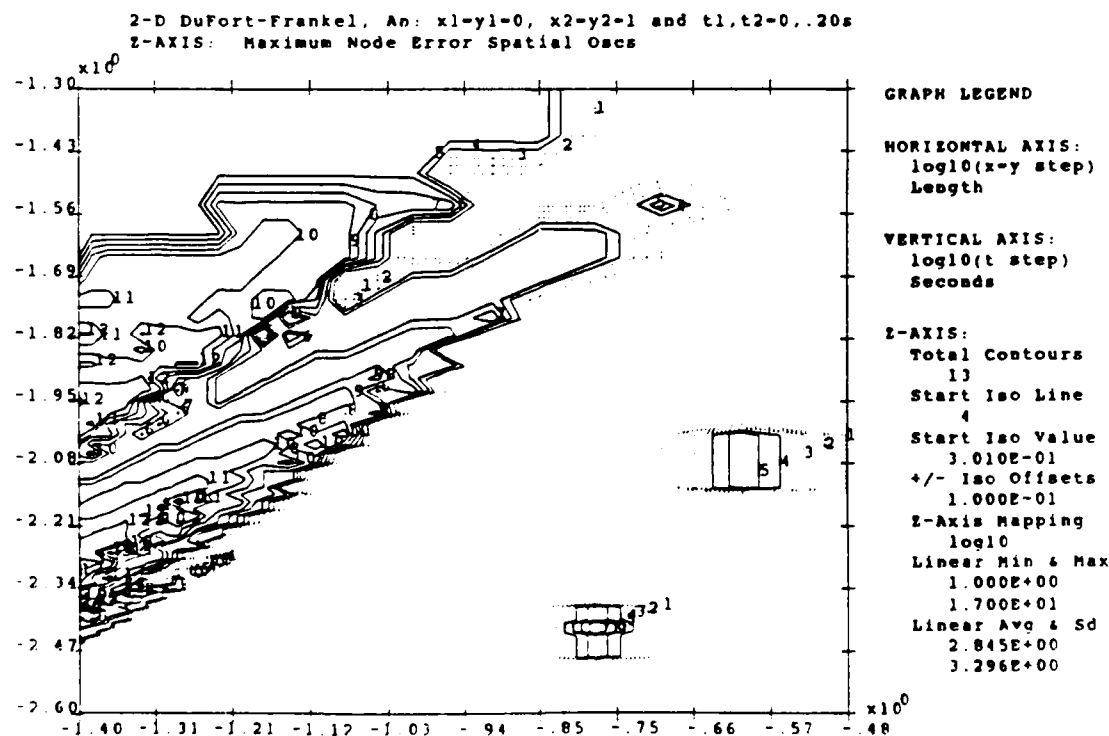
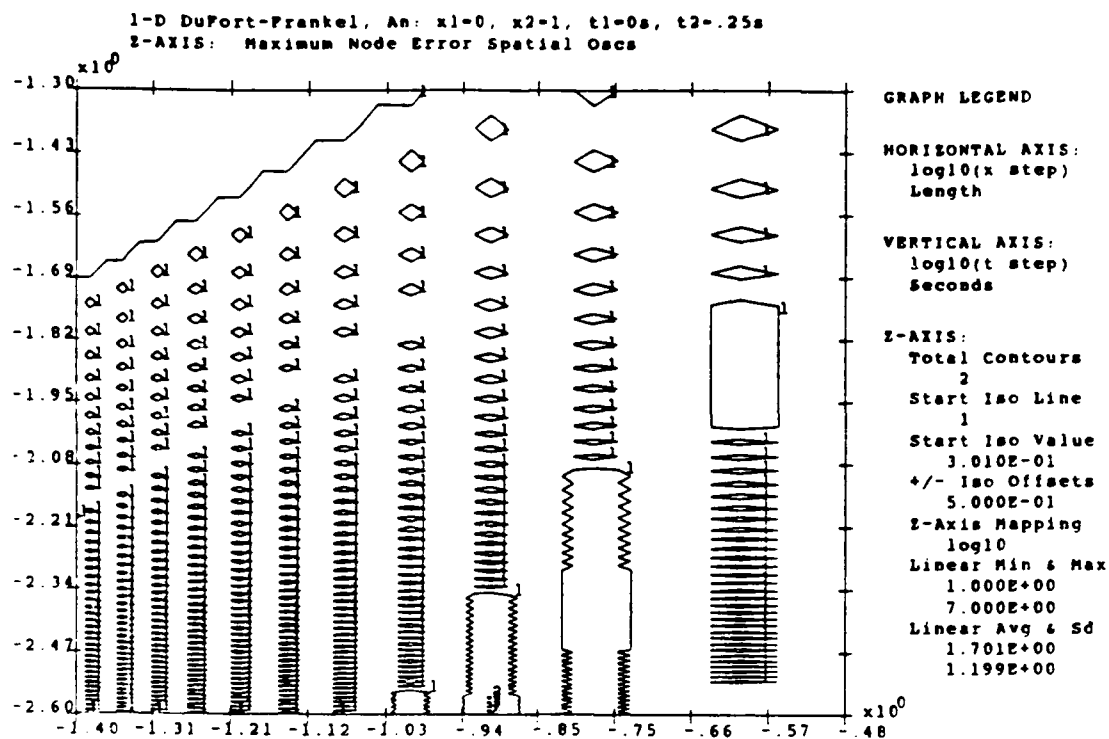


Figure 13. DF Maximum Spatial Error Oscillations, Analytic Start

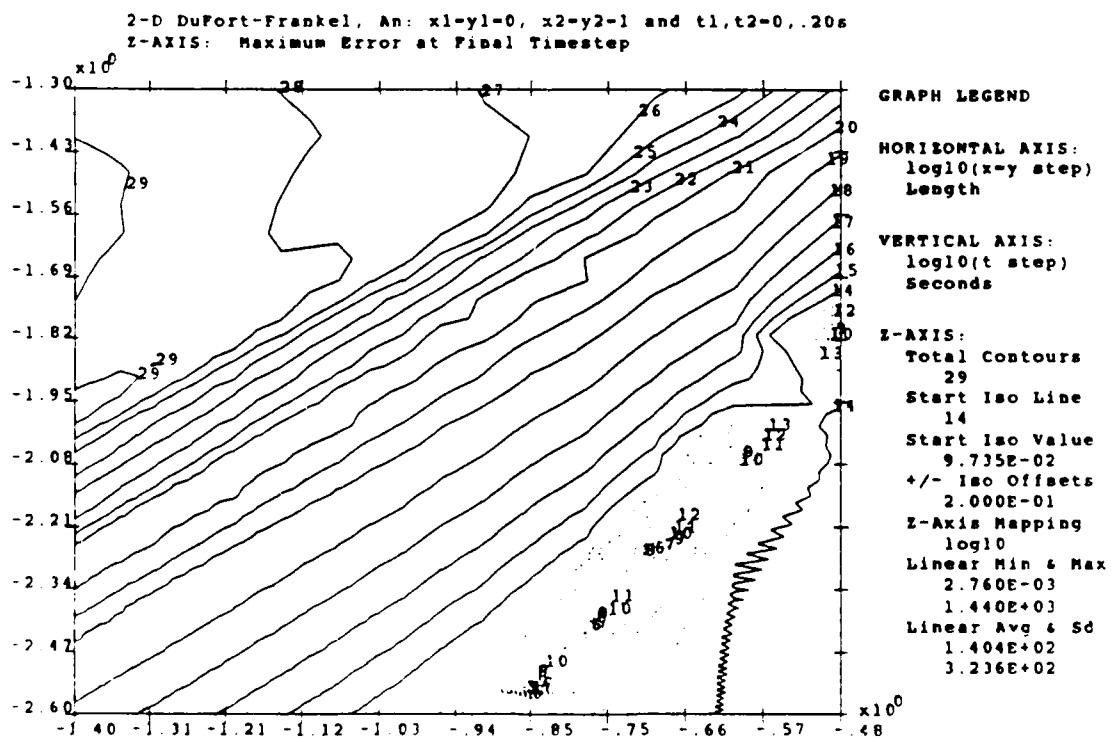
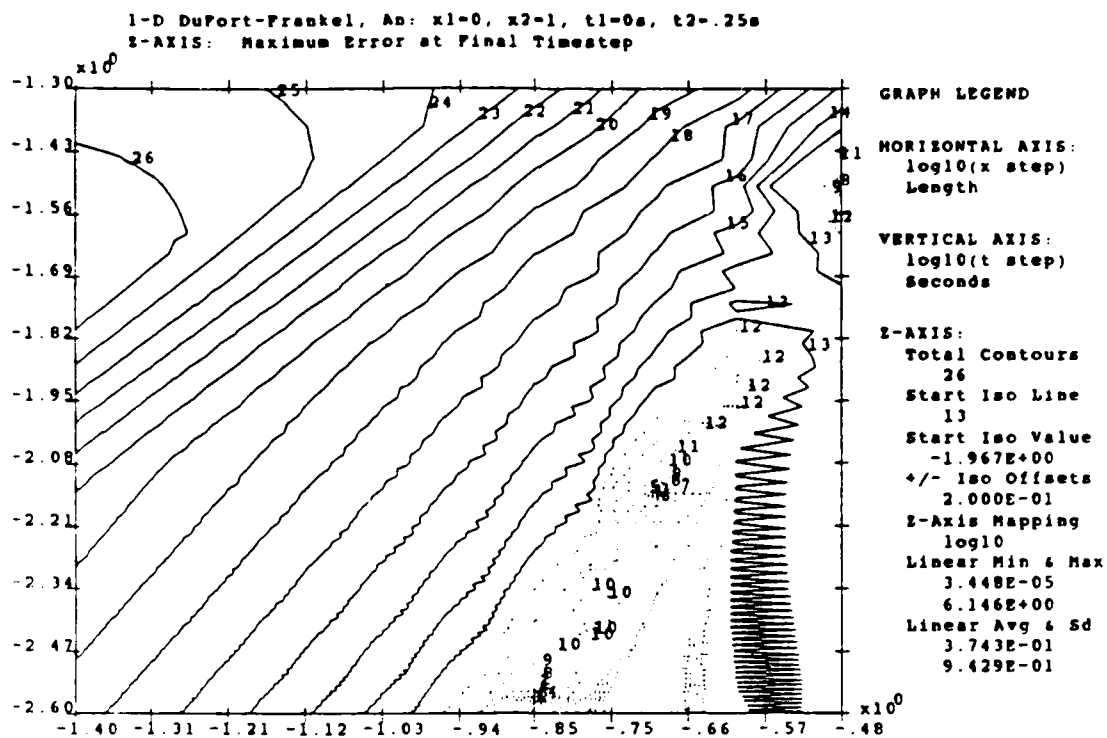


Figure 14. DF Maximum Errors, Analytic Start

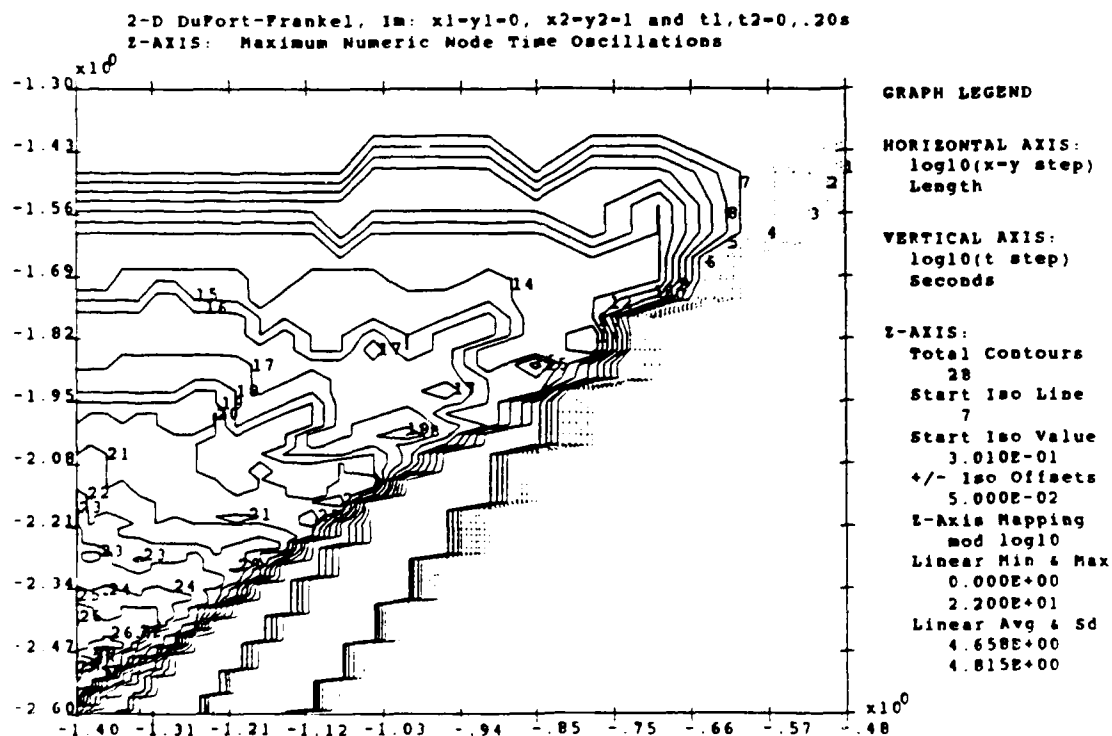
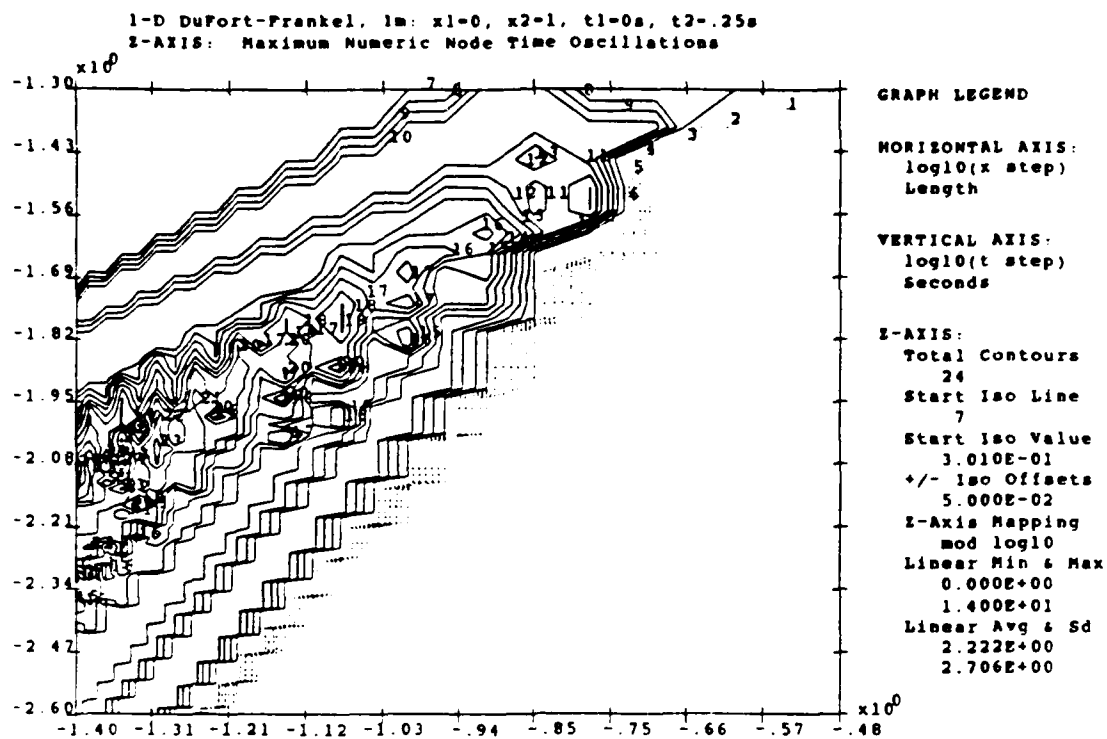


Figure 15. DF Maximum Numeric Time Oscillations, IM Start

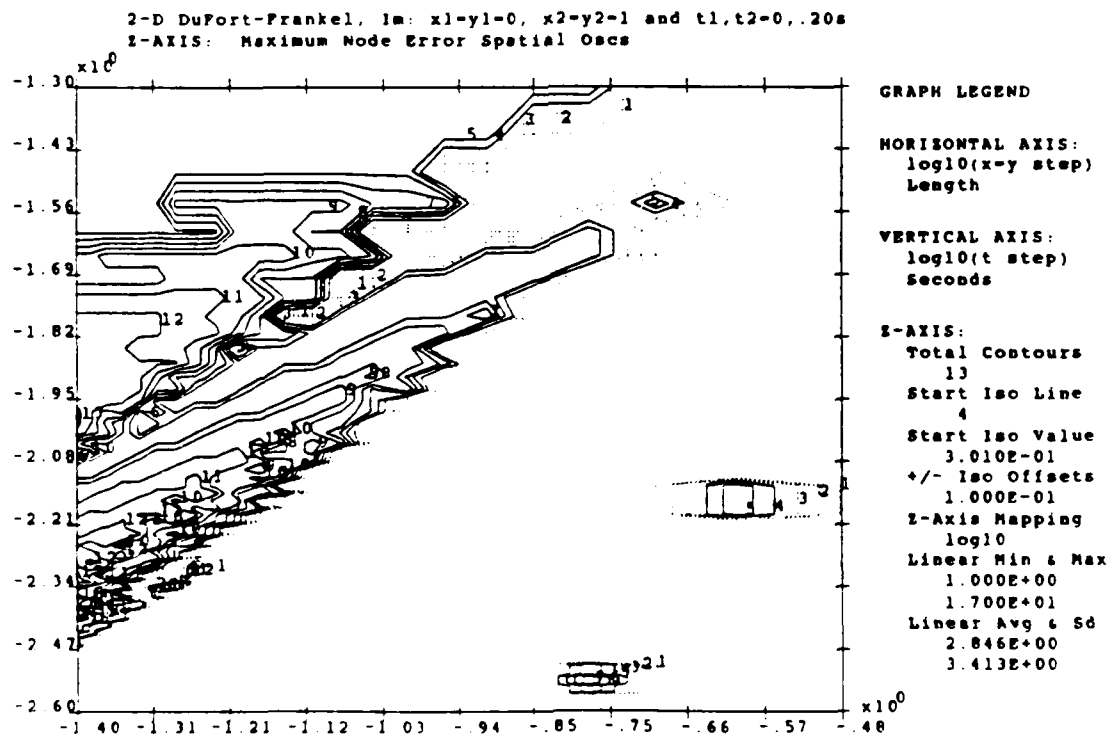
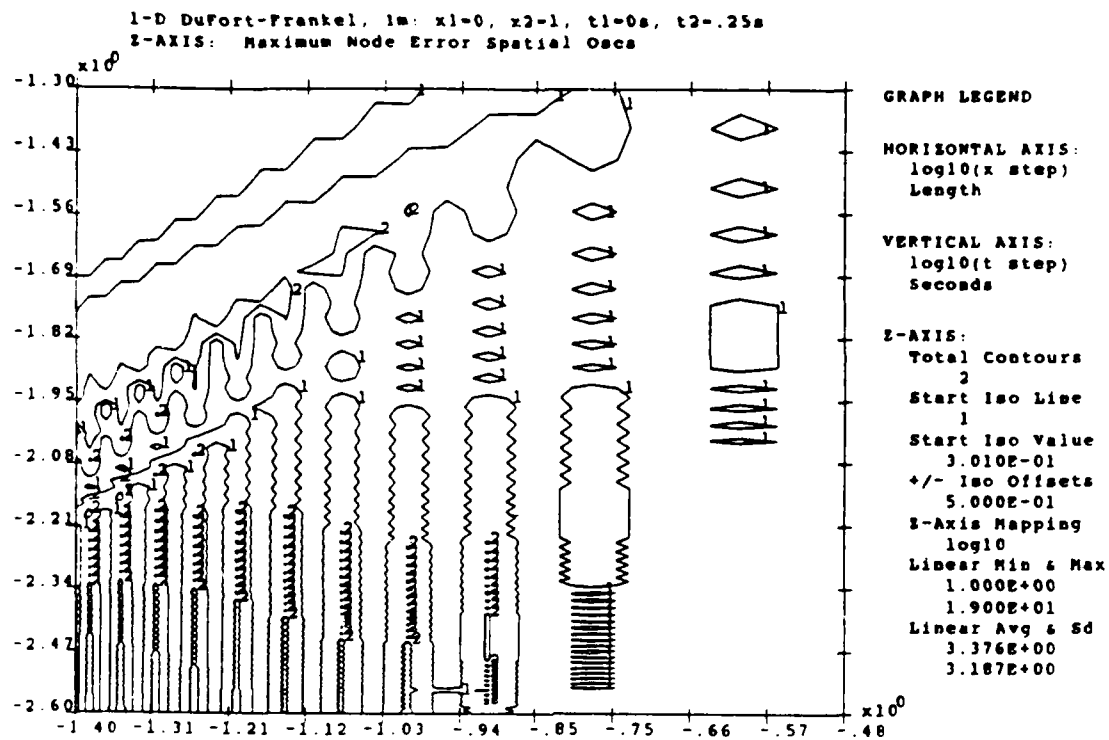


Figure 16. DF Maximum Spatial Error Oscillations, IM Start

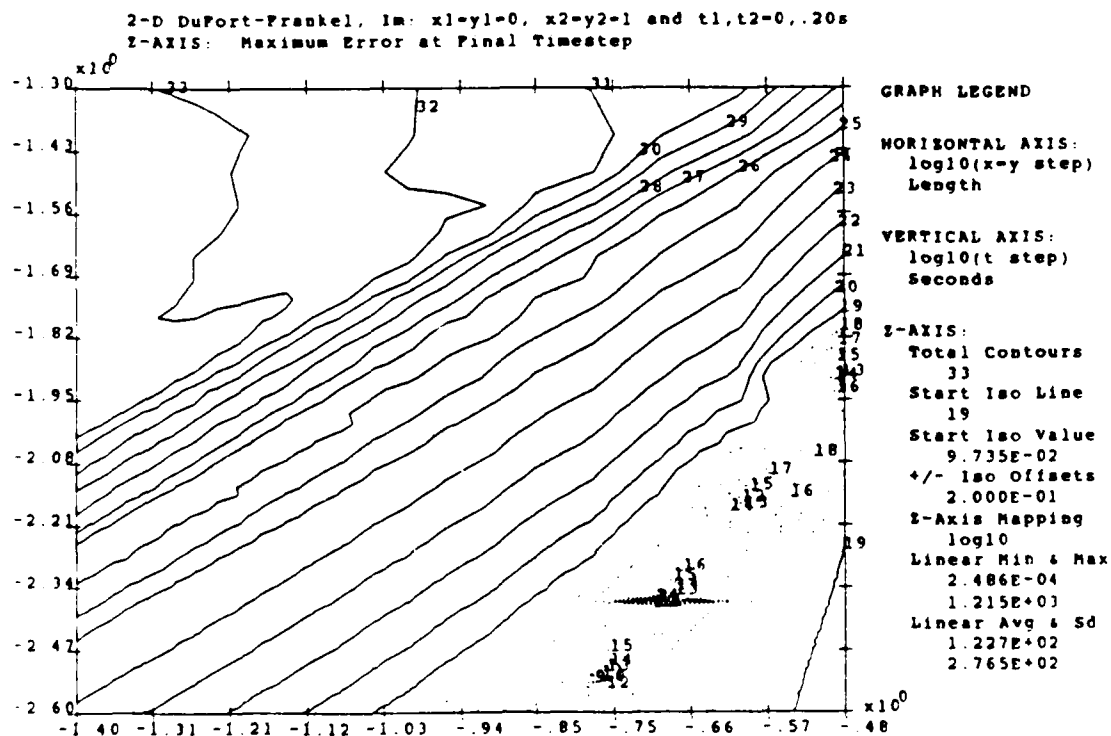
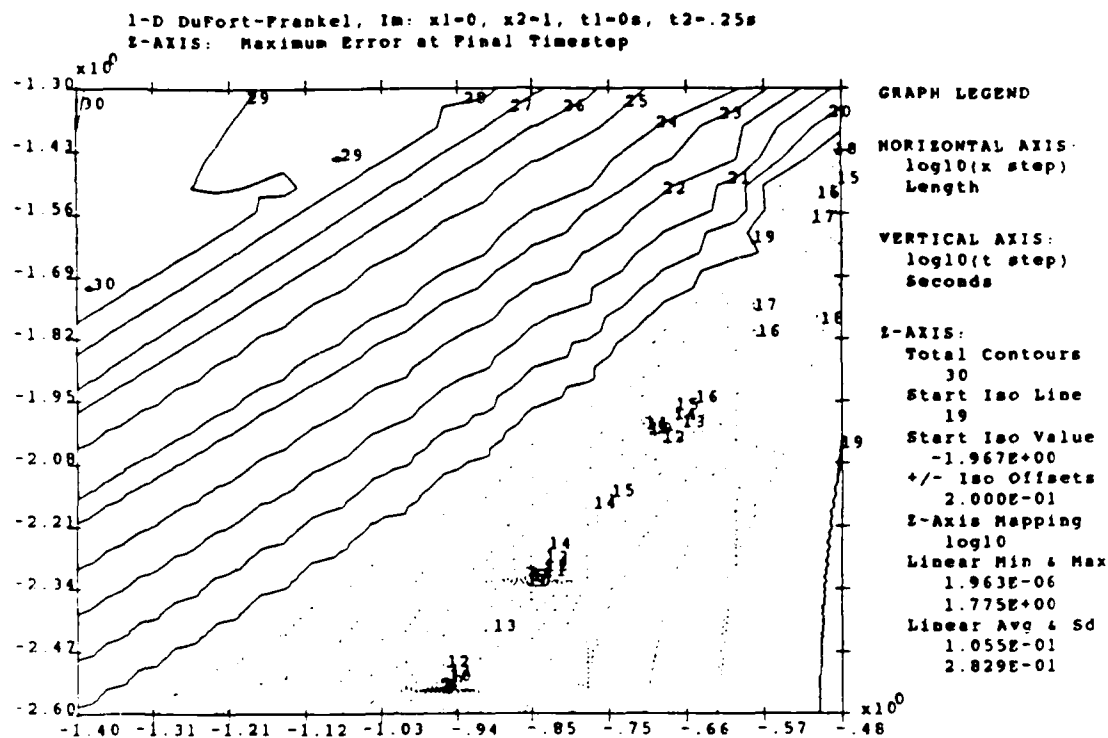


Figure 17. DF Maximum Errors, IM Start

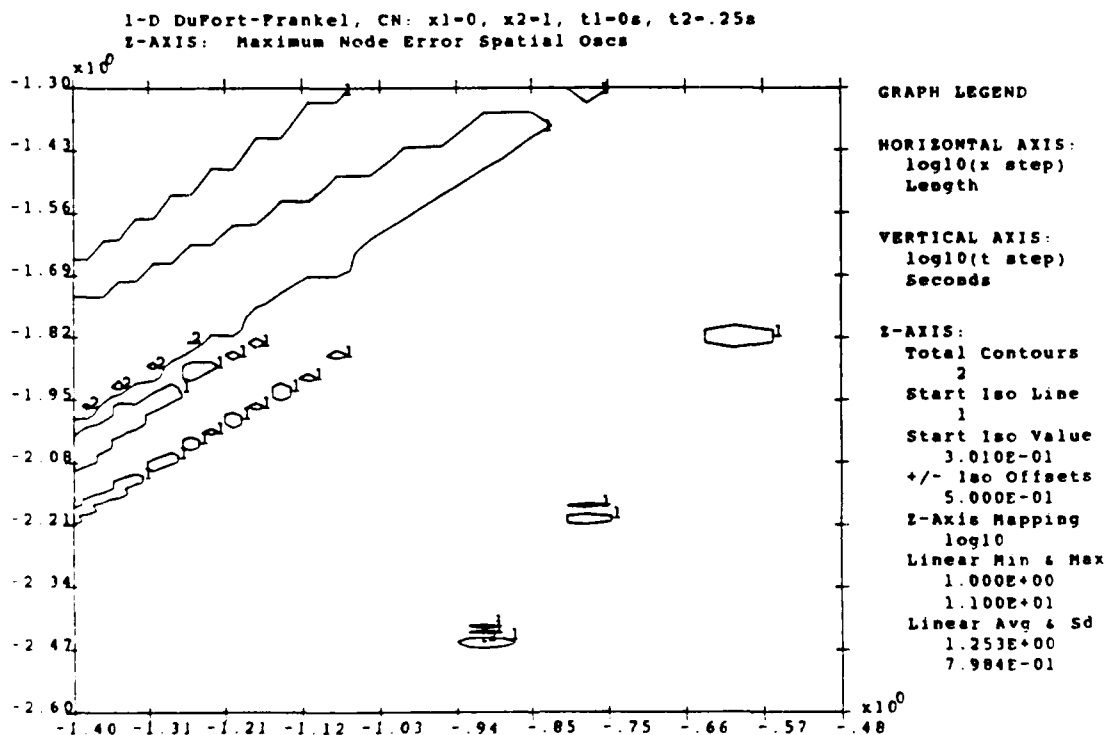
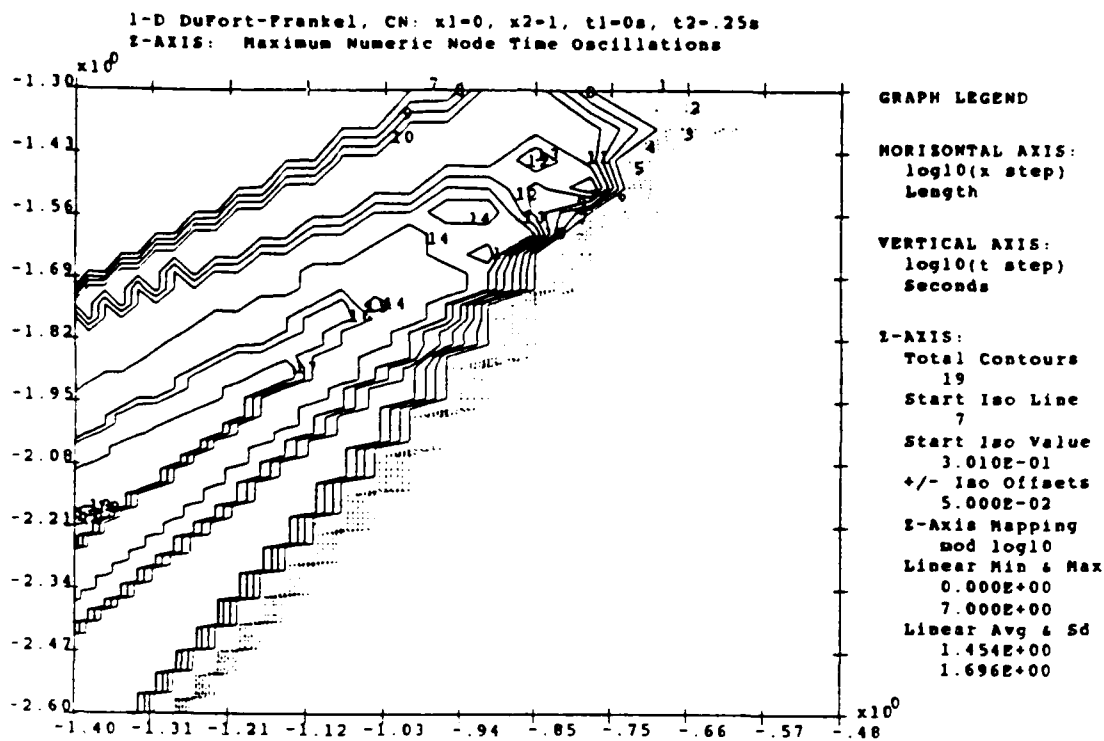


Figure 18. DF Maximum Numeric Time Oscillations, CN Start;
DF Maximum Spatial Error Oscillations, CN Start

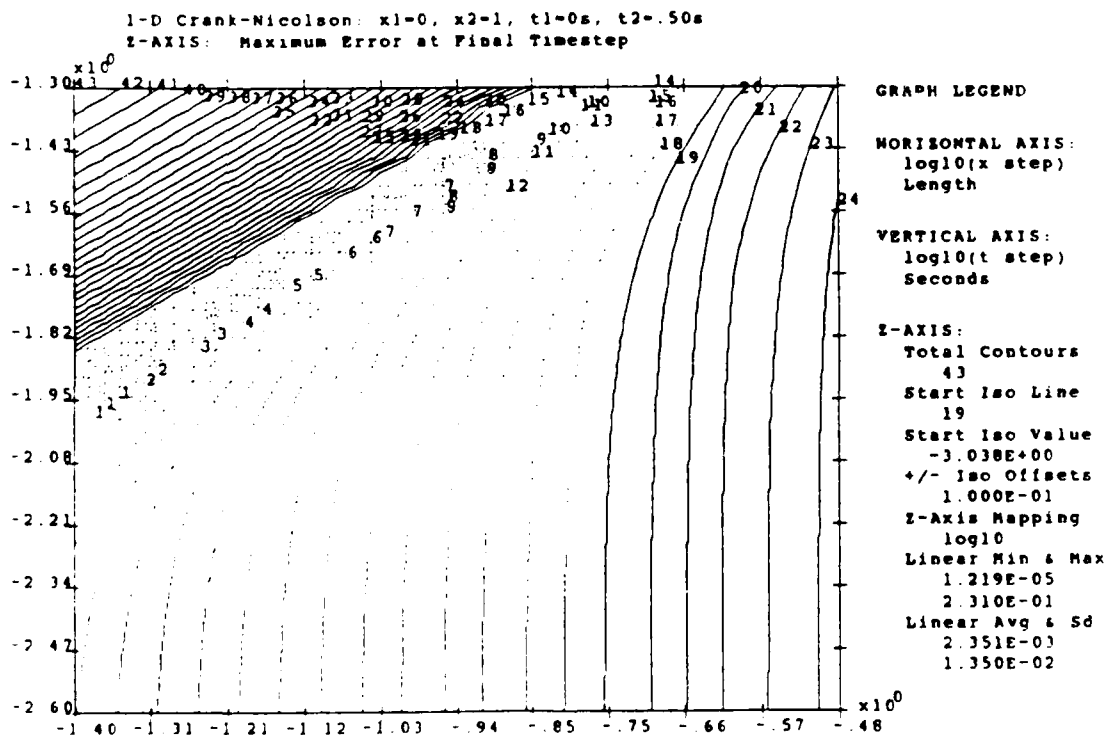
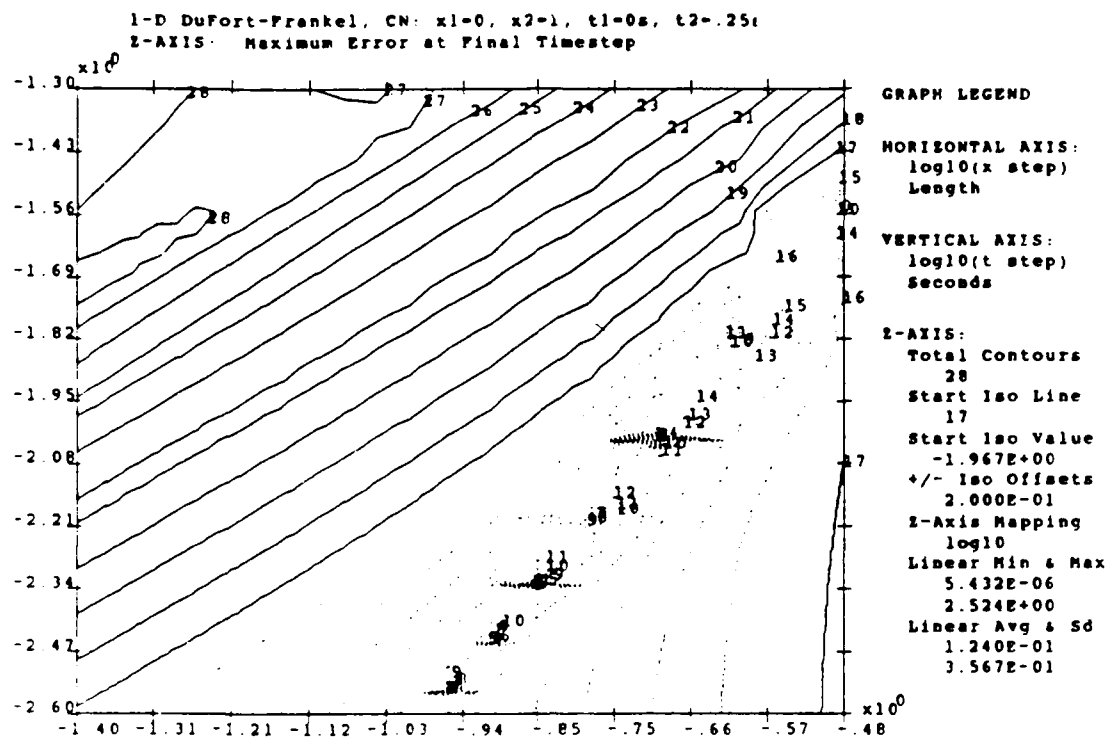


Figure 19. DF Maximum Errors, CN Start, and
 CN Maximum Errors, $t=0.50s$

The time oscillatory behavior displayed by the DF method is much more complex than that of the EX method. However, all the time oscillation graphs show high r correlations in the slopes of the lines best fitting where the oscillations begin. But, unlike the EX method, the number of oscillations at first increases with increasing r values, and then begins to decrease again, and even stops oscillating for larger values of r . This is a remarkable result, and should be looked into in more detail. Unfortunately, the full matrix method eigenvalues are complicated, even for the 1-D case, since for values of r greater than about 0.5, the eigenvalues generally become complex valued. Due to the complex eigenvalues of the amplification matrix for the 1-D and 2-D DF, a complete analysis of the DF method was not completed. Furthermore, complications can arise when h is approximately equal to k because "the computed solution may involve waves associated with the hyperbolic character of the PDE (4.4.3), with which it is consistent" (9:167). This hyperbolic wave region of the h - k domain also includes the region observed to have temporal and spatial oscillations decreasing to zero. Waves in the jump start solution may also be the reason that the CN jump start has the lowest resulting oscillatory behavior. The reason for this behavior needs further study, since the observed behavior would be expected to be just the opposite, with the analytic having the least, the IM more, and the CN jump start the most oscillations for the same h - k domain. However, since the errors for such large values of r are

generally increasing, even though no oscillations may be occurring, the solutions are unusable. In fact, the solutions are about 2 orders of magnitude worse than the IM method, which doesn't oscillate in high r regions either.

For the 1-D and 2-D DF, the coefficient method predicted $r > 0.5$ and $r > 0.25$ respectively, for the start of oscillatory behavior. The domain graphs show that the actual values of r are between 0.50 to 1.0 and between 0.25 and 0.50 for the 1-D and 2-D results respectively. However, the analytic 1-D jump start takes exception, with the major r correlation best fit line for the start of oscillations falling at slightly less than $r = 0.5$. Also, for the 1-D CN jump start, the best fit r line moves to about $r = 1.0$. As such, the coefficient method predicted behavior is generally good at predicting when the oscillations do not occur, but doesn't do as well as predicting where the oscillations actually begin. This is expected, since for any given test problems, the behavior of the FDM should be better and not worse than the worst predicted behavior. Finally, the coefficient method is inadequate as a tool for explaining any of the complex behavior seen in the DF, while the matrix method may provide some insights.

The spatial oscillations for the DF generally have a more linear power function form, since they have less slope than the r coefficient lines designating the start of oscillations. Two other results are worth noting. One, the 1-D case for the

analytic and IM jump starts oscillate spatially throughout most of the domain, except in the high r region where h is approximately equal to k . Secondly, the 1-D DF CN jump start and both of the 2-D DF jump starts exhibit a more linear functional constraint on where oscillations start. Plus, the domain graphs look similar, with low peaks of oscillations occurring at locations in the domain containing least maximum error potholes. This is suspicious of a lack of accuracy and precision, or both, creating artificial error oscillations in the final solution. None the less, it seems these are actually oscillations. Because the smallest maximum errors in the domain involve 5 to 7 digits of precision, while the program should be accurate to at least 10 digits of precision, neither accuracy nor precision seem to be the cause. Regardless, the oscillations occur at minimum potholes of the maximum error, and can be completely ignored from a practical engineering standpoint. Concluding spatial oscillations, the correlation between time oscillations predicted by stability and actual spatial oscillations is shown to be a poor one, and that spatial oscillations should not be used to validate stability oscillation predictions, as is often inferred.

The maximum error domain graphs show that the least errors in the domain generally lie in valleys with high r correlations, where water would flow from the domain if it were three dimensional, and with the r coefficient becoming more linear as the 10% solid contour lines are reached. The valleys for the 1-D DF are approximately centered between

$r=1/8$ to $1/2$ ($1/4$ average) for the 1-D cases, and between $r=1/16$ to $1/4$ ($1/8$ average) for the 2-D cases. The analytic jump starts resulted in the smallest, most severe, r values.

Crank-Nicolson Results

Figures 21-23 show the standard problems at the standard times for the one and two dimensional cases. Figures 19-20 also show the 1-D CN results, but at a final solution time of 0.50 seconds, instead of the standard 0.25 seconds. This was done to see if the characteristics of the domain graphs would change, and they did not. The similar characteristics for the different times were expected. Since the domains were kept constant, the predictions remained constant as well. The only major variation was that the time=0.50 second domains required using twice as many time steps to create the same domain graph. Therefore the maximum number of time oscillations that can be supported by the nodes also doubled, increasing the turbulent zone area required to reach maximum time oscillations slightly, but still starting at exactly the same r value centered at $r=2.0$. Whereas the spatial oscillation line is parallel for both times, it become less constraining and moved up higher in the domain for the $t=0.50$ second case. The domain itself supports about the same number of spatial oscillations, though a slight decrease was observed. The 10% maximum error line falls exactly in the same place for both cases. However, the valley (again where water would flow) of

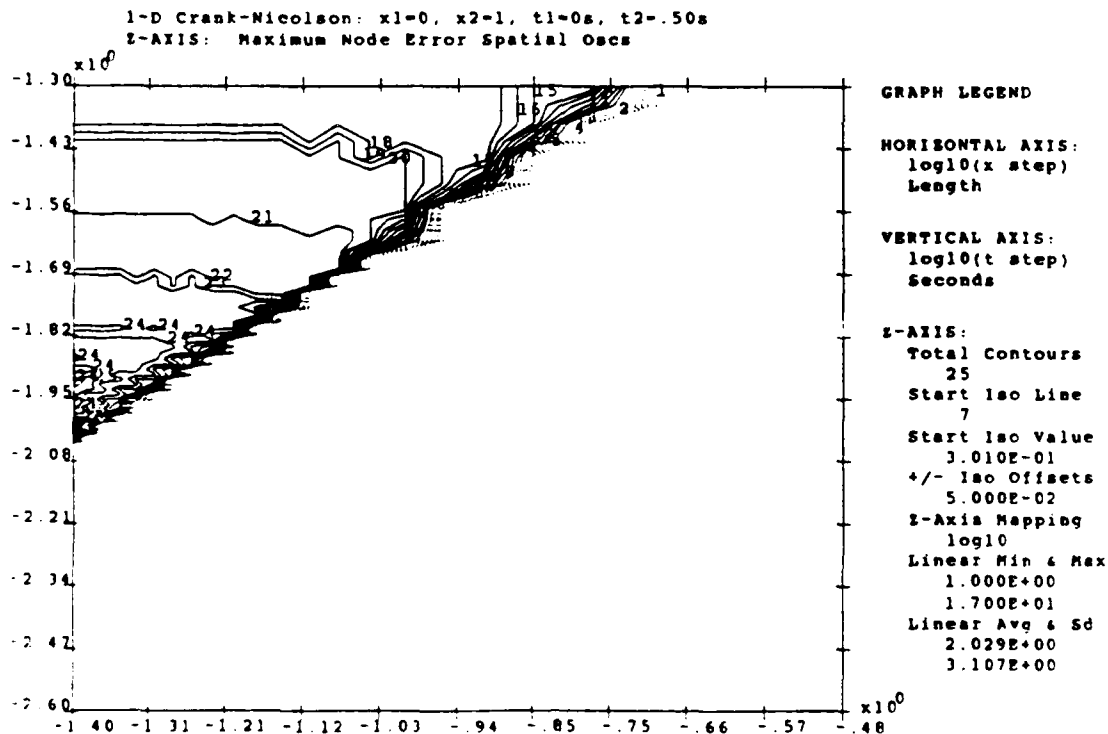
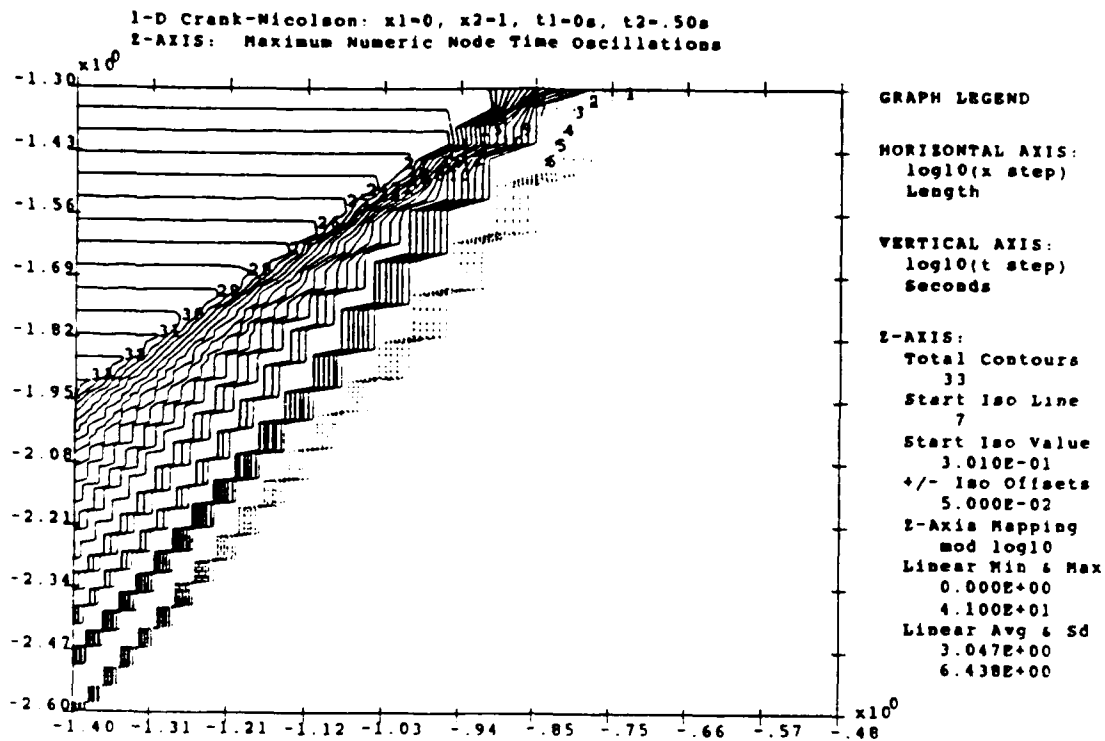


Figure 20. CN Maximum Numeric Time Oscillations, $t=0.50$ s;
CN Maximum Spatial Error Oscillations, $t=0.50$ s

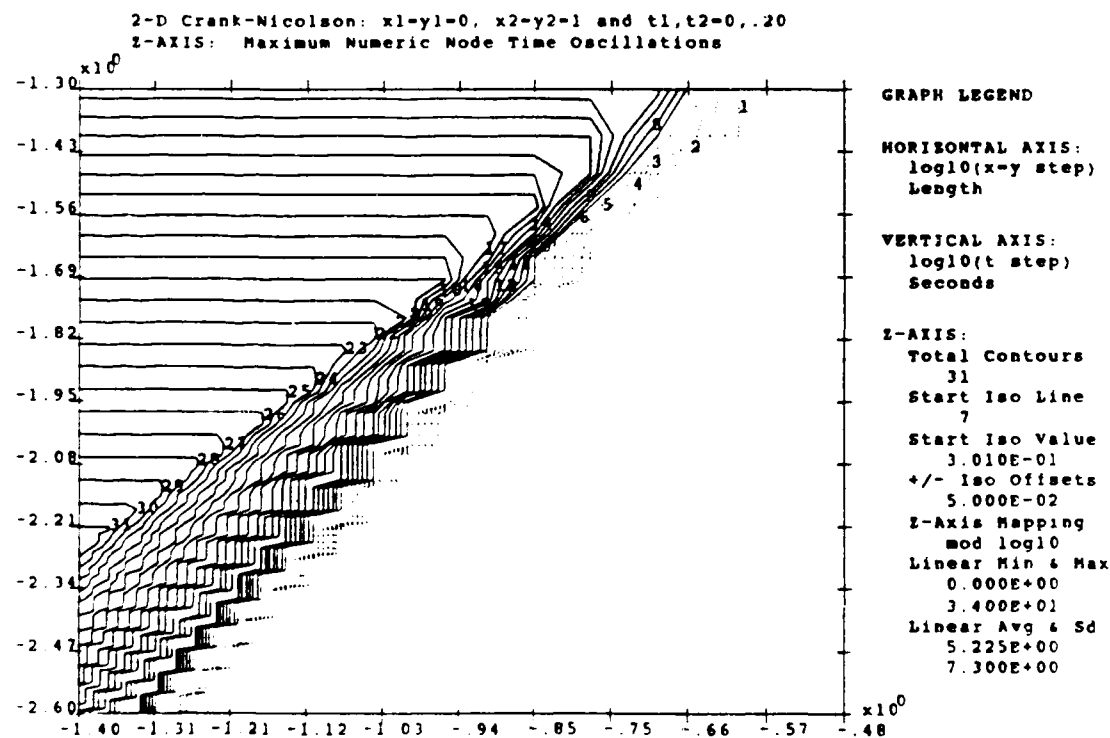
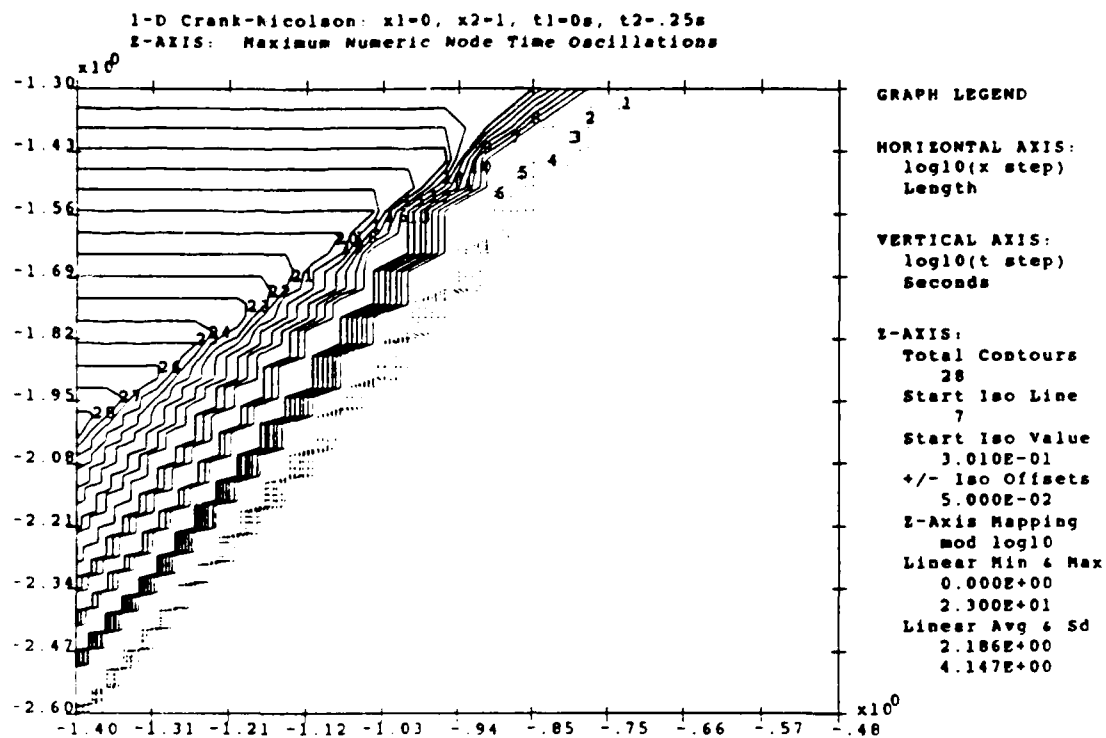


Figure 21. CN Maximum Numeric Time Oscillations

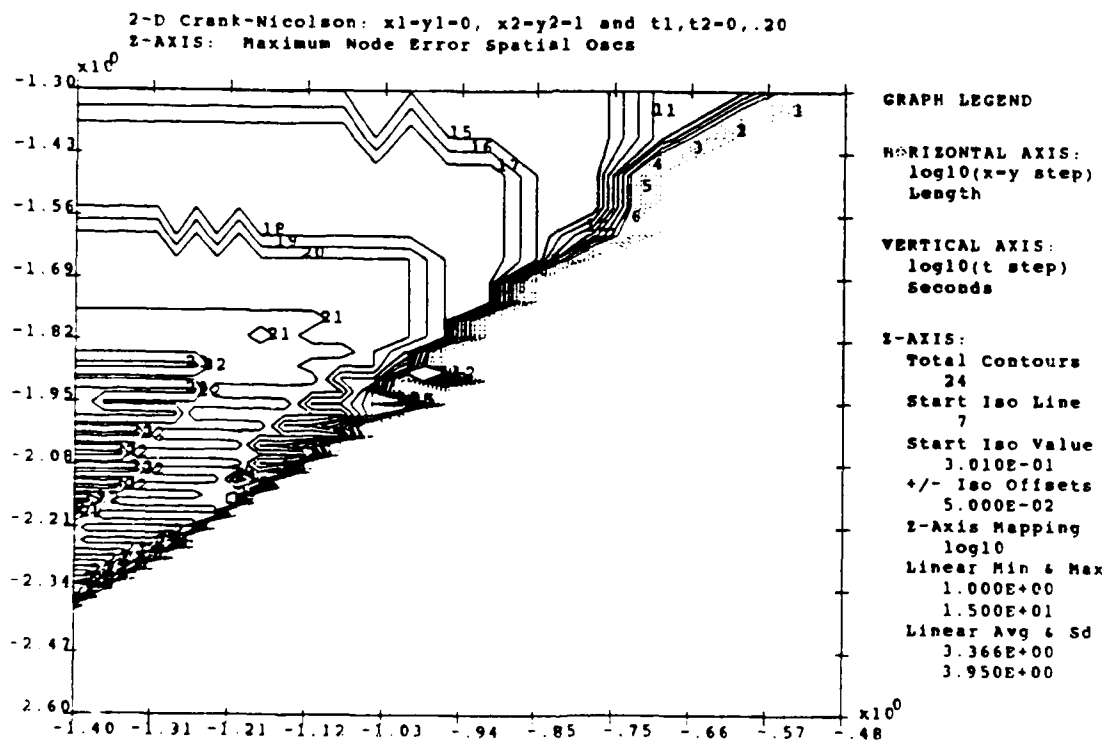
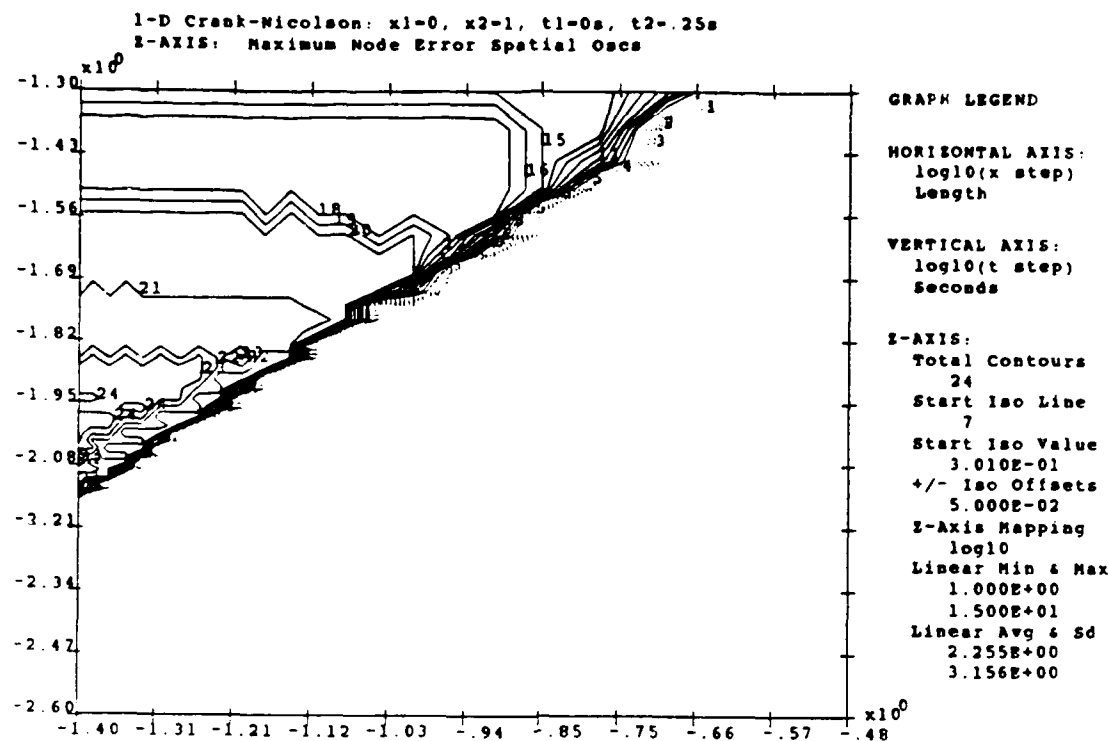


Figure 22. CN Maximum Spatial Error Oscillations

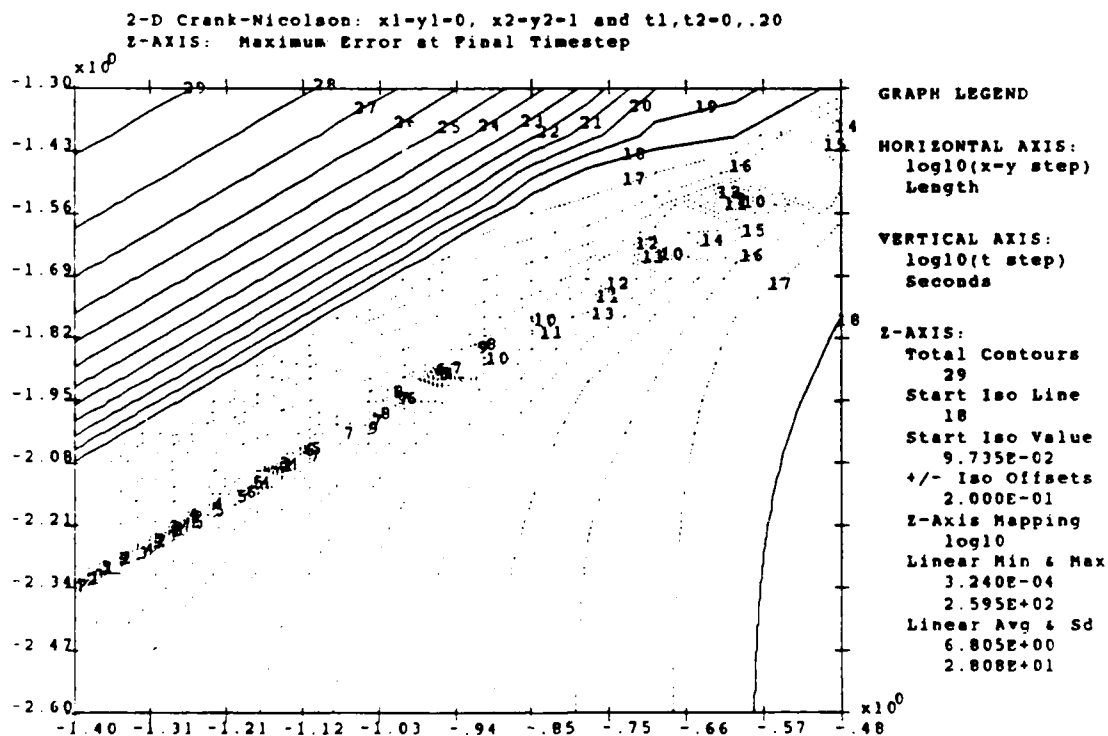
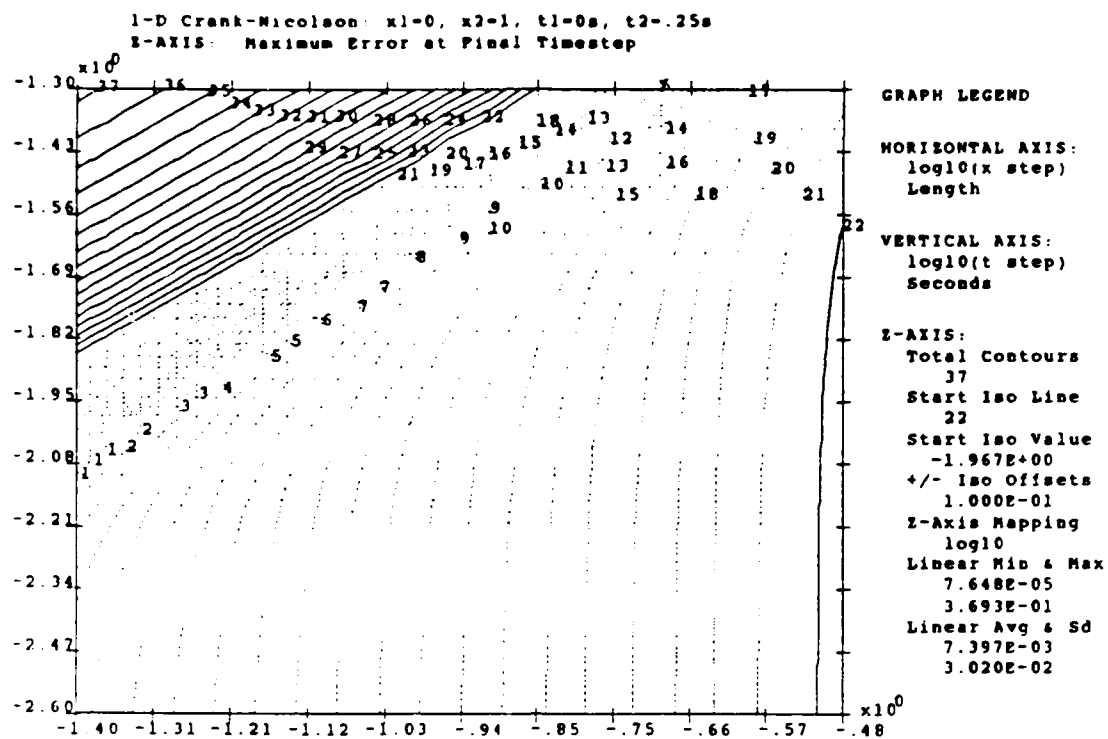


Figure 23. CN Maximum Errors

least errors, though remaining parallel for both cases, became flatter and broader, and the center of the valley shifted toward higher r values. Note that the center of the valley, as well as the 10% line, are roughly parallel and linear. By comparison with Figure 2 (top), all of the CN FDMs and cases studied satisfied the 10% criteria of the full matrix method, which predicted the linear relationship. Finally, the range of maximum errors decreases with the increased time as expected, since the transient heat equation has more time to reach a smaller range of values as it approaches the temperature of the boundary conditions, and it allows the FDM to damp the solution more since it is unconditionally stable, and approach the almost steady state solution with no discrete boundaries.

Returning to the standard 1-D and 2-D comparisons, the CN case provides, similar to the EX, clear results in the h - k domain. For time oscillations, very high r correlations exist. The starting time oscillation lines start cleanly at about $r=2.0$ and $r=1.0$ for the 1-D and 2-D cases respectively, and are both twice as high as predicted by the coefficient method, and four times higher than predicted by the more severe full matrix predictions. Hence, the time oscillation predictions are both conservative, as they should be, but by a large margin as well. As with the DF spatial oscillations, the CN spatial oscillations are more linear where they start, and do not correlate well, functionally, with the predicted time oscillations based on stability considerations.

Peaceman-Rachford ADI Results

The ADI results for two dimensions are shown in Figures 24 and 25. Similar to the DF method, the ADI method exhibits complicated behavior in the h - k domain. In order to correctly read the h - k domain, consideration of how h is presented on the graph relates to h used in the calculation of r is needed. The ADI program breaks the user given time step into two time steps to perform the two step ADI method, where each of the two time steps has an r that is one half that which the user input time step would indicate. Since the user given time step is graphed on the vertical axis, the observed value of r on the h - k domain needs to be divided by two to get the actual r values being predicted.

Note that unlike the other methods examined, the ADI has a valley, with high r correlation, where it oscillates at a minimum in time, with shallow hills of oscillation on either side. The shallow hills are a range of time oscillations which only vary from 1 to 4, and other than the IM method, show the smallest range for any of the 1-D or 2-D cases examined in this thesis. So, in fact, the ADI method is seen to be oscillatory in time for all regions in the h - k domain for this sample problem, and therefore appears to be unconditionally oscillatory for this problem. The minimum valley of time oscillation was found to occur at a value of one time oscillation, located between $r=0.75$ to $r=2.0$, with less than two oscillations occurring for all values of $r \leq 2.0$

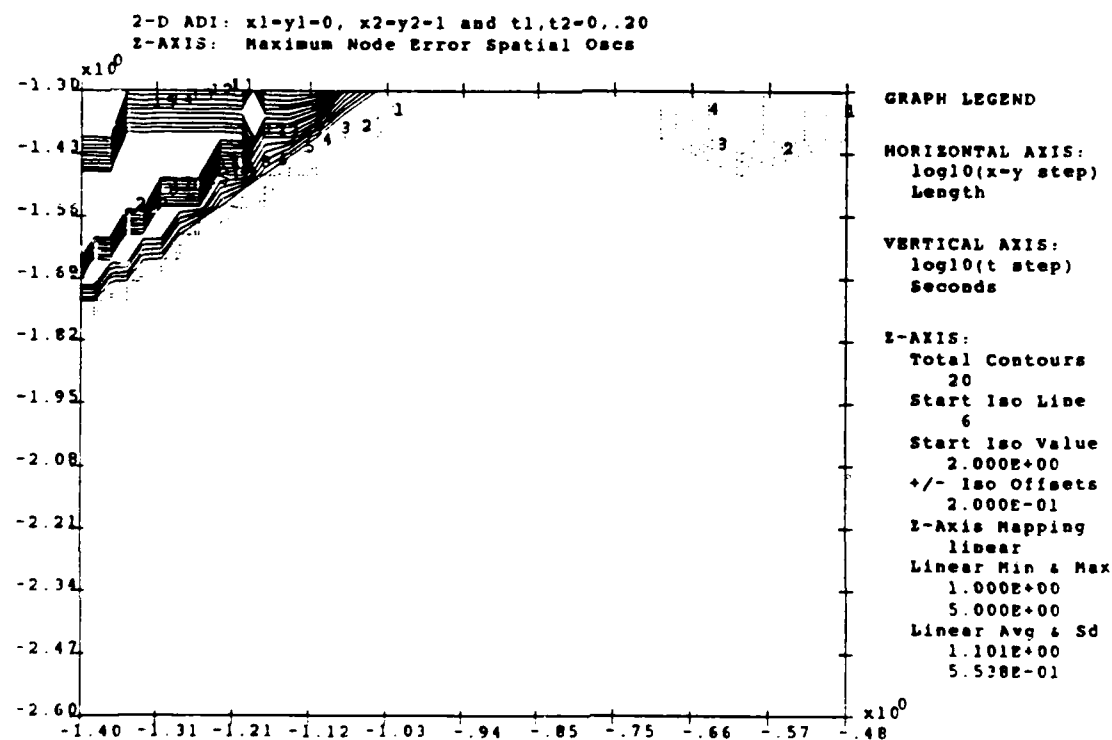
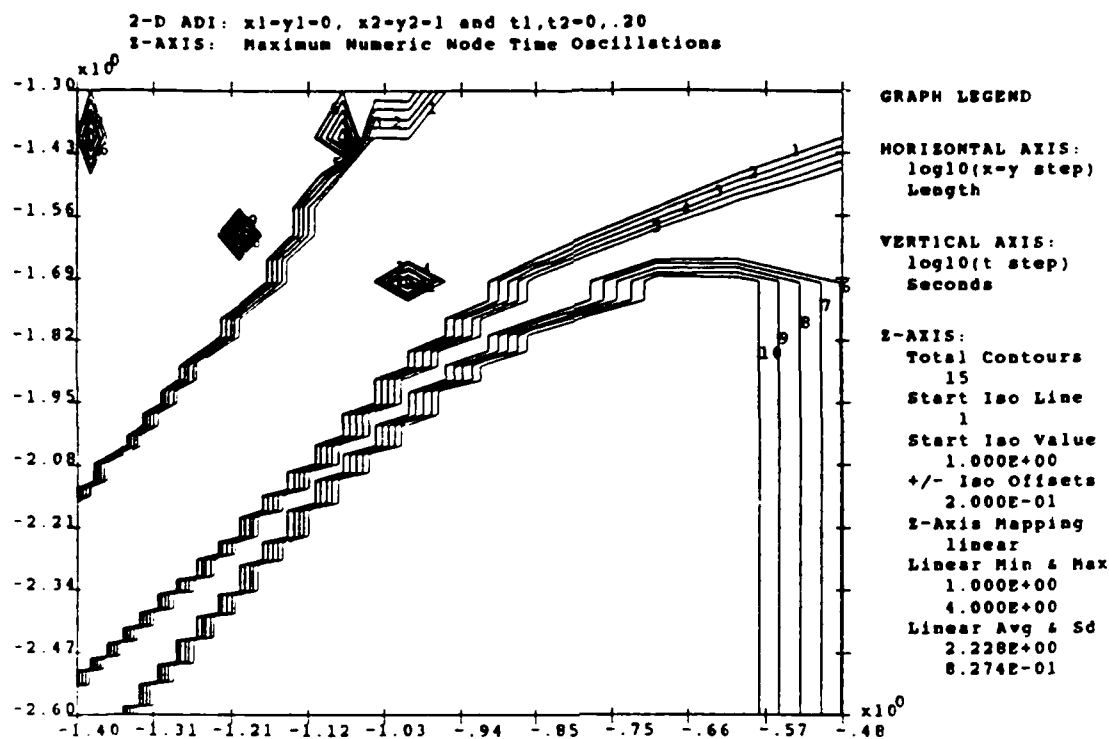


Figure 24. ADI Maximum Numeric Time Oscillations, and
 ADI Maximum Spatial Error Oscillations

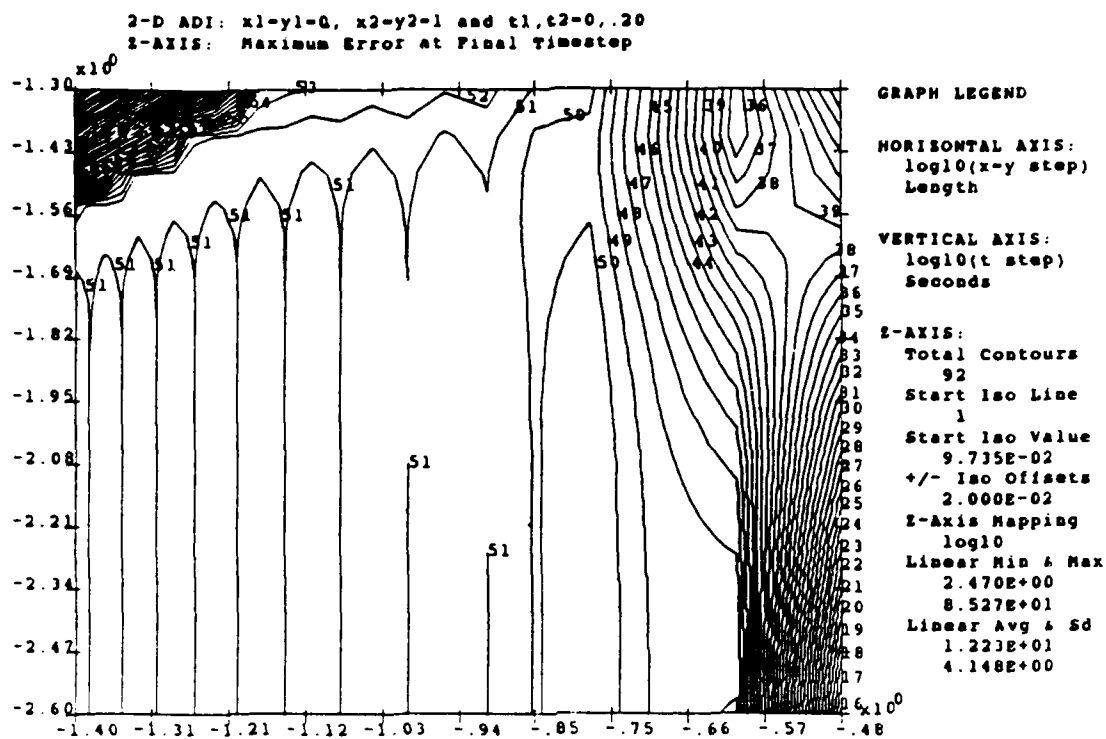


Figure 25. ADI Maximum Errors

in the domain. The coefficient method predicts time oscillations to occur at $r > 1/2$. As can be seen, the coefficient method does not do a good job at predicting the complex behavior of the ADI oscillations.

Looking at the spatial oscillations, the more familiar result is observed: an approximate r correlation, though more linear, is found. Spatial oscillations start at a line that is the one of the highest in the h - k domain of all the FDMs surveyed in this study (not counting no lines for the IM method). The starting line varies from above $r=3.0$ to $r=6.0$ in the domain.

Maximum errors of the ADI method never become larger than 85 degrees, nor smaller than 2.5 degrees, throughout the domains studied. This is not highly accurate, and never gets better than 10%. But the maximum error is never greater than 12.5 degrees at contour line 51, which covers most of the domain, and includes values of approximately $r \leq 4.0$. Note that the DF and CN methods do worse, with maximum errors reaching 1200 and 260 degrees in the domain, respectively. Of course, the DF and CN methods also do much better, with the smallest maximum errors reaching 2.5×10^{-4} and 3.2×10^{-4} degrees, respectively. And since 12.5 degrees is the range of values of the analytic solution, 12.5 degrees probably represents unacceptable error in the final solution, as it can equal 100% of the range of the exact solution. Full matrix predictions were not completed for the ADI method, so they have not been tested against the observed results.

VI. Conclusions and Recommendations

Conclusions

Based on the results of this study, conclusions will now be presented concerning two topics: 1) the coefficient and matrix methods of predicting stability and oscillations, and 2) the numerical results obtained from the h - k domain graphs.

The Pade' method was found to be equivalent to the full matrix method for predicting stability, where only the approach to deriving the amplification matrix differed. Further, the coefficient method p -ratio was found to be equivalent to the expectation value of the matrix method's amplification matrix eigenvalues for two-level FDMs. In effect, for two-level FDMs, the coefficient method p -ratios can be derived from the matrix method. The coefficient method was found to be an easy to use and apply method for predicting stability behavior, though not as powerful as the matrix method. However, the coefficient method should do well at predicting two-level FDM stability, since the coefficient method predictions are equivalent to the expectation value of the matrix predictions.

The matrix approach, on the other hand, is much more difficult to apply, especially to three-level systems, such as the DF. Even if the amplification matrix can be derived, it may be very complicated to analyze to determine FDM behavior.

Further, the Pade' approach to deriving the amplification matrix can be more difficult, if not impossible, to apply to some FDMs, such as the DF, which does not seem to be easily factored into various S,T approximants. Another problem with the Pade' approach is that once factored into several S,T approximants and recombined, such as in the case of the ADI method, one has to interpret how to replace the split block matrices with eigenvalues in the resulting amplification matrix. Even when the eigenvalues of the [B] and [C] matrices are known, split forms involve using several Pade' approximants that do not reproduce the desired FDM's matrix unless appropriate truncations are carried out. In general, it is simpler and safer to use the FDM itself to construct the amplification matrix, and avoid the Pade' approach, when analyzing a given FDM for stability.

Due to the more mathematically rigorous nature of the matrix method, its predictions, though severe, should generally be more exact when applied to an infinite set of problems. A great advantage of the matrix approach is that one is also able to understand and predict when the oscillations lead to errors that are not disastrous. Consequently, a less severe functional relationship in the h-k domain can be derived, since in practice, small errors induced by oscillations can still lead to acceptable solutions.

The h-k domain graphs were an excellent means of comparing predictions based on stability analysis and for finding interesting FDM behavior. The h-k domain graphs

showed that neither the coefficient nor matrix method predictions were significantly violated for the two-level FDMs studied. However, unusual DF and ADI behavior was observed which wasn't predicted by the coefficient method. Conclusions based on the h-k domain graphs will be covered in the following order: general expected and unexpected results, incorrect diagnostics, oscillatory behavior compared to the coefficient and matrix method predictions, and comments on maximum errors.

Except for the IM method, all of the FDMs surveyed in the h-k domain showed varying degrees of r correlations, as was expected from the major role r plays in predicting behavior. Also expected was the result that the 1-D and 2-D contour graphs, while very different among the five FDMs examined, were very similar for the same FDM. This similarity was maintained regardless of the different problems, final solution times, number of spatial dimensions, or differences in DF jump starts used.

Unexpected results were observed for both the DF and ADI FDMs. For the DF FDM, oscillations were not found in regions with large values of r , though those regions had large errors. Moreover, oscillations were found in regions with smaller than predicted values of r , though those regions had errors which were quite small. Also, the DF FDM showed unexpected behavior when the analytic solution, IM, and CN methods were used to jump start the first time level. The analytic solution jump

resulted in the worst time oscillations and errors in the final solution. The CN jump start, an FDM known to be able to oscillate, actually resulted in the least time oscillations, while the IM jump start gave the most accuracy. Finally, the ADI method always displayed time oscillations over the whole domain, though its spatial oscillations were more normal in appearance, being approximately linear and only occurring high in the h - k domain.

Two stability diagnostics, spatial oscillations and maximum error versus time, were found to be misleading and incorrect. Based on stability analysis of FDMs, oscillations with respect to time (i.e. time steps) are predicted. Unfortunately, spatial oscillations are often used to confirm stability oscillation predictions. But, in this study, spatial oscillations, except for the EX FDM, were found to be more linear ($k=bh$, where b is a constant) than the time oscillations ($k=rh^2$). So while it was generally observed that spatial oscillations usually occurred in regions with time oscillations, as would be expected, it was found that time oscillations also occurred in regions of the domain that were not oscillating spatially. Therefore, spatial oscillations used to prove or infer stability predictions based on time oscillations can be misleading. At best, such demonstrations often require that larger than necessary r values be used to find oscillations, and thereby tend to inflate the r values that stability analysis is suppose to predict. At worst, the use of spatial oscillations confuses the concepts embodied in

stability predictions as well as providing incorrect results. Another misleading diagnostic is the use of the maximum error versus time. Maximum error versus time is not a good stability (stable decay and stable oscillation) indicator since stability is a necessary, but not a sufficient, condition for accuracy.

Oscillatory behavior in time was verified to exist, as predicted by the coefficient method, for the EX, DF, CN, and ADI FDMs. The coefficient method did not predict oscillations for the IM method, and none were found. Predicted r values for the start of oscillations in the EX, CN, and DF were very good at predicting values below which oscillations were not occurring, but were less accurate about predicting when the oscillations actually began. Such conservative predictions are expected as other test problems could start oscillating in time at values closer to the predicted r values. Overall, the coefficient method, as expected, proved to be good at predicting two-level FDM stability behavior. The DF and ADI methods exhibited more complex behavior. In comparison, the coefficient method only showed general r correlations which only approximately predicted the oscillatory behavior observed in the DF and ADI FDMs.

The matrix method was completely derived and applied to the IM, EX and CN methods. As with the coefficient method, the matrix method correctly predicted no oscillations for the IM method. Since the predicted r values (based on the extreme

eigenvalues of the matrix method) were smaller, usually one half the value of the predicted coefficient method values, the matrix method was even more severe, more conservative in its predictions than the coefficient method. This severity was expected, since from the derivations, the matrix method stability predictions are worst case predictions that should never be violated. The non-disastrous oscillations predictions proved to be useful in determining less severe restrictions on h and k , roughly resulting in maximum absolute errors of less than 10% of the final range of temperatures for the problems studied.

Neither the coefficient nor the matrix method was proven to be substantially incorrect by these test problems, number of dimensions, or final solution times for two-level FDMs. In addition, the coefficient method provided acceptable results without the severe constraints of the matrix method. Analysis of the DF and ADI methods using the matrix method could not be finished, but for these methods the eigenvalues of the amplification matrices indicate that more complicated behavior is probable. Therefore, the matrix method may be able to explain the unexpected results seen in the DF and ADI, whereas the simple coefficient method could not. Further, the eigenvalues of the amplification matrices predicted different behavior, which was observed in the test problems, for the 1-D DF, 2-D CN, and 2-D ADI, whereas the coefficient method only predicted the same behavior.

The worst maximum error increased, for the same domains

and for both the 1-D and 2-D cases, in the following order: IM, ADI, CN, DF, EX, with EX having the worst maximum error due to its conditional stability being violated. The least maximum error generally decreased in the following order: ADI, IM, CN, EX, DF, with the DF have the least maximum error of all over the domain. Generally, the CN method proved to be one of the best methods for small maximum errors based upon a nearly linear restriction, as predicted by the matrix method, on the values of k/h , versus the more general r constraints based on k/h^2 . For h and k of any size in the domain, the IM method provided the smallest worst maximum error, as well as having the smallest range of maximum errors over the entire h - k domain.

Recommendations

As a result of this study, the following are proposed:

1. Finish analyzing the 1-D DF, 2-D DF and ADI FDMs using the full matrix method. Explain the unexpected behavior, not predicted by the coefficient method, observed in the DF and ADI methods. Relate the coefficient method p -ratios to the matrix method for three-level FDMs.
2. Confirm or reject the ADI results for the p -ratio, amplification matrix eigenvalues, and computer graphs in this study. Since these results were the last achieved in this study, they were not as completely tested and checked as other results, and represent the only probable areas where

AD-A189 591

PREDICTING OSCILLATORY FINITE DIFFERENCE SOLUTIONS TO

2/2

THE HEAT EQUATION: (U) AIR FORCE INST OF TECH

WRIGHT-PATTERSON AFB OH SCHOOL OF ENGI

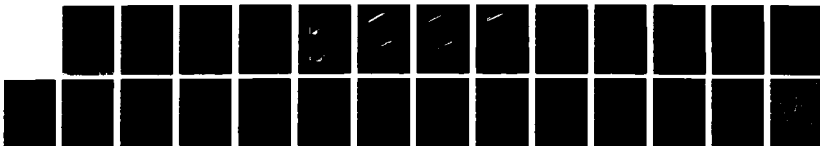
T M DIPP

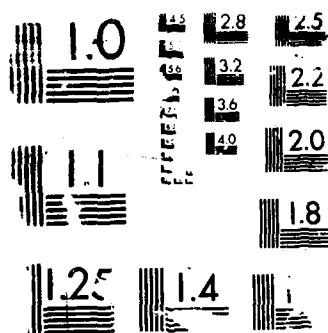
UNCLASSIFIED

DEC 87 AFIT/GEP/ENP/87D-5

F/G 12/1

NL





100-1000 RESOLUTION TEST CHART

significant errors could have occurred in this study.

3. Use Gauss-Seidel iteration to completely jump start the DF method using the DF method itself, which is what the stability predictions are based on, and see if better or more predictable results are obtained then by using the analytic solution, IM, or CN.

4. Compare the stability predictions based on the probabilistic and fourier techniques with the domain graphs of this study.

5. Run the programs for other problems at various times to see if the less rigorous coefficient method can be found to be significantly violated in its predicted non-oscillatory r values. Is the matrix method ever violated?

6. Run the programs to see if the probabilistic method, as applied to explicit schemes, is ever violated. Also compare the probabilistic method with the matrix method, which considers all the nodes, to determine if they are equivalent or not. Does a relationship similar to that of the coefficient and matrix methods exist?

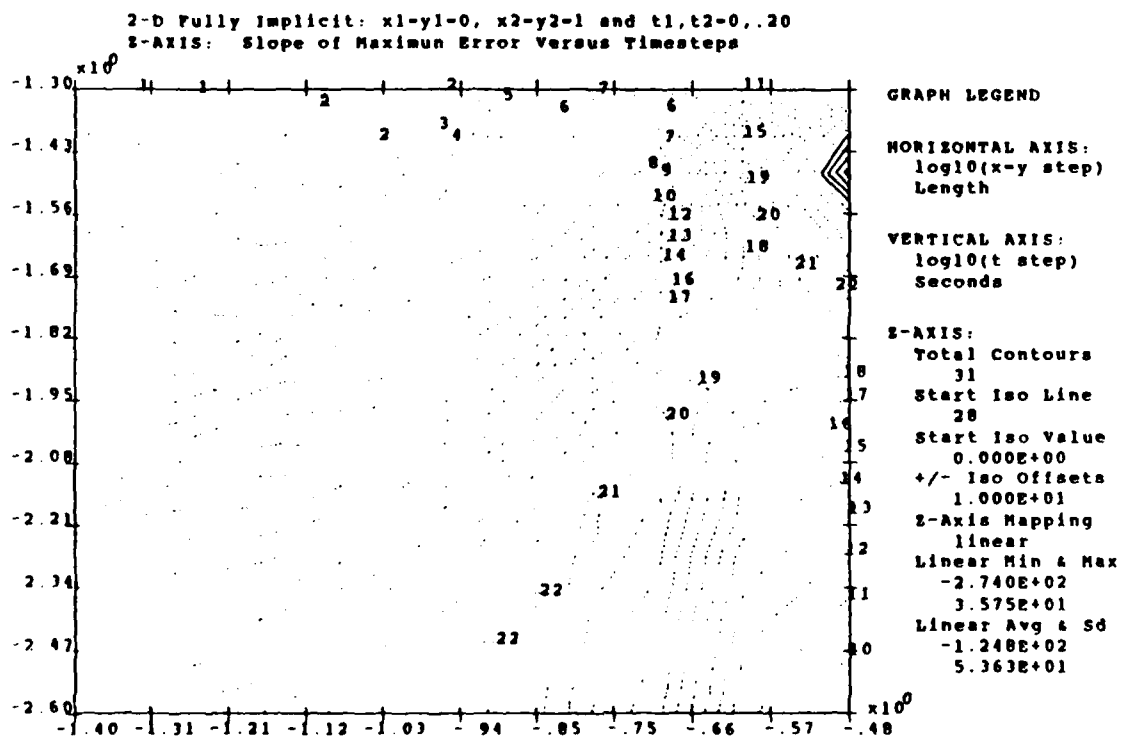
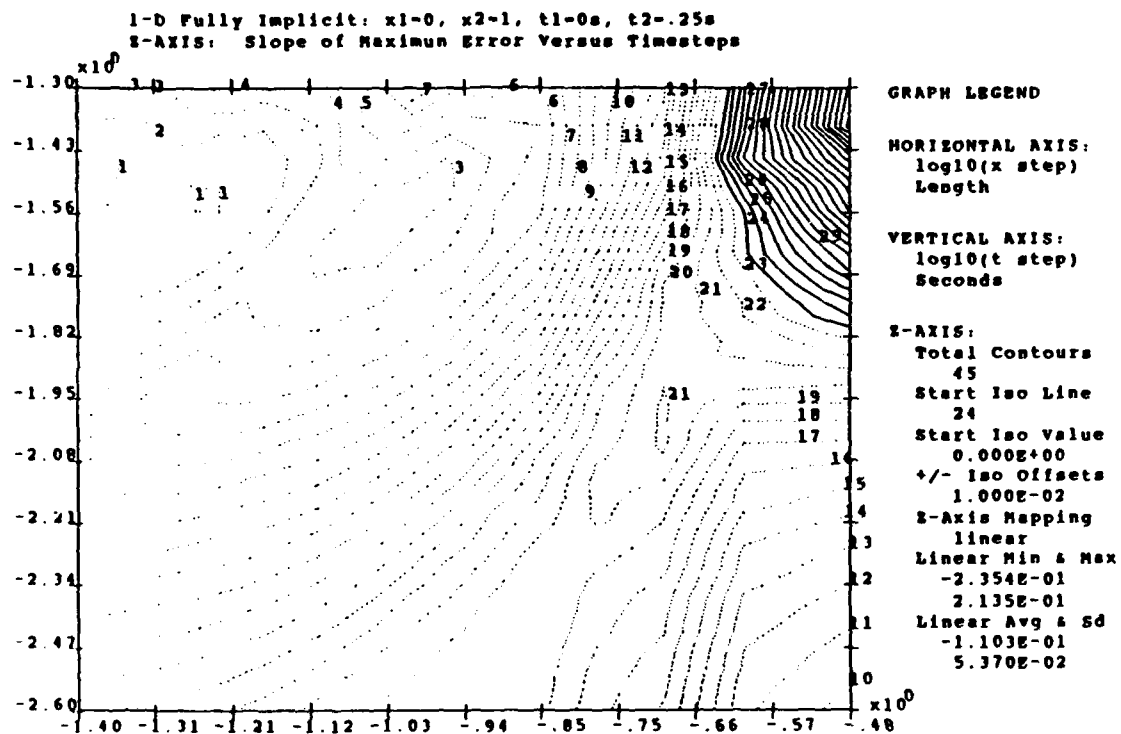
7. Develop an algorithm to plot stability in the h - k domain, using the numerical solution being bounded as a trial diagnostic.

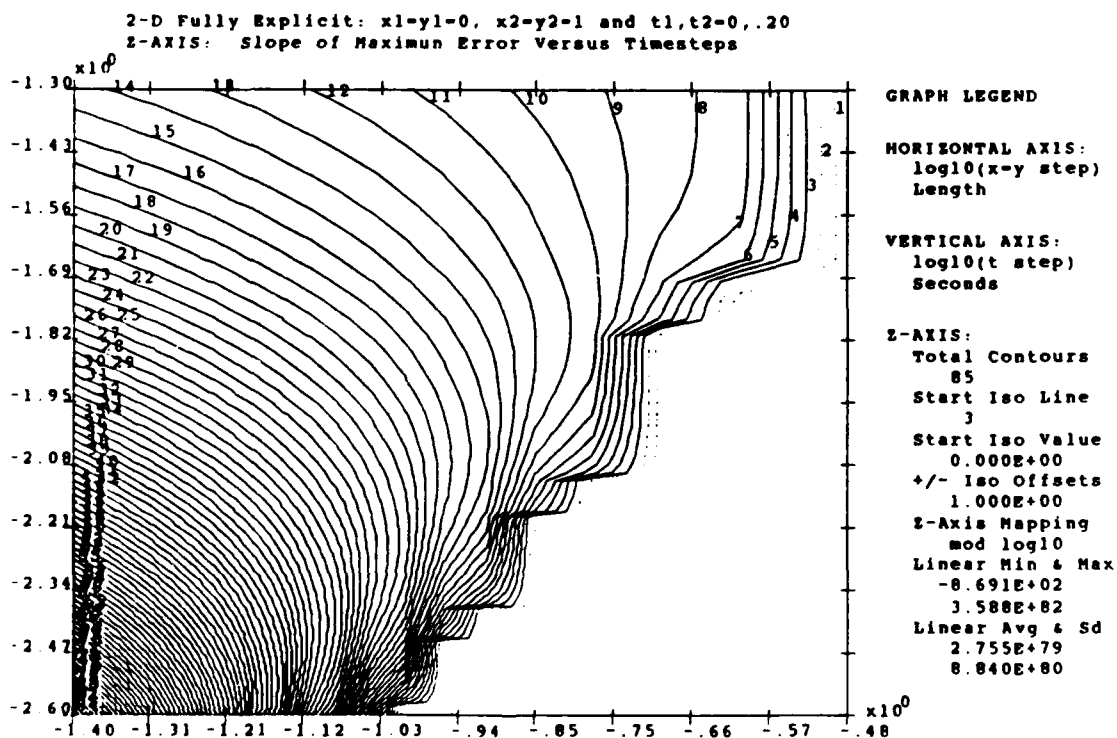
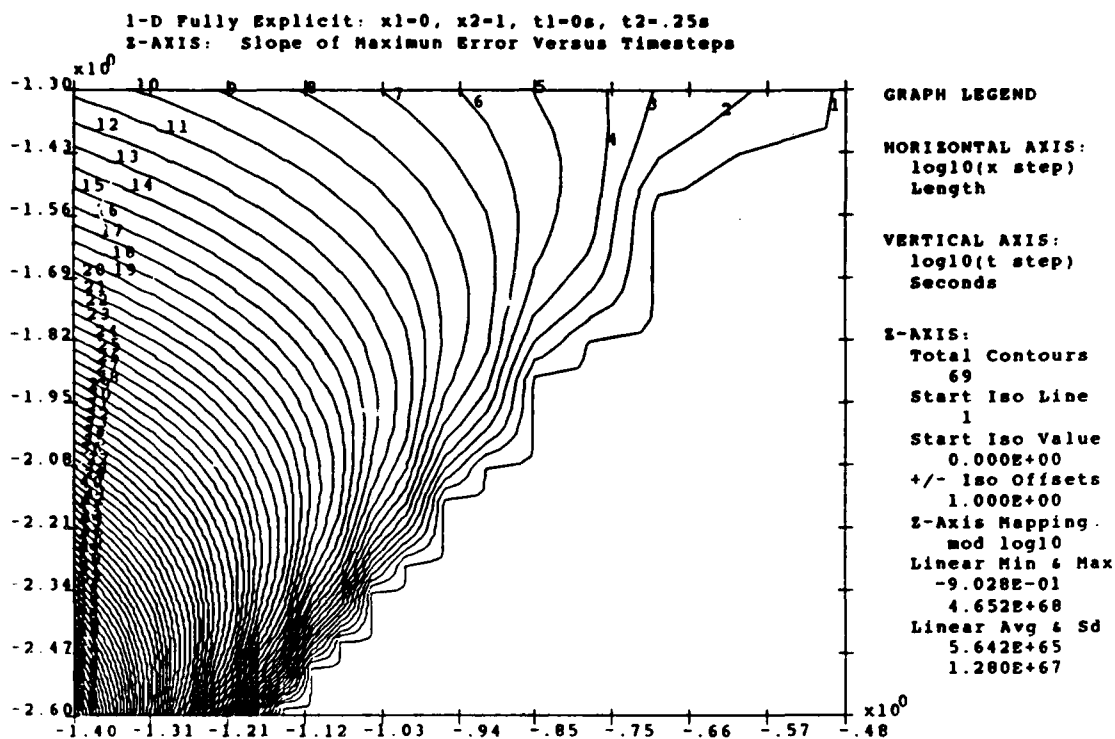
8. Apply the FDMs studied in this paper to problems with derivative or mixed boundary conditions, since these effect stability. How do the various methods of predicting stability compare with the new domain results?

9. Use the domain graph approach to explore newly

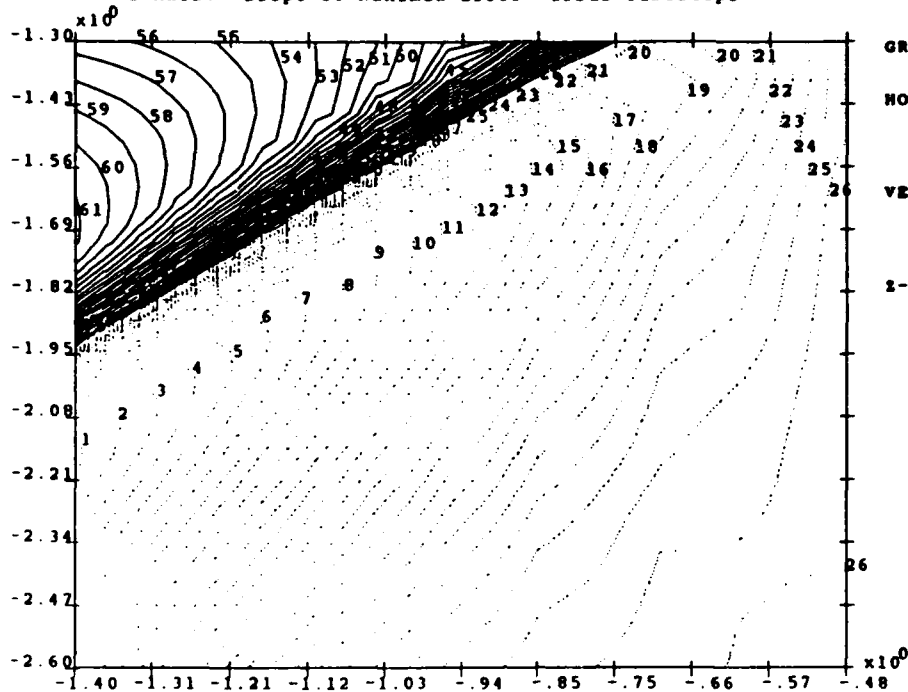
developed FDMs to see if they oscillate and to determine if the errors are disastrous.

Appendix A: h-k Domain Graphs for the Slope of the Maximum Error Versus Time





1-D DuFort-Frankel, An: $x_1=0$, $x_2=1$, $t_1=0s$, $t_2=.25s$
 Z-AXIS: Slope of Maximum Error Versus Timesteps



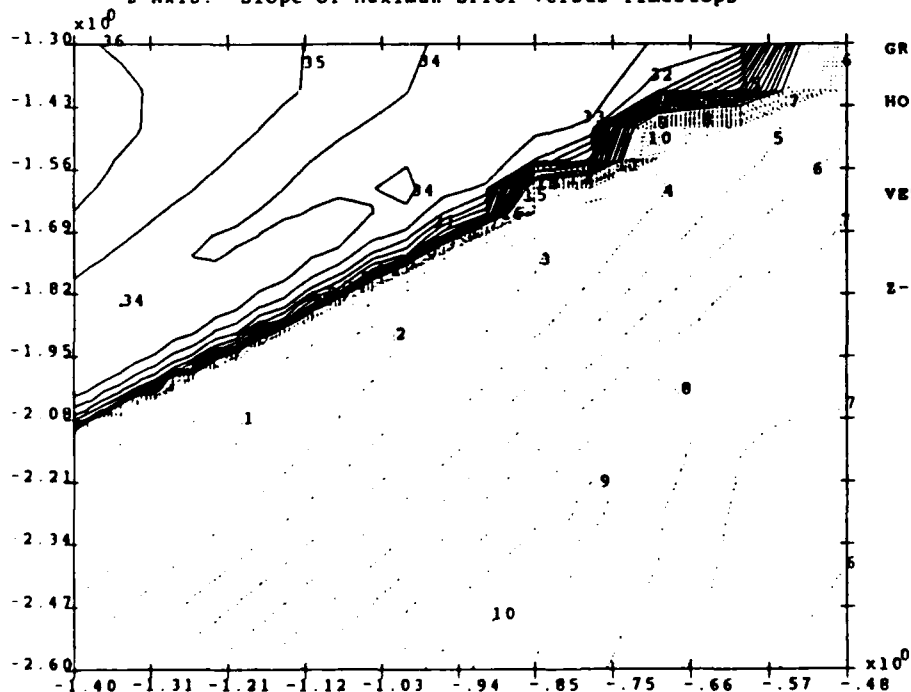
GRAPH LEGEND

HORIZONTAL AXIS:
 $\log_{10}(x \text{ step})$
 Length

VERTICAL AXIS:
 $\log_{10}(t \text{ step})$
 Seconds

Z-AXIS:
 Total Contours
 61
 Start Iso Line
 27
 Start Iso Value
 0.000E+00
 +/- Iso Offsets
 4.000E-02
 Z-Axis Mapping
 mod log10
 Linear Min & Max
 -1.018E+01
 2.232E+01
 Linear Avg & Sd
 -1.741E+00
 4.845E+00

2-D DuFort-Frankel, An: $x_1=y_1=0$, $x_2=y_2=1$ and $t_1, t_2=0, .20s$
 Z-AXIS: Slope of Maximum Error Versus Timesteps

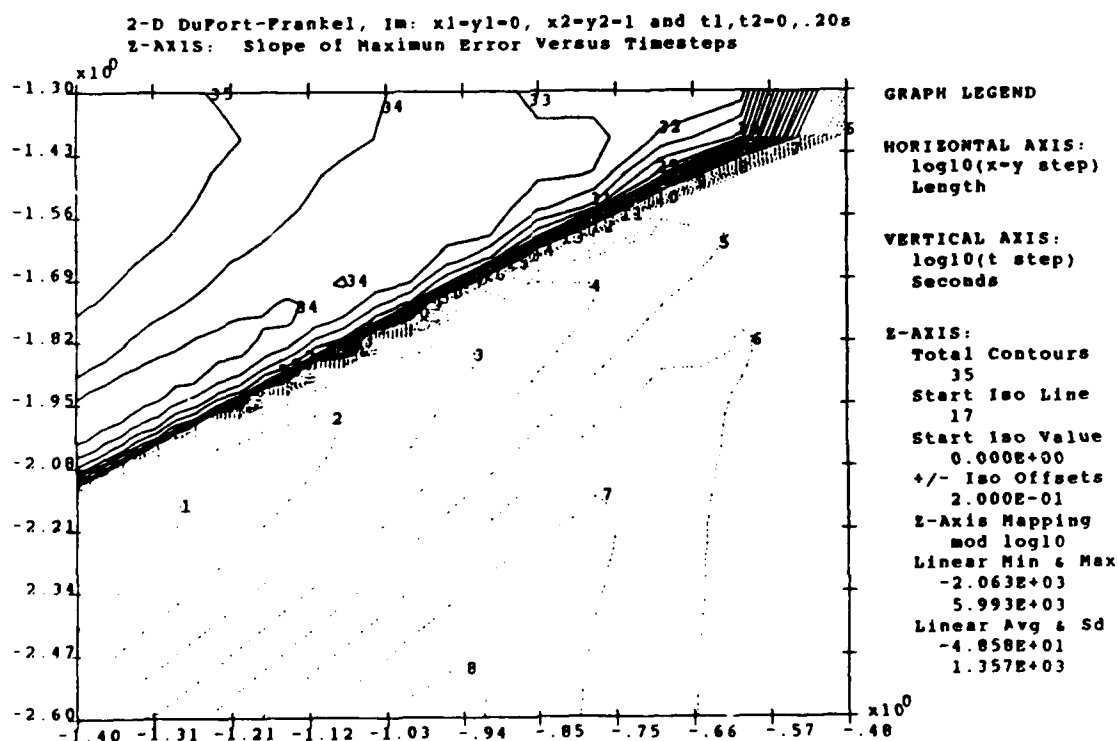
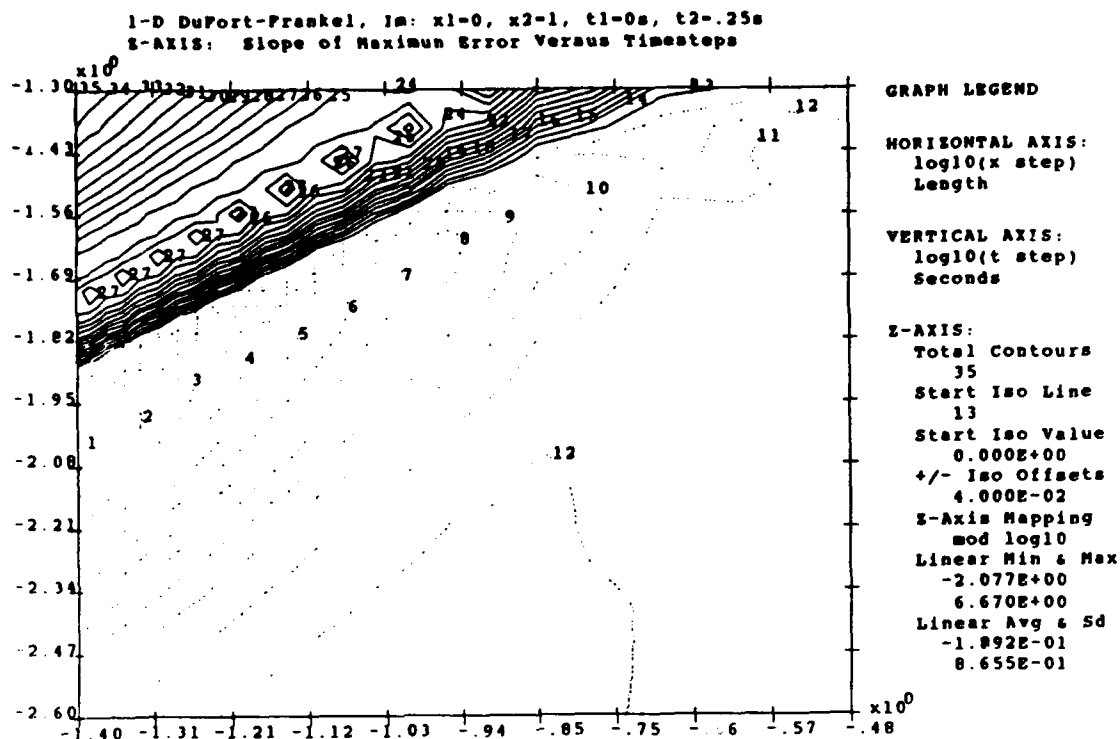


GRAPH LEGEND

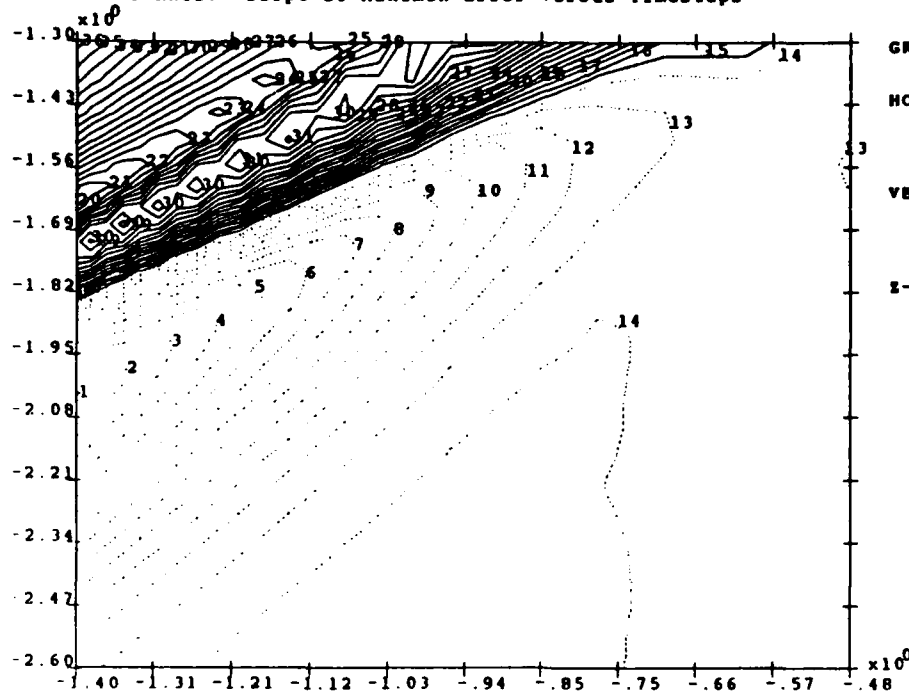
HORIZONTAL AXIS:
 $\log_{10}(x-y \text{ step})$
 Length

VERTICAL AXIS:
 $\log_{10}(t \text{ step})$
 Seconds

Z-AXIS:
 Total Contours
 36
 Start Iso Line
 17
 Start Iso Value
 0.000E+00
 +/- Iso Offsets
 2.000E-01
 Z-Axis Mapping
 mod log10
 Linear Min & Max
 -2.469E+03
 7.507E+03
 Linear Avg & Sd
 -5.074E+01
 1.595E+03



1-D DuPort-Frankel, CN: x1=0, x2=1, t1=0s, t2=.25s
 Z-AXIS: Slope of Maximum Error Versus Timesteps



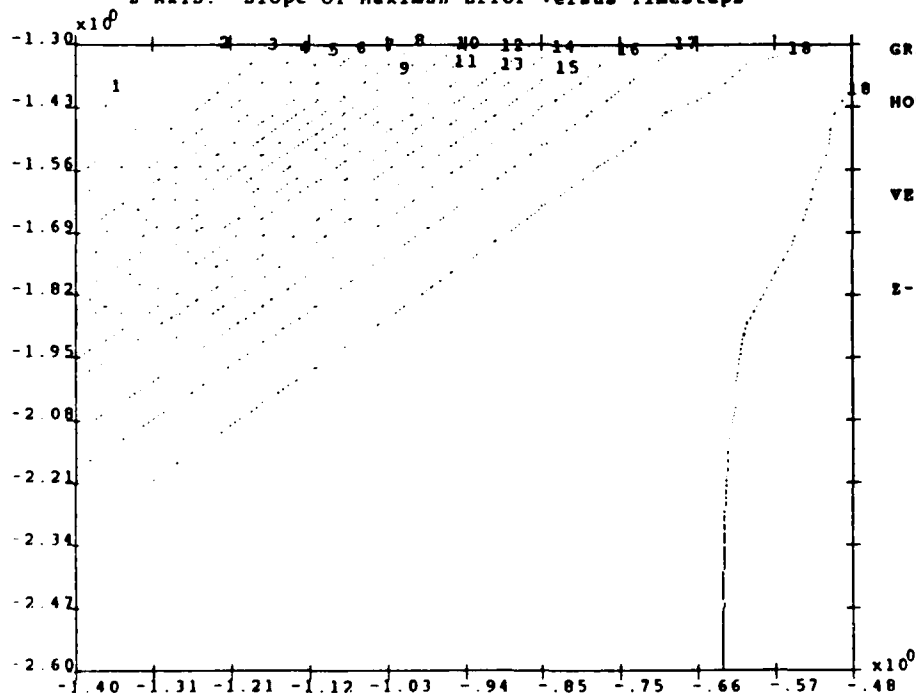
GRAPH LEGEND

HORIZONTAL AXIS:
 $\log_{10}(x \text{ step})$
 Length

VERTICAL AXIS:
 $\log_{10}(t \text{ step})$
 Seconds

Z-AXIS:
 Total Contours
 36
 Start Iso Line
 15
 Start Iso Value
 0.000E+00
 +/- Iso Offsets
 4.000E-02
 Z-Axis Mapping
 mod log10
 Linear Min & Max
 -2.653E+00
 6.226E+00
 Linear Avg & Sd
 -2.618E-01
 8.467E-01

1-D Crank-Nicolson: x1=0, x2=1, t1=0s, t2=.50s
 Z-AXIS: Slope of Maximum Error Versus Timesteps

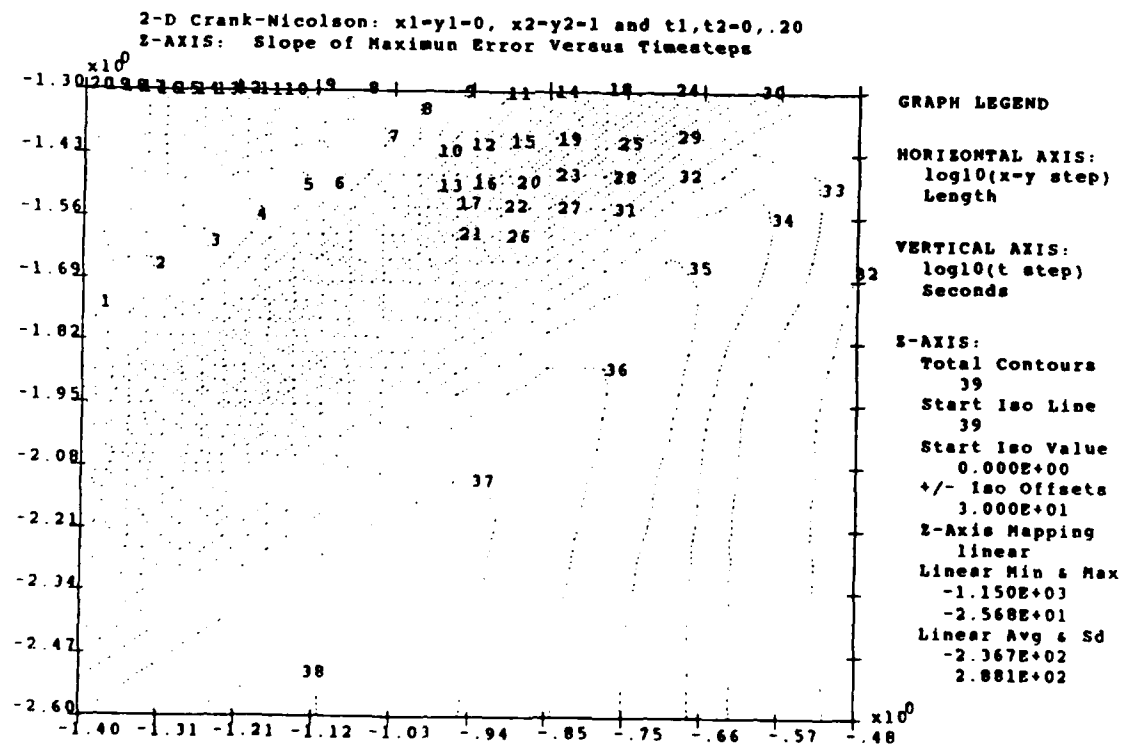
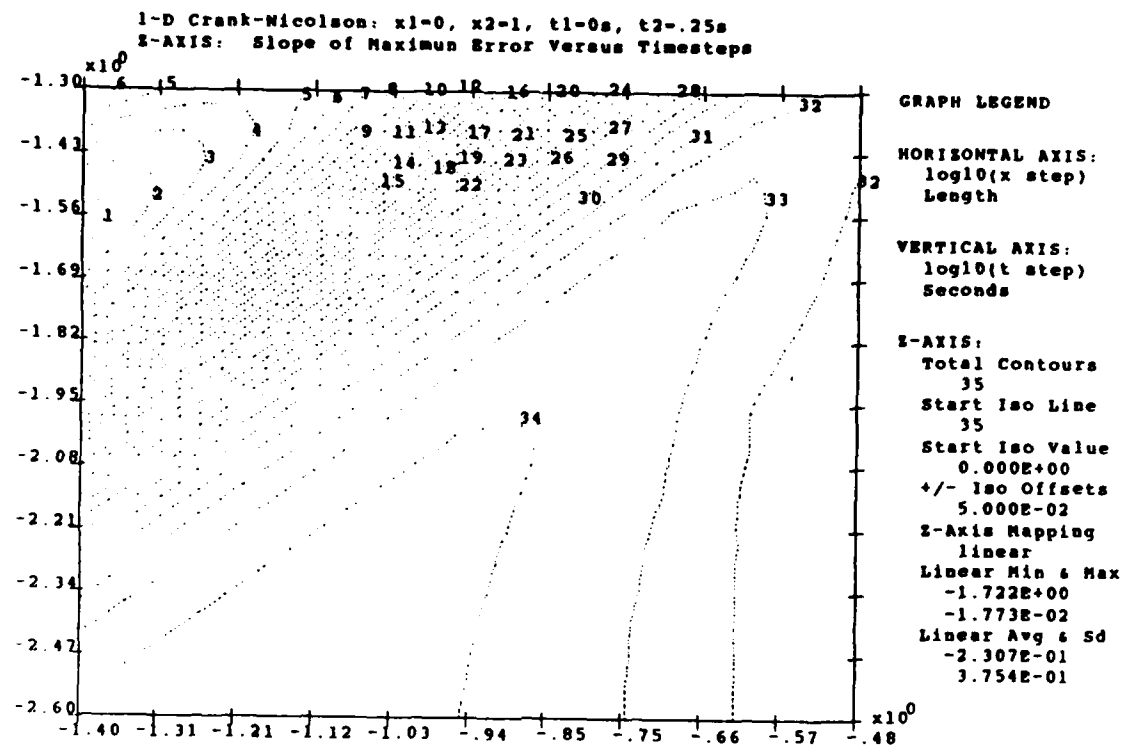


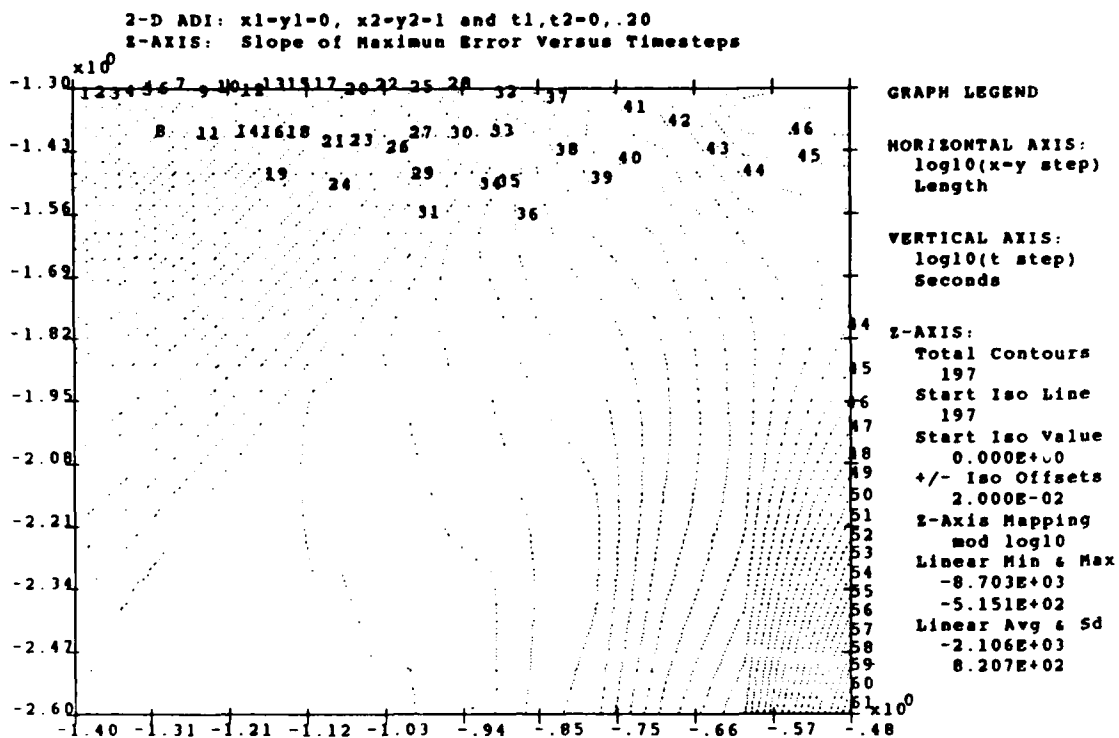
GRAPH LEGEND

HORIZONTAL AXIS:
 $\log_{10}(x \text{ step})$
 Length

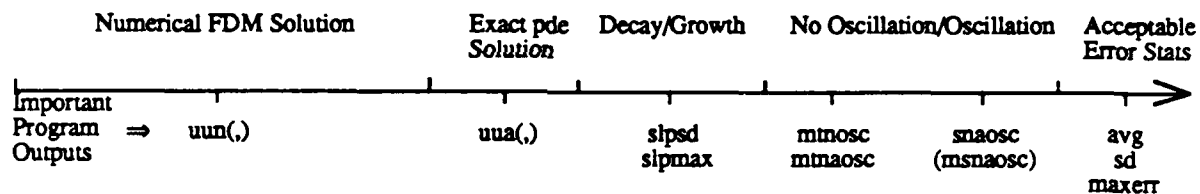
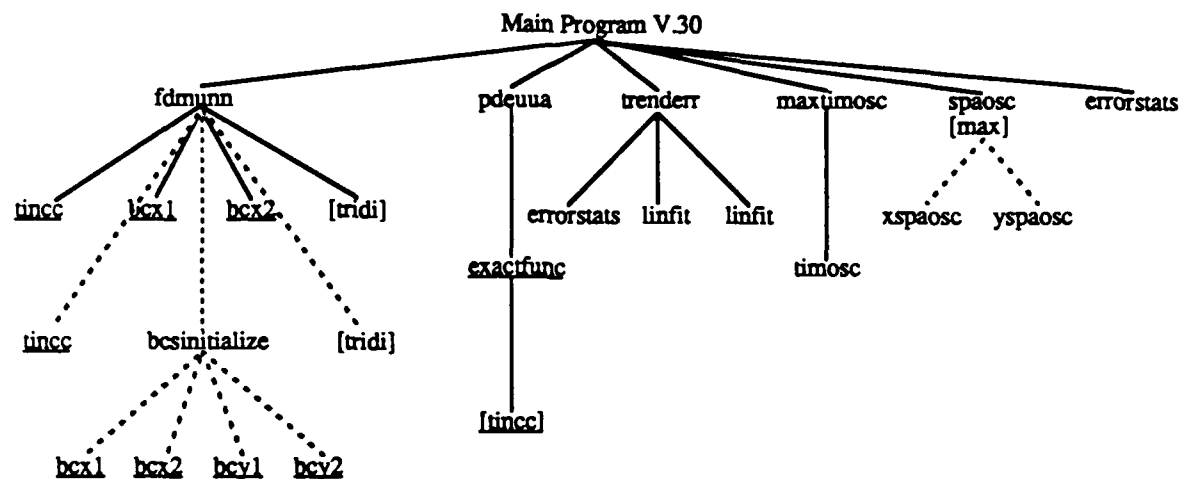
VERTICAL AXIS:
 $\log_{10}(t \text{ step})$
 Seconds

Z-AXIS:
 Total Contours
 19
 Start Iso Line
 19
 Start Iso Value
 0.000E+00
 +/- Iso Offsets
 5.000E-02
 Z-Axis Mapping
 linear
 Linear Min & Max
 -9.140E-01
 -5.341E-03
 Linear Avg & Sd
 -8.144E-02
 1.621E-01





Appendix B: General Structure Diagram of Programs



Solid Lines — 1-D and 2-D paths if only solid lines from root

Dotted Lines — 2-D paths, followed instead of solid lines from a root

[] — optional, if required

Underline — function

No Underline — procedure

Definitions of Structure Diagram Terms

fdmuun:	calculates and stores all Finite Difference Method (FDM) solutions in uun (ix, it) for all nodes, all timesteps
pdeuua:	calculates and stores all partial differential equation (pde) solutions in uua (ix, it) for all nodes, all timesteps
trenderr:	calculates sd and max error slopes of absolute (numeric solution – analytic solution) errors at each timestep versus that timestep
maxtimosc:	calculates maximum N and $N - A * \text{time}$ oscillations from all spatial nodes
spaosc:	calculates total spatial oscillations at <u>any</u> timestep — here it is used for final timestep, n_t
errorstats:	calculates error statistics for <u>all</u> nodes (includes BCs) for <u>any</u> timestep — here it is used for final timestep, n_t
<u>tincc</u> :	temperature initial condition (IC)
<u>bcx1</u> :	left boundary condition (BC)
<u>bcx2</u> :	right boundary condition (BC)
[tridi]	tridiagonal solver (if needed)
<u>exactfunc</u> :	exact analytic series solution to pde
errorstats:	calculates error statistics (avg, sd, max absolute errors) over <u>all</u> nodes for <u>any</u> timestep
linfit:	least squares curve fitting routine to calculate error slopes (sd & max) for trending error behavior
timosc:	calculates total time oscillations at any spatial node for N and $N - A *$ solutions

* N — Numeric Solution, A — Exact Analytic Solution

Calculation of Program Run Time

$$n_x = \frac{(x_2 - x_1)}{\Delta x}$$

$$n_t = \frac{(t_2 - t_1)}{\Delta t}$$

Approximate total node points solved in h-k domain:

$$1\text{-D: } \frac{(\max n_x)^2 (\max n_t)^2}{4}$$

$$2\text{-D: } \frac{(\max n_x)^3 (\max n_t)^2}{6} \quad \text{for } \Delta x = \Delta y \text{ plane (used in this thesis, with } n_x = n_y \text{ also)}$$

$$2\text{-D: } \frac{(\max n_x)^2 (\max n_y)^2 (\max n_t)^2}{8} \quad \text{for all } \Delta x \text{ and } \Delta y$$

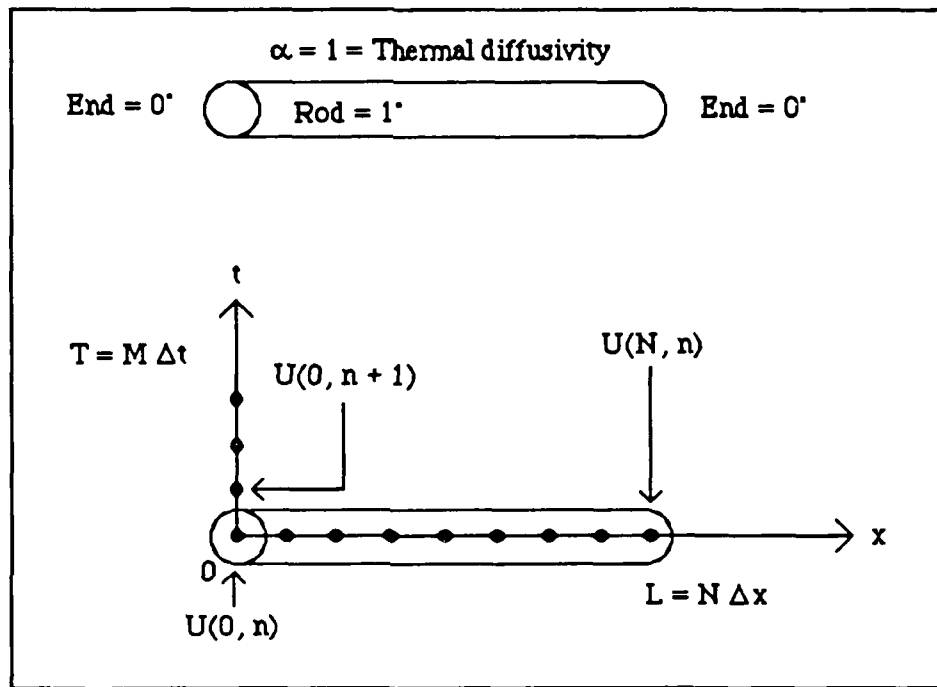
Note: ICC can solve for 1.125 million node points per hour on average, with 0.675 to 2.25 million node points per hour for ± 3 standard deviations.

Example: 1-D: $n_x = 3 \text{ to } 100$, $n_t = 3 \text{ to } 100 \Rightarrow \approx 25 \text{ million points} \approx 22 \text{ hours to run}$

2-D: $n_x = n_y = 3 \text{ to } 25$, $n_t = 3 \text{ to } 100 \Rightarrow \approx 26 \text{ million nodes} \approx 23 \text{ hours}$

Appendix C: Example Stability Derivations

1-D EX Example



$$\frac{\partial U}{\partial t} \approx \alpha \frac{\partial^2 U}{\partial x^2} \quad \text{continuous}$$

$$\frac{\partial U}{\partial t} \approx \frac{U(x, t + \Delta t) - U(x, t)}{\Delta t} \quad \text{to}$$

$$\frac{\partial^2 U}{\partial x^2} \approx \frac{U(x + \Delta x, t) - 2U(x, t) + U(x - \Delta x, t)}{\Delta x^2} \quad \text{discrete}$$

Substitute derivative approximations into pde and rearrange terms to get explicit form:

$$U(x, t + \Delta t) = rU(x - \Delta x, t) + (1 - 2r)U(x, t) + rU(x + \Delta x, t)$$

where $r = \frac{\Delta t}{2 \Delta x^2}$

which can be written in matrix form as:

$$\begin{bmatrix} 1-2r & r & & & \\ r & 1-2r & r & & \\ & & & & \\ & & & r & 1-2r & r \\ & & & r & 1-2r \end{bmatrix} \begin{bmatrix} U_{1,n} \\ U_{2,n} \\ - \\ U_{N-2,n} \\ U_{N-1,n} \end{bmatrix} + \begin{bmatrix} rU_{0,n} \\ 0 \\ - \\ 0 \\ rU_{N,n} \end{bmatrix} = \begin{bmatrix} U_{1,n+1} \\ U_{2,n+1} \\ - \\ U_{N-2,n+1} \\ U_{N-1,n+1} \end{bmatrix}$$

Coefficient Method:

$$p = \frac{U(x, t + \Delta t)}{U(x, t)} = \frac{1-2r}{1} = 1-2r \quad \begin{cases} r=0 \text{ to } 1/2 & \text{stable decay} \\ r=1/2 \text{ to } 1 & \text{stable osc} \\ r>1 & \text{unstable osc} \end{cases}$$

Matrix Method:

$$\text{Tridi Matrix } Z_s = b + 2\sqrt{ac} \cos \frac{s\pi}{N} \quad s = 1, 2, \dots, N-1$$

$$\mu_s \equiv G_s = 1 - 2r + 2r \cos \frac{s\pi}{N} = 1 - 4r \sin^2 \frac{s\pi}{2N}$$

$$\langle \mu_s \rangle = 1 - 2r = \text{coefficient method } p\text{-ratio}$$

$$\text{Extremes: } \mu_1 \approx 1, \quad \mu_{N-1} \approx 1 - 4r \quad \text{for large } N$$

$$1 - 4r \begin{cases} r=0 \text{ to } 1/4 & \text{stable decay} \\ r=1/4 \text{ to } 1/2 & \text{stable osc} \\ r>1/2 & \text{unstable osc} \end{cases} \quad \text{for eigenvalue extremes}$$

$$\text{Non-disastrous oscillations condition: } |\mu_{N-1}| < |\mu_1|$$

$$r < \frac{1}{2 + \frac{\pi^2}{2N^2}} \quad \text{or} \quad r < 1/2 \text{ approximately for large } N$$

Matrix Non-Disastrous Oscillations

$$\text{Condition: } |\mu_{N-1}| < |\mu_1|$$

$$-\mu_1 < \mu_{N-1} < \mu_1$$

$$-1 + 4r \sin^2 \frac{\pi}{2N} < 1 - 4r \sin^2 \frac{(N-1)\pi}{2N} < 1 - 4r \sin^2 \frac{\pi}{2N}$$

$$\text{RHS: } \sin^2 \frac{(N-1)\pi}{2N} > \sin^2 \frac{\pi}{2N} \quad \text{is always satisfied}$$

$$\text{LHS: } 4r \sin^2 \frac{\pi}{2N} < 2 - 4r \sin^2 \frac{(N-1)\pi}{2N}$$

$$\text{LET: } \left\{ \begin{array}{l} \sin^2 \frac{\pi}{2N} \approx \frac{\pi^2}{4N^2} \\ \sin^2 \frac{(N-1)\pi}{2N} \approx 1 \end{array} \right\} \quad \text{for large N}$$

$$\text{THEN: } 4r \frac{\pi^2}{4N^2} < 2 - 4r \quad r \left(\frac{\pi^2}{N^2} + 4 \right) < 2 \quad r < \frac{2}{\frac{\pi^2}{N^2} + 4} \quad \text{therefore}$$

$$r < \frac{1}{2 + \frac{\pi^2}{2N^2}} \quad \text{condition for non-disastrous oscillations}$$

NOTE: Approaches $r < 1/2$ for large N, where μ_s varies from -1 to 1 for $\mu_{N-1} \approx 1 - 4r$.
Therefore, agrees with the condition based on $|\text{eigenvalues}| < 1$.

Derivation of the Two Dimensional EX Full Matrix Parameters using the Pade' Method

Let $\mu_{m,n} \equiv G_{m,n} \equiv$ Amplification Matrix Eigenvalues

From the 2-D EX Pade' Approximant: $\mu_{m,n} = 1 + kZ_{m,n}$

$$\text{where } Z_{m,n} = -\frac{4}{h^2} \left(\sin^2 \frac{m\pi}{2N} + \sin^2 \frac{n\pi}{2N} \right)$$

$$\text{and } m = 1(1)N-1; \quad n = 1(1)N-1$$

$$\text{so } \mu_{m,n} = 1 - 4r \left(\sin^2 \frac{m\pi}{2N} + \sin^2 \frac{n\pi}{2N} \right) \quad , \quad \text{then}$$

$$\langle \mu_{m,n} \rangle = 1 - 4r = \text{coefficient method p-ratio}$$

$$\text{Extremes: } \mu_{1,1} \approx 1, \quad \mu_{N-1,N-1} \approx 1 - 8r$$

$$1 - 8r \begin{cases} r = 0 \text{ to } 1/8 & \text{stable decay} \\ r = 1/8 \text{ to } 1/4 & \text{stable osc} \\ r > 1/4 & \text{unstable osc} \end{cases} \quad \text{for eigenvalue extremes}$$

For non-disastrous oscillations, the high frequency components must decay faster than the low frequency components so that

$$\text{Condition: } \left| \mu_{N-1, N-1} \right| < \left| \mu_{1,1} \right|$$

$$-\mu_{1,1} < \mu_{N-1, N-1} < \mu_{1,1}$$

RHS: is always satisfied

$$\text{LHS: } -1 - kZ_{1,1} < 1 + kZ_{N-1, N-1}$$

$$-kZ_{1,1} < 2 + kZ_{N-1, N-1}$$

$$\text{LET: } \left\{ \begin{array}{l} Z_{1,1} \approx -\frac{4}{h^2} \left(\frac{\pi^2}{4N^2} + \frac{\pi^2}{4N^2} \right) \\ Z_{N-1, N-1} \approx -\frac{8}{h^2} \end{array} \right\} \text{ for large } N$$

$$\text{THEN: } 4r \frac{2\pi^2}{4N^2} < 2 - 8r \quad r \left(\frac{2\pi^2}{N^2} + 8 \right) < 2 \quad r < \frac{2}{\frac{2\pi^2}{N^2} + 8} \text{ therefore}$$

$$r < \frac{1}{4 + \frac{\pi^2}{N^2}} \quad \text{condition for non-disastrous oscillations}$$

Appendix D: Relating Coefficient and Matrix Methods

Amplification Matrix Eigenvalues

1-D EX	$1 - 4r \sin^2 \frac{s\pi}{2N}$	2-D EX	$1 - 4r \left(\sin^2 \frac{i\pi}{2N} + \sin^2 \frac{j\pi}{2N} \right)$
1-D IM	$\frac{1}{1 + 4r \sin^2 \frac{s\pi}{2N}}$	2-D IM	$\frac{1}{1 + 4r \left(\sin^2 \frac{i\pi}{2N} + \sin^2 \frac{j\pi}{2N} \right)}$
1-D CN	$\frac{1 - 2r \sin^2 \frac{s\pi}{2N}}{1 + 2r \sin^2 \frac{s\pi}{2N}}$	2-D CN	$\frac{1 - 2r \left(\sin^2 \frac{i\pi}{2N} + \sin^2 \frac{j\pi}{2N} \right)}{1 + 2r \left(\sin^2 \frac{i\pi}{2N} + \sin^2 \frac{j\pi}{2N} \right)}$
1-D DF	$\frac{2r \cos \frac{s\pi}{N} \pm \sqrt{1 - 4r^2 \sin^2 \frac{s\pi}{N}}}{1 + 2r}$		
2-D DF	$\frac{2r \left(\cos \frac{i\pi}{N} + \cos \frac{j\pi}{N} \right) \pm \sqrt{1 - 4r^2 \left[4 - \left(\cos \frac{i\pi}{N} + \cos \frac{j\pi}{N} \right)^2 \right]}}{1 + 4r}$		
2-D ADI	$\frac{1 - 2r \sin^2 \frac{j\pi}{2N}}{1 + 2r \sin^2 \frac{i\pi}{2N}}$		$\frac{1 - 2r \sin^2 \frac{i\pi}{2N}}{1 + 2r \sin^2 \frac{j\pi}{2N}}$

where $s = 1, 2, \dots, N - 1$

$i = 1, 2, \dots, N - 1$

$j = 1, 2, \dots, N - 1$

Expectation Values

$$\left\langle \sin^2 \frac{s\pi}{N} \right\rangle = \left\langle \sin^2 \frac{2s\pi}{2N} \right\rangle = \left\langle \cos^2 \frac{s\pi}{N} \right\rangle = \left\langle \cos^2 \frac{2s\pi}{2N} \right\rangle = \frac{1}{2} \quad N \geq 2 \quad s = 1, 2, \dots, N-1$$

$$\left\langle \cos \frac{i\pi}{N} \right\rangle = 0 \quad N \geq 2 \quad i = 1, 2, \dots, N-1$$

$$\left\langle \sin^2 \frac{i\pi}{2N} + \sin^2 \frac{j\pi}{2N} \right\rangle = \left\langle \sin^2 \frac{i\pi}{2N} \right\rangle + \left\langle \sin^2 \frac{j\pi}{2N} \right\rangle = 1 \quad N \geq 2 \quad i = 1, 2, \dots, N-1$$

$$j = 1, 2, \dots, N-1$$

$$\left\langle \left(\cos \frac{i\pi}{N} + \cos \frac{j\pi}{N} \right)^2 \right\rangle = 1 \quad \text{for large } N$$

$$= 0 \quad N = 2 \quad i = 1, 2, \dots, N-1$$

$$j = 1, 2, \dots, N-1$$

$\langle \rangle$ indicates expectation value of enclosed quantity, defined as:

$$\langle k Z_s \rangle \equiv \frac{1}{N-1} \sum_{s=1}^{N-1} k Z_s \quad \text{or}$$

$$\langle k Z_s \rangle \approx \frac{\int_0^{\pi/2} -4r \sin^2 \theta \, d\theta}{\int_0^{\pi/2} d\theta} \quad \text{for large } N$$

Comparison of Coefficient P-Ratio and
Expectation Values of Amplification Matrix Eigenvalues

FDM	Coef P-Ratio	$\langle G_s \rangle$ or $\langle G_{m,n} \rangle$
1-D EX	$1 - 2r$	Same
2-D EX	$1 - 4r$	Same
1-D IM	$\frac{1}{1 + 2r}$	Same
2-D IM	$\frac{1}{1 + 4r}$	Same
1-D CN	$\frac{1 - r}{1 + r}$	Same
* 2-D CN	$\frac{1 - 2r}{1 + 2r}$	Same
* 1-D DF	$\frac{1 - 2r}{1 + 2r}$	$\frac{\pm \sqrt{1 - 2r^2}}{1 + 2r}$
** 2-D DF	$\frac{1 - 4r}{1 + 4r}$	$\frac{\pm \sqrt{1 - 12r^2}}{1 + 4r}$ for large N
* 2-D ADI	$\frac{1 - 2r}{1 + 2r}$	$\frac{1 - 2r + r^2}{1 + 2r + r^2}$

* Have same Coef P-Ratio

** $\frac{\pm \sqrt{1 - 16r^2}}{1 + 4r}$ for N = 2

Bibliography

1. Burden, R. L. and J. D. Faires. Numerical Analysis (Third Edition). Boston: Prindle, Weber & Schmidt Publishers, 1985.
2. Carslaw, H. S. and J. C. Jaeger. Conduction of Heat in Solids (Second Edition). Great Britain: Clarendon Press, 1959.
3. Clark, M., Jr. and K. F. Hansen. Numerical Methods of Reactor Analysis. New York: Academic Press, 1964.
4. Cuthrell, Joseph E. Oscillatory Behavior of Finite Difference Methods for the Solution of the Two Dimensional Transient Heat (Diffusion) Equation. MS Thesis. School of Engineering, Air Force Institute of Technology (AU), Wright-Patterson AFB OH, March 1986.
5. Gellert, W., H. Kustner, M. Hellwich and H. Kastner (Editors). The VNR Concise Encyclopedia of Mathematics. New York: Van Nostrand Reinhold Company, 1975.
6. Hornbeck, Robert W. Numerical Methods. New York: Quantum Publishers Inc., 1975.
7. Kaplan, Bernard. "A Probabilistic Derivation of the Stability Condition of the Difference Equation for the Diffusion Equation," American Journal of Physics, 51 (5): 459-460 (May 1983).
8. Kropf, Roger F. Oscillatory Solutions of the Peaceman-Rachford Alternating Direction Implicit Method and A Comparison of Methods for the Solution of the Heat Equation. MS Thesis. School of Engineering, Air Force Institute of Technology (AU), Wright-Patterson AFB OH, January 1985.
9. Lapidus, Leon and George F. Pinder. Numerical Solutions of Partial Differential Equations in Science and Engineering. New York: John Wiley and Sons, 1982.
10. Lawson, J. D. and J. L. Morris. "The Extrapolation of First Order Methods for Parabolic Partial Differential Equations," I', SIAM Journal Numerical Analysis, 15 (6), 1212-1224 (1978).
11. Lupo, J. A., Professor of Physics. Personal Interviews. School of Engineering, Air Force Institute of Technology

(AU), Wright-Patterson AFB OH, August-September 1987.

12. Myers, Glen E. Analytical Methods in Conduction Heat Transfer. New York: McGraw-Hill Book Company, 1971.
13. Smith, G. D. Numerical Solution of Partial Differential Equations: Finite Difference Methods (Third Edition). New York: Oxford University Press, 1985.
14. Twizell, E. H. Computational Methods for Partial Differential Equations. New York: Halsted Press, 1984.
15. White, J. W. An Elementary Introduction to Finite Difference Equations. Lawrence Livermore Laboratory, University of California, Livermore, CA, May 1976.

VITA

Captain Thomas M. Dipp was born on 13 October 1959 in Boise, Idaho. He graduated from high school in Gilchrist, Oregon in 1978 and went on to enlist in the Air Force. Continuing his education, he received a Bachelor of Science degree in Physics from the United States Air Force Academy in June of 1983. After graduation, he spent a tour of duty at Vandenberg AFB, CA working in the Western Space and Missile Center, until entering the Air Force Institute of Technology in June 1986. His next assignment is to the Air Force Weapons Lab, Kirtland AFB, New Mexico.

Permanent address: P.O. Box 69

Crescent, Oregon 97733

UNCLASSIFIED

SECURITY CLASSIFICATION OF THIS PAGE

REPORT DOCUMENTATION PAGE

Form Approved
OMB No. 0704-0188

1a. REPORT SECURITY CLASSIFICATION UNCLASSIFIED			1b. RESTRICTIVE MARKINGS		
2a. SECURITY CLASSIFICATION AUTHORITY			3. DISTRIBUTION / AVAILABILITY OF REPORT		
2b. DECLASSIFICATION / DOWNGRADING SCHEDULE			Approved for public release; distribution unlimited		
4. PERFORMING ORGANIZATION REPORT NUMBER(S) AFIT/GEP/ENP/87D-5			5. MONITORING ORGANIZATION REPORT NUMBER(S)		
6a. NAME OF PERFORMING ORGANIZATION Air Force Institute of Technology Wright-Patterson AFB, OH 45433		6b. OFFICE SYMBOL (if applicable)	7a. NAME OF MONITORING ORGANIZATION		
6c. ADDRESS (City, State, and ZIP Code)			7b. ADDRESS (City, State, and ZIP Code)		
8a. NAME OF FUNDING / SPONSORING ORGANIZATION		8b. OFFICE SYMBOL (if applicable)	9. PROCUREMENT INSTRUMENT IDENTIFICATION NUMBER		
8c. ADDRESS (City, State, and ZIP Code)			10. SOURCE OF FUNDING NUMBERS		
PROGRAM ELEMENT NO.		PROJECT NO.	TASK NO.	WORK UNIT ACCESSION NO.	
11. TITLE (Include Security Classification) See Box 19					
12. PERSONAL AUTHOR(S) Thomas M. Dipp, B.S., Capt, USAF					
13a. TYPE OF REPORT MS Thesis		13b. TIME COVERED FROM _____ TO _____		14. DATE OF REPORT (Year, Month, Day) 1987 December	
15. PAGE COUNT 120					
16. SUPPLEMENTARY NOTATION					
17. COSATI CODES			18. SUBJECT TERMS (Continue on reverse if necessary and identify by block number)		
FIELD	GROUP	SUB-GROUP	Numerical Analysis, Heat Conduction (Diffusion), Finite Differences, Partial Differential Equations, Heat Transfer		
12	01				
19. ABSTRACT (Continue on reverse if necessary and identify by block number)					
<p>Title: PREDICTING OSCILLATORY FINITE DIFFERENCE SOLUTIONS TO THE HEAT EQUATION: A COMPARATIVE STUDY OF THE COEFFICIENT AND MATRIX METHODS</p> <p>Thesis Chairman: Dr. Bernard Kaplan Professor of Physics</p> <p style="text-align: right;">Approved for public release: LAW AFR 190-17 24 Feb 88</p>					
20. DISTRIBUTION / AVAILABILITY OF ABSTRACT <input type="checkbox"/> UNCLASSIFIED/UNLIMITED <input checked="" type="checkbox"/> SAME AS RPT <input type="checkbox"/> DTIC USERS			21. ABSTRACT SECURITY CLASSIFICATION UNCLASSIFIED		
22a. NAME OF RESPONSIBLE INDIVIDUAL Dr. Bernard Kaplan			22b. TELEPHONE (Include Area Code) (513) 255-4498		22c. OFFICE SYMBOL AFIT/ENP

This thesis compared the coefficient method with the full matrix method for predicting stability and oscillatory behavior of Finite Difference Methods, FDMs, used in solving the one and two dimensional transient heat (diffusion) equation with Dirichlet boundary conditions. Five FDMs were used: the fully implicit, fully explicit, DuFort-Frankel, Crank-Nicolson, and Peaceman-Rachford ADI.

Analytically, the Pade' method was found to be equivalent to the matrix method in predicting stability and oscillations. The matrix method was shown to be more severe than the coefficient method in predicting both stable and non-oscillatory step size constraints. Also, the matrix method, while mathematically more rigorous, proved to be more difficult to derive and analyze, possibly limiting its usefulness. Ultimately, it was found that the coefficient method's predictions could be derived from the matrix method for two-level FDMs.

Numerically, all methods were solved repeatedly and the results investigated for oscillatory behavior and maximum errors in the h - k , or space and time step, domain. These results allowed functional comparison with stability and oscillatory predictions made by the coefficient and full matrix methods. Neither the coefficient nor matrix method's stability and oscillatory predictions were significantly violated for two-level FDMs. Finally, the matrix method could generally predict when non-disastrous oscillations would occur, based on moderate step size constraints.

END

DATE

3-88

DTIC